2017

ANALYTICAL STRIP METHOD FOR THIN CYLINDRICAL SHELLS

John T. Perkins
University of Kentucky, taylor.perkins@stantec.com
Digital Object Identifier: https://doi.org/10.13023/ETD.2017.369

STUDENT AGREEMENT:

I represent that my thesis or dissertation and abstract are my original work. Proper attribution has been given to all outside sources. I understand that I am solely responsible for obtaining any needed copyright permissions. I have obtained needed written permission statement(s) from the owner(s) of each third-party copyrighted matter to be included in my work, allowing electronic distribution (if such use is not permitted by the fair use doctrine) which will be submitted to UKnowledge as Additional File.

I hereby grant to The University of Kentucky and its agents the irrevocable, non-exclusive, and royalty-free license to archive and make accessible my work in whole or in part in all forms of media, now or hereafter known. I agree that the document mentioned above may be made available immediately for worldwide access unless an embargo applies.

I retain all other ownership rights to the copyright of my work. I also retain the right to use in future works (such as articles or books) all or part of my work. I understand that I am free to register the copyright to my work.

REVIEW, APPROVAL AND ACCEPTANCE

The document mentioned above has been reviewed and accepted by the student's advisor, on behalf of the advisory committee, and by the Director of Graduate Studies (DGS), on behalf of the program; we verify that this is the final, approved version of the student's thesis including all changes required by the advisory committee. The undersigned agree to abide by the statements above.

John T. Perkins, Student

Dr. Issam Elias Harik, Major Professor

Dr. Yi-Tin Wang, Director of Graduate Studies

ANALYTICAL STRIP METHOD FOR THIN CYLINDRICAL SHELLS

_____

DISSERTATION

_____

A dissertation submitted in partial fulfillment of the
requirements for the degree of Doctor of Philosophy in the
College of Engineering
at the University of Kentucky

By
John Taylor Perkins

Lexington, Kentucky

Director: Dr. Issam Elias Harik, Professor of Civil Engineering

Lexington, Kentucky

2017

ABSTRACT OF DISSERTATION

ANALYTICAL STRIP METHOD FOR THIN CYLINDRICAL SHELLS

The Analytical Strip Method (ASM) for the analysis of thin cylindrical shells is presented in this dissertation. The system of three governing differential equations for the cylindrical shell are reduced to a single eighth order partial differential equation (PDE) in terms of a potential function. The PDE is solved as a single series form of the potential function, from which the displacement and force quantities are determined. The solution is applicable to isotropic, generally orthotropic, and laminated shells. Cylinders may have simply supported edges, clamped edges, free edges, or edges supported by isotropic beams. The cylindrical shell can be stiffened with isotropic beams in the circumferential direction placed anywhere along the length of the cylinder. The solution method can handle any combination of point loads, uniform loads, hydrostatic loads, sinusoidal loads, patch loads, and line loads applied in the radial direction. The results of the ASM are compared to results from existing analytical solutions and numerical solutions for several examples; the results for each of the methods were in good agreement. The ASM overcomes limitations of existing analytical solutions and provides an alternative to approximate numerical and semi-numerical methods.

KEYWORDS: Analytical modeling, Thin shells, Laminates, bending-extension coupling, Composite shells

    John Taylor Perkins
Student's Signature

    08/03/2017
Date

ANALYTICAL STRIP METHOD FOR THIN CYLINDRICAL SHELLS

By

John Taylor Perkins

Dr. Issam E. Harik
Director of Dissertation

Dr. Yi-Tin Wang
Director of Graduate Studies

08/03/2017
Date

ACKNOWLEDGEMENTS

This dissertation would not be possible without the guidance of my advisor Dr. Issam Harik, who has supported me through this non-traditional journey. He has offered unconditional support and encouragement. He challenged and inspired me to take on this research topic, which has transformed into something neither of us imagined. More than anything, it has been his infinite patience that has allowed me to pursue this dream in cooperation with my professional career.

I would like to thank my advisory committee members, Dr. Hans Gesund, Dr. George Blandford, and Dr. Mark Hanson. Their time, commitment, insight, and suggestions are much appreciated. Appreciation is also extended to the Department of Civil Engineering, who has provided tuition support through this process.

I am extremely grateful for my foundation of support outside of the University. Tony Hunley, Ph.D, has provided mentorship and inspiration both professionally and academically. It was his support that allowed me to pursue this research in conjunction with my professional career. I thank my Parents for their belief and dedication, I thank my In-Laws for their assistance, and I thank my friends for their moral encouragement. Above all I thank my wife, Lauren, whose sacrifice, and commitment to this process has rivaled my own. She has provided constant and unwavering belief in me; her optimism, encouragement, and enthusiasm has been a beacon in the most discouraging of times. Finally, I am thankful for my son, who is here to witness the end of this long and winding journey.

TABLE OF CONTENTS

Chapter 5   ANALYTICAL STRIP METHOD FOR THIN LAMINATED CYLINDRICAL SHELLS

LIST OF TABLES

LIST OF FIGURES

CHAPTER 1
INTRODUCTION

1.1 Background

Cylindrical Shells are important structural elements with widespread applications in various fields such as civil, environmental, mechanical, and aerospace engineering. On a larger scale they are used as storage tanks, buried conduits, pressure vessels, towers, and chimneys. On a smaller scale they can be used as functional components of a larger system. To design these cylindrical shell structures effectively and efficiently it is critical to understand their behavior.

Unlike plates, whose geometry lies within a plane, shells can have curvature in two orthogonal directions. Cylindrical shells are a special case with curvature in a single direction. This curvature complicates the governing equations since there is coupling between transverse shearing forces and bending moments. To simplify the solution to the governing equations, it is often necessary to rely on specialized shell theories that implement simplifications based on assumptions of stress and strain distributions through the thickness of the shell.

The most basic cylindrical shells are constructed from isotropic materials. The use of composite materials is also embraced because of the unique benefits they provide. Composite materials are created by combining two or more constituent materials at the macroscopic level to produce a product with desirable performance characteristics. Composite materials may exhibit superior strength and stiffness-to-weight ratio, corrosion resistance, high fatigue life, and enhanced thermal performance.

The most common use of composites in engineering applications is laminated composites. These materials are made of individual orthotropic layers, lamina, stacked in a configuration that optimizes performance for the desired application. The lamina consists of fibers, either unidirectional or bidirectional, encased in a supporting matrix. The fiber material, fiber distribution, number of layers, layer thickness, and angular fiber

orientation within each layer are all parameters than may be adjusted to optimize the performance of the material.

Laminates with a symmetric configuration about the middle surface of the shell behave orthotropic at the macromechanical level. Symmetric angle-ply laminates exhibit a coupling between extensional and shearing stresses. Laminates with an antisymmetric lamination scheme about the middle surface exhibit coupling between extensional and bending or twisting forces. These coupling effects significantly complicate the behavior of the laminate and make the development of analytical solutions more difficult.

1.2 Literature Review

1.2.1 Shell Theory

Finding the exact stress and deformational response of a cylindrical shell subjected to static loading is a complex problem that requires solution of the three-dimensional elasticity equations. Elasticity solutions may be possible for problems with simplified loading or boundary conditions, but for anything more complex, the governing elasticity equations must be reduced to simplify the problem. Shell theories apply assumptions of stress and strain distribution through the thickness of the shell to reduce the three-dimensional structure to a two-dimensional plane stress problem.

The most basic shell theory is known as the theory of thin elastic shells, also referred to as classical shell theory or Love's first approximation. Thin shell theories are based on the following, known as Love's assumptions (Love, 1944)

- Thickness of the shell is small compared with the other dimensions
- Strains and displacements are sufficiently small so that the quantities of second- and higher-order magnitude in the strain-displacement relations may be neglected in comparison with the first-order terms
- The transverse normal stress is negligible.

- Normals to the undeformed middle surface remain straight and normal to the deformed middle surface and undergo no change in length during deformation.

There are a wide number of thin shell theories available, including those formulated by Donnell (1933, 1938), Mushtari (1938), Love (1988, 1944), Timoshenko and Woinowsky-Krieger (1959), Reissner (1941), Naghdi and Berry (1964), Vlasov (1944, 1949), Sanders (1959), Byrne (1944), Flügge (1934, 1962), Goldenveizer (1961), Lur'ye (1940), and Novozhilov (1964). These theories vary by the level of simplification implemented in the strain-displacement equations and the governing equilibrium equations. Leissa (1973) provides an excellent review of available thin shell theories.

Three notable thin shell theories are those developed by Donnell (1933, 1938), Love (1944), and Naghdi and Berry (1964). Donnell's theory is analogous to plate theory, as it neglects the component of transverse shearing force from the equilibrium of forces in the circumferential direction, and is applicable to shallow shells. This greatly simplifies the governing differential equations for cylindrical shells, but can lead to inaccuracies as the ratio of thickness-to-radius and thickness-to-length of the shell increases (Kraus, 1967). Love's equations are commonly adopted for thin shell problems because they provide reliable results while maintaining adequate simplicity to facilitate the solution process. A disadvantage of the Love's equations is that it does not produce a symmetric system of governing differential equations. Shell theory of Naghdi and Berry implement the same set of assumptions as Love but produce a symmetric set of governing equations (Leissa, 1973).

Love's assumptions are appropriate for thin shells, but as the thickness of the shell increases relative to the radius and length they can lead to inaccuracies. This has necessitated the development of higher-order shell theories that relax one or more of Love's assumptions. In particular, the fourth of Love's assumption is relaxed to allow for transverse shearing deformations through the thickness of the shell. The order of the shell theory correlates to the assumed distribution of transverse shearing stresses. Example higher order theories are those proposed by Hildebrand, Reissner, and Thomas

(1949), Reissner (1952), and Naghdi (1957). Due to the complexity of the governing equations, solutions utilizing these theories are often limited to numerical methods.

The above shell theories were originally derived based on isotropic shells, but can be easily extended to laminated composite shells by generalizing the assumed material constitutive relationships. Ambartsumian (1961, 1966) and Bert (1975) both presented a theory for laminated orthotropic shells, which incorporated extensional-bending coupling. Dong, Pister, and Taylor (1962) developed a theory of thin shells laminated with anisotropic layers based on Donnell's assumptions (1933), while Cheng and Ho (1963) developed equations based on Flügge's shell theory (1962). The fourth of Love's assumptions, which assumes undeformable normals to the middle surface of the shell, becomes quite significant for laminated shells as it can lead to more than 30% error for deflections, stresses, and frequencies (Reddy, 2004). Whitney and Sun (1974), Reddy (1984), Vasilenko and Golub (1984), and Barbero et al. (1990) have developed shear deformational theories for laminated shells, but these theories suffer from the same limitations as higher-order isotropic shell theories due to complexity of the governing equations.

1.2.2 Analytical Solutions

An analytical solution (Timoshenko, 1961) to a problem is one that satisfies the governing equations at every point in the domain, as well as the boundary and initial conditions. An analytical solution may be formulated as either closed-form or as an infinite series. Analytical solutions for cylindrical shells often necessitate infinite series solutions.

Analytical solutions to isotropic cylindrical shells subjected to axisymmetric loads are widely available. Timoshenko and Woinowsky-Krieger (1959) provide solutions for cylindrical shells with uniform internal pressure as well as cylindrical tanks subjected to hydrostatic loads. Due to the introduction of a second variable in the circumferential direction, non-axisymmetric type loadings are difficult to incorporate in the solution. Bijlaard (1955) developed a double series solution for cylindrical shells subjected to a

patch load as well as a similar solution for point loads. Odqvist (1946), Hoff et. al. (1954), Cooper (1957), and Naghdi (1968) have developed unique solutions for cylindrical shells subjected to a uniform line load along a generator. Meck (1961) presented a solution for line loads applied along the circumferential direction.

For laminated composite shells, three-dimensional elasticity solutions and higher order shell theories are well suited for thick to moderately thick shells. Elasticity solutions for laminated composite shells are widely available (Ren, 1987, 1995; Chandrashekhara and Nanjunda Rao, 1997, 1998; Varadan and Bhaskar, 1991). Noor and Burton (1990) provide and exhaustive review of available solutions. The applicability of these solutions is generally constrained to shells of infinite length or with simplified loading conditions. Although thin shell theories poorly capture the behavior of shells with low radius-to-thickness ratio, they perform reliably for high radius-to-thickness ratios (Ren, 1987), and the simplifying assumptions in the theory facilitate the incorporation of complex loading and boundary conditions.

One of the primary uses for analytical solutions is as a benchmark to validate and compare solutions attained from other methods. For example, an analytical solution developed for a thin shell theory may be used to validate the accuracy of a finite element solution or may be used as a basis of comparison for a higher-order shell theory for which only numerical solutions methods are possible.

1.2.3 Numerical Solutions

A numerical solution is one that approximates the solution to a governing differential equation including boundary and initial conditions. Analytical solutions are not always available for problems with complex geometries and boundary conditions, nonlinearity, and higher-order deformation response. These limitations, however, do not preclude the use of numerical methods. Two common numerical solution methods are the finite difference and finite element methods. Finite element solutions for laminated cylindrical shells have been developed by Saviz et al. (2009), Singha et al. (2006), Liew et al. (2002), and Saviz and Mohammadpourfard (2010).

The finite element method requires the structure to be discretized into elements of regular geometric shape. The response of each element is approximated by shape functions, which when assembled, dictate the global response of the structure. Consequently, more refinement of the domain discretization yields a more accurate approximation to the structural response. The finite element solution requires the solution of a system of equations, the order of which depends on the discretization of the domain. Efficient solutions to numerical methods may require considerable computational demand and storage capacity.

Numerical methods provide versatility not available for most existing analytical solutions. They are, however, limited by the implementation of loading and boundary conditions. Additionally, most numerical solutions are not continuous for all pertinent displacement and forces components of the domain.

1.3 Research Objective

The objective of this paper is to develop an analytical strip method (ASM) of solution for stiffened isotropic and laminated composite thin cylindrical shells.

The ASM was first developed by Harik and Salamoun (1986, 1988) for the analysis of thin orthotropic and stiffened rectangular plates subjected to uniform, partial uniform, patch, line, partial line and point loads, or any combination thereof. The solution method was subsequently extended to laminated plates by Sun (2009). The solution procedure requires that the structure be divided into strips based on the geometric discontinuities and applied loads. Figure 1.1 shows the necessary strip discretization for a stiffened cylindrical shell subjected to a combination of loadings. The governing differential equation for each strip is solved analytically, and the applicable continuity and boundary conditions are used to combine the solutions for the strips.

1.4 Research Significance

Available analytical solutions to cylindrical shells are currently limited; many require simplifications such as infinite length boundary conditions, axisymmetric loading, and

omission of terms in the governing equations. Methods that don't require these simplifications lack generality in terms of end boundary conditions, variations in wall thickness, and incorporation of stiffeners. The ASM overcomes these limitations.

Numerical methods provide an alternative to analytical solutions. Numerical methods, such as finite element solutions, often require significant effort to discretize the domain and to perform refinement studies to validate the accuracy of the results. In the ASM, the structure is divided into strips based on discontinuities in the shell geometry and applied loads. Unlike numerical methods, the accuracy of the ASM results are dependent on the number of modes summed in the solution rather than the number of strips that sub-divide the structure.

1.5 Dissertation Outline

The dissertation consists of six chapters organized as follows:

- Chapter 2 presents the governing equations for isotropic and laminated cylindrical shells.

- Chapter 3 details the derivation of the ASM solution.

- Chapter 4 summarizes the ASM for isotropic thin cylindrical shells and provides numerical examples that compare the ASM results with existing analytical solutions and highlights the features of the ASM.

- Chapter 5 summarizes the ASM for laminated thin cylindrical shells and provides numerical examples that compare the ASM results with existing analytical solutions and highlights the features of the ASM.

- Chapter 6 presents a summary of the significant findings from this research, and conclusions are drawn with regards to its relevance. Future research needs are identified and discussed.
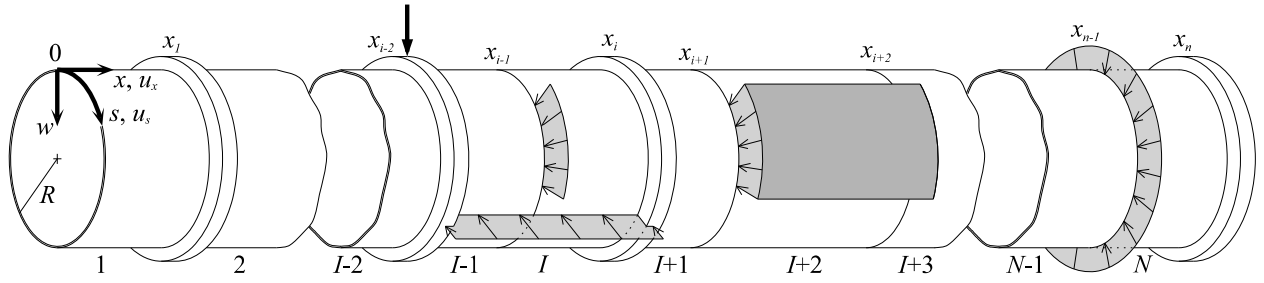
Figure 1.1. Stiffened cylindrical shell with strip and edge loadings

Note: The stiffeners are concentric with the shell

CHAPTER 2
GOVERNING EQUATIONS

2.1 Introduction

This chapter presents the derivation of the governing differential equations for isotropic and laminated cylindrical shells (Figure 2.1). Laminated shells can have any generalized layer configuration and ply-angle scheme, such that the shell behaves anisotropically.

The derivation of the governing differential equations are based on the following assumptions:

- The shell materials are linear and elastic.

- The lamina are homogeneous and orthotropic.

- The stacked lamina are perfectly bonded, thus no delamination at the layer interfaces.

- The shell walls are thin and Love's assumptions (Love, 1944) are applicable

    - Thickness of the shell is small compared with the other dimensions.

    - Strains and displacements are sufficiently small so that the magnitudes of the second-order and higher-order terms in the strain-displacement relations may be neglected in comparison with the first-order terms.

    - The transverse normal stress is negligible.

    - Normals to the undeformed middle surface remain straight and normal to the deformed middle surface, and undergo no change in length during deformation.

2.2 Strain-Displacement Equations

The surface coordinate system used in the derivation of the governing equations for the cylindrical shell is shown in Figure 2.1. The strain-displacement equations associated with thin shell theory are given as (Kraus, 1967)

$$\epsilon_x = \frac{\partial u_x}{\partial x} \tag{2.1a}$$

$$\epsilon_s = \frac{\partial u_s}{\partial s} + \frac{w}{R} \tag{2.1b}$$

$$\gamma_{xs} = \frac{\partial u_s}{\partial x} + \frac{\partial u_x}{\partial s} \tag{2.1c}$$

$$\kappa_x = -\frac{\partial^2 w}{\partial x^2} \tag{2.1d}$$

$$\kappa_s = \frac{\partial}{\partial s}\left(\frac{u_s}{R} - \frac{\partial w}{\partial s}\right) \tag{2.1e}$$

$$\kappa_{xs} = \frac{1}{R}\frac{\partial u_s}{\partial x} - 2\frac{\partial^2 w}{\partial x \partial s} \tag{2.1f}$$

2.3 Constitutive Equations

2.3.1 Isotropic Shells

The constitutive equations for a single isotropic layer are provided by Jones (1999).

$$\begin{Bmatrix} N_x \\ N_s \\ N_{xs} \end{Bmatrix} = \begin{bmatrix} A & \nu A & 0 \\ \nu A & A & 0 \\ 0 & 0 & \frac{1-\nu}{2}A \end{bmatrix} \begin{Bmatrix} \epsilon_x \\ \epsilon_s \\ \gamma_{xs} \end{Bmatrix} \tag{2.2a}$$

$$\begin{Bmatrix} M_x \\ M_s \\ M_{xs} \end{Bmatrix} = \begin{bmatrix} D & \nu D & 0 \\ \nu D & D & 0 \\ 0 & 0 & \frac{1-\nu}{2}D \end{bmatrix} \begin{Bmatrix} \kappa_x \\ \kappa_s \\ \kappa_{xs} \end{Bmatrix} \tag{2.2b}$$

where A and D are the extensional and bending stiffness of the shell

$$A = \frac{Et}{1-\nu^2} \tag{2.3a}$$

$$D = \frac{Et^3}{12(1-\nu^2)} \tag{2.3b}$$

2.3.2 Laminated Shells

The stress-strain relationships for a single orthotropic lamina are (Jones, 1999)

$$\begin{Bmatrix} \sigma_x \\ \sigma_s \\ \tau_{xs} \end{Bmatrix} = \begin{bmatrix} \bar{Q}_{11} & \bar{Q}_{12} & \bar{Q}_{16} \\ \bar{Q}_{12} & \bar{Q}_{22} & \bar{Q}_{26} \\ \bar{Q}_{16} & \bar{Q}_{26} & \bar{Q}_{66} \end{bmatrix} \begin{Bmatrix} \epsilon_x \\ \epsilon_s \\ \gamma_{xs} \end{Bmatrix} \tag{2.4}$$

where $\bar{Q}_{ij}$ are the transformed reduced stiffness coefficients given by (Jones, 1999)

$$\bar{Q}_{11} = Q_{11}\cos^4\beta + 2(Q_{12} + 2Q_{66})\sin^2\beta\cos^2\beta + Q_{22}\sin^4\beta \tag{2.5a}$$

$$\bar{Q}_{12} = (Q_{11} + Q_{22} - 4Q_{66})\sin^2\beta\cos^2\beta + Q_{12}(\sin^4\beta + \cos^4\beta) \tag{2.5b}$$

$$\bar{Q}_{22} = Q_{11}\sin^4\beta + 2(Q_{12} + 2Q_{66})\sin^2\beta\cos^2\beta + Q_{22}\cos^4\beta \tag{2.5c}$$

$$\bar{Q}_{16} = (Q_{11} - Q_{12} - 2Q_{66})\sin\beta\cos^3\beta + (Q_{12} - Q_{22} + 2Q_{66})\sin^3\beta\cos\beta \tag{2.5d}$$

$$\bar{Q}_{26} = (Q_{11} - Q_{12} - 2Q_{66})\sin^3\beta\cos\beta + (Q_{12} - Q_{22} + 2Q_{66})\sin\beta\cos^3\beta \tag{2.5e}$$

$$\bar{Q}_{26} = (Q_{11} + Q_{22} - 2Q_{12} - 2Q_{66})\sin^2\beta\cos^2\beta + Q_{66}(\sin^4\beta + \cos^4\beta) \tag{2.5f}$$

and β is the orientation angle of the lamina principal direction, measured counterclockwise from the x-axis of the cylinder. The reduced stiffness coefficients, Q_{ij}, are (Jones, 1999)

$$Q_{11} = \frac{E_1}{1-\nu_{12}\nu_{21}} \tag{2.6a}$$

$$Q_{12} = \frac{\nu_{21}E_1}{1-\nu_{12}\nu_{21}} = \frac{\nu_{12}E_2}{1-\nu_{12}\nu_{21}} \tag{2.6b}$$

$$Q_{22} = \frac{E_2}{1 - \nu_{12}\nu_{21}} \tag{2.6c}$$

$$Q_{66} = G_{12} \tag{2.6d}$$

The constitutive relationships for the laminated shell are (Jones, 1999)

$$\begin{Bmatrix} N_x \\ N_s \\ N_{xs} \end{Bmatrix} = \begin{bmatrix} A_{11} & A_{12} & A_{16} \\ A_{12} & A_{22} & A_{26} \\ A_{16} & A_{26} & A_{66} \end{bmatrix} \begin{Bmatrix} \epsilon_x \\ \epsilon_s \\ \gamma_{xs} \end{Bmatrix} + \begin{bmatrix} B_{11} & B_{12} & B_{16} \\ B_{12} & B_{22} & B_{26} \\ B_{16} & B_{26} & B_{66} \end{bmatrix} \begin{Bmatrix} \kappa_x \\ \kappa_s \\ \kappa_{xs} \end{Bmatrix} \tag{2.7a}$$

$$\begin{Bmatrix} M_x \\ M_s \\ M_{xs} \end{Bmatrix} = \begin{bmatrix} B_{11} & B_{12} & B_{16} \\ B_{12} & B_{22} & B_{26} \\ B_{16} & B_{26} & B_{66} \end{bmatrix} \begin{Bmatrix} \epsilon_x \\ \epsilon_s \\ \gamma_{xs} \end{Bmatrix} + \begin{bmatrix} D_{11} & D_{12} & D_{16} \\ D_{12} & D_{22} & D_{26} \\ D_{16} & D_{26} & D_{66} \end{bmatrix} \begin{Bmatrix} \kappa_x \\ \kappa_s \\ \kappa_{xs} \end{Bmatrix} \tag{2.7b}$$

where A_{ij} are the extensional stiffnesses, B_{ij} are the bending-extensional coupling stiffnesses, and D_{ij} are the bending stiffnesses. The stiffness coefficients are given by Reddy (2004) and are defined as

$$\{A_{ij}, B_{ij}, D_{ij}\} = \int_{-\frac{t}{2}}^{\frac{t}{2}} \bar{Q}_{ij}\{1, z, z^2\}dz; \quad i, j = 1,2,6 \tag{2.8}$$

where t is the thickness of the shell.

In symmetric laminates, $B_{ij} = 0$ in Eq. (2.7). In antisymmetric cross-ply laminates, $B_{12} = B_{16} = B_{26} = B_{66} = 0$ and $B_{22} = -B_{11}$ in Eq. (2.7). In antisymmetric angle-ply laminates, $B_{11} = B_{12} = B_{22} = B_{66} = 0$ in Eq. (2.7).

The reduced constitutive relations for a single generally orthotropic layer as well as cross-ply and angle-ply symmetric and antisymmetric laminates is

$$\begin{Bmatrix} N_x \\ N_s \\ N_{xs} \end{Bmatrix} = \begin{bmatrix} A_{11} & A_{12} & A_{16} \\ A_{12} & A_{22} & A_{26} \\ A_{16} & A_{26} & A_{66} \end{bmatrix} \begin{Bmatrix} \epsilon_x \\ \epsilon_s \\ \gamma_{xs} \end{Bmatrix} + \begin{bmatrix} B_{11} & 0 & B_{16} \\ 0 & B_{22} & B_{26} \\ B_{16} & B_{26} & 0 \end{bmatrix} \begin{Bmatrix} \kappa_x \\ \kappa_s \\ \kappa_{xs} \end{Bmatrix} \tag{2.9a}$$

$$\begin{Bmatrix} M_x \\ M_s \\ M_{xs} \end{Bmatrix} = \begin{bmatrix} B_{11} & 0 & B_{16} \\ 0 & B_{22} & B_{26} \\ B_{16} & B_{26} & 0 \end{bmatrix} \begin{Bmatrix} \epsilon_x \\ \epsilon_s \\ \gamma_{xs} \end{Bmatrix} + \begin{bmatrix} D_{11} & D_{12} & D_{16} \\ D_{12} & D_{22} & D_{26} \\ D_{16} & D_{26} & D_{66} \end{bmatrix} \begin{Bmatrix} \kappa_x \\ \kappa_s \\ \kappa_{xs} \end{Bmatrix} \tag{2.9b}$$

2.4 Equilibrium Equations

The equilibrium equations for the cylindrical shell are given as (Kraus, 1967)

$$\frac{\partial N_x}{\partial x} + \frac{\partial N_{sx}}{\partial s} + q_x = 0 \tag{2.10a}$$

$$\frac{\partial N_{xs}}{\partial x} + \frac{\partial N_s}{\partial s} + \frac{Q_s}{R} + q_s = 0 \tag{2.10b}$$

$$\frac{\partial Q_x}{\partial x} + \frac{\partial Q_s}{\partial s} - \frac{N_s}{R} + q = 0 \tag{2.10c}$$

$$\frac{\partial M_x}{\partial x} + \frac{\partial M_{xs}}{\partial s} - Q_x = 0 \tag{2.10d}$$

$$\frac{\partial M_{xs}}{\partial x} + \frac{\partial M_s}{\partial s} - Q_s = 0 \tag{2.10e}$$

The five equilibrium equations are reduced to three by substituting Eq. (2.10d) and Eq. (2.10e) into Eq. (2.10c).

$$\frac{\partial N_x}{\partial x} + \frac{\partial N_{sx}}{\partial s} + q_x = 0 \tag{2.11a}$$

$$\frac{\partial N_{xs}}{\partial x} + \frac{\partial N_s}{\partial s} + \frac{Q_s}{R} + q_s = 0 \tag{2.11b}$$

$$\frac{\partial^2 M_x}{\partial x^2} + 2\frac{\partial^2 M_{xs}}{\partial x \partial s} + \frac{\partial^2 M_s}{\partial s^2} - \frac{N_s}{R} + q = 0 \tag{2.11c}$$

2.5 Coupled Governing Differential Equations

2.5.1 Isotropic Shells

The three coupled differential equations for isotropic cylindrical shells are derived by substituting the strain-displacement equations, Eq. (2.1), into the constitutive relationships of Eq. (2.2) to get the force-displacement relationships. The force-displacement relationships are then substituted into the equilibrium equations of Eq. (2.11). The system of differential equations may be presented as

13

$$\begin{bmatrix} L_{11} & L_{12} & L_{13} \\ L_{12} & L_{22} & L_{23} \\ L_{13} & L_{23} & L_{33} \end{bmatrix} \begin{Bmatrix} u_x \\ u_s \\ w \end{Bmatrix} = \begin{Bmatrix} q_x \\ q_s \\ q \end{Bmatrix} \tag{2.12}$$

where L_{ij} are differential operators

$$L_{11} = A\frac{\partial^2}{\partial x^2} + \frac{1-v}{2}A\frac{\partial^2}{\partial s^2} \tag{2.13a}$$

$$L_{12} = \frac{1+v}{2}A\frac{\partial^2}{\partial x \partial s} \tag{2.13b}$$

$$L_{13} = \frac{v}{R}A\frac{\partial}{\partial x} \tag{2.13c}$$

$$L_{22} = \left(\frac{1-v}{2}A + \frac{1-v}{2R^2}D\right)\frac{\partial^2}{\partial x^2} + (A + D)\frac{\partial^2}{\partial s^2} \tag{2.13d}$$

$$L_{23} = \frac{1}{R}A\frac{\partial}{\partial s} - \frac{1}{R}D\frac{\partial^3}{\partial x^2 \partial s} - \frac{1}{R}D\frac{\partial^3}{\partial s^3} \tag{2.13e}$$

$$L_{33} = \frac{1}{R^2}A + D\frac{\partial^4}{\partial x^4} + 2D\frac{\partial^4}{\partial x^2 \partial s^2} + D\frac{\partial^4}{\partial s^4} \tag{2.13f}$$

A and D are the extensional and bending stiffness of the shell given by Eq. (2.3). The differential equations of Eq. (2.12) and Eq. (2.13) are consistent with the thin shell theory developed by Naghdi and Berry (1964).

2.5.2 Laminated Shells

The three coupled differential equations for laminated cylindrical shells are derived by substituting the strain-displacement equations, Eq. (2.1), into the constitutive relationships of Eq. (2.9) to get the force-displacement relationships. The force-displacement relationships are then substituted into the equilibrium equations of Eq. (2.11). The system of differential equations may be presented as

$$\begin{bmatrix} L_{11} & L_{12} & L_{13} \\ L_{12} & L_{22} & L_{23} \\ L_{13} & L_{23} & L_{33} \end{bmatrix} \begin{Bmatrix} u_x \\ u_s \\ w \end{Bmatrix} = \begin{Bmatrix} q_x \\ q_s \\ q \end{Bmatrix} \tag{2.14}$$

where L_{ij} are differential operators

$$L_{11} = A_{11}\frac{\partial^2}{\partial x^2} + 2A_{16}\frac{\partial^2}{\partial x \partial s} + A_{66}\frac{\partial^2}{\partial s^2} \tag{2.15a}$$

$$L_{12} = \left(A_{16} + \frac{1}{R}B_{16}\right)\frac{\partial^2}{\partial x^2} + \left(A_{12} + A_{66} + \frac{1}{R}B_{12} + \frac{1}{R}B_{66}\right)\frac{\partial^2}{\partial x \partial s} +$$

$$\left(A_{26} + \frac{1}{R}B_{26}\right)\frac{\partial^2}{\partial s^2} \tag{2.15b}$$

$$L_{13} = -B_{11}\frac{\partial^3}{\partial x^3} + \frac{1}{R}A_{12}\frac{\partial}{\partial x} - 3B_{16}\frac{\partial^3}{\partial x^2 \partial s} - (B_{12} + 2B_{66})\frac{\partial^3}{\partial x \partial s^2} + \frac{1}{R}A_{26}\frac{\partial}{\partial s} -$$

$$B_{26}\frac{\partial^3}{\partial s^3} \tag{2.15c}$$

$$L_{22} = \left(A_{66} + \frac{1}{R^2}D_{66} + \frac{2}{R}B_{66}\right)\frac{\partial^2}{\partial x^2} + 2\left(\frac{1}{R^2}D_{26} + \frac{2}{R}B_{26} + A_{26}\right)\frac{\partial^2}{\partial x \partial s} +$$

$$\left(A_{22} + \frac{2}{R}B_{22} + \frac{1}{R^2}D_{22}\right)\frac{\partial^2}{\partial s^2} \tag{2.15d}$$

$$L_{23} = \left(-B_{16} - \frac{1}{R}D_{16}\right)\frac{\partial^3}{\partial x^3} + \frac{1}{R}\left(\frac{1}{R}B_{26} + A_{26}\right)\frac{\partial}{\partial x} -$$

$$\left(\frac{2}{R}D_{66} + \frac{1}{R}D_{12} + B_{12} + 2B_{66}\right)\frac{\partial^3}{\partial x^2 \partial s} + \left(-3B_{26} - \frac{3}{R}D_{26}\right)\frac{\partial^3}{\partial x \partial s^2} +$$

$$\frac{1}{R}\left(A_{22} + \frac{1}{R}B_{22}\right)\frac{\partial}{\partial s} + \left(-B_{22} - \frac{1}{R}D_{22}\right)\frac{\partial^3}{\partial s^3} \tag{2.15e}$$

$$L_{33} = \frac{1}{R^2}A_{22} + D_{11}\frac{\partial^4}{\partial x^4} + 4D_{16}\frac{\partial^4}{\partial x^3 \partial s} + (2D_{12} + 4D_{66})\frac{\partial^4}{\partial x^2 \partial s^2} - \frac{2}{R}B_{12}\frac{\partial^2}{\partial x^2}$$

$$-\frac{4}{R}B_{26}\frac{\partial^2}{\partial x \partial s} + 4D_{26}\frac{\partial^4}{\partial x \partial s^3} - \frac{2}{R}B_{22}\frac{\partial^2}{\partial s^2} + D_{22}\frac{\partial^4}{\partial s^4} \tag{2.15f}$$

and A_{ij} are the extensional stiffnesses, B_{ij} are the bending-extensional coupling stiffnesses, and D_{ij} are the bending stiffnesses given by Eq. (2.8).

2.6 Single Uncoupled Governing Differential Equation

2.6.1 Isotropic Shells

This section reduces the system of three coupled differential equations for the isotropic cylindrical shell into a single eighth-order partial differential equation. For the case of radial loads only, $q_x = q_s = 0$ in Eq. (2.12) reducing the system to

$$\begin{bmatrix} L_{11} & L_{12} & L_{13} \\ L_{12} & L_{22} & L_{23} \\ L_{13} & L_{23} & L_{33} \end{bmatrix} \begin{Bmatrix} u_x \\ u_s \\ w \end{Bmatrix} = \begin{Bmatrix} 0 \\ 0 \\ q \end{Bmatrix} \tag{2.16}$$

The displacements in the x, s, and r direction, u_x, u_s, and w, can be written in terms of the potential function $\Phi(x, s)$ (Sharma et al., 1980)

$$u_x = (L_{12}L_{23} - L_{13}L_{22})\Phi(x, s) \tag{2.17a}$$

$$u_s = (L_{13}L_{21} - L_{23}L_{11})\Phi(x, s) \tag{2.17b}$$

$$w = (L_{11}L_{22} - L_{12}L_{21})\Phi(x, s) \tag{2.17c}$$

where the differential operators L_{ij} are presented in Eq. (2.13).

The first two equations in the system of governing differential equations of Eq. (2.16) are identically satisfied by Eq. (2.17). Substituting Eq. (2.17) into the third equation of Eq. (2.16) yields (Sharma et al., 1980)

$$\left(L_{11}L_{22}L_{33} - L_{12}{}^2L_{33} - L_{23}{}^2L_{11} + 2L_{13}L_{12}L_{23} - L_{13}{}^2L_{22}\right)\Phi(x, s) = q(x, s) \tag{2.18}$$

Expansion of Eq. (2.18) gives the eighth-order partial differential equation

$$F_{80}\frac{\partial^8\Phi}{\partial x^8} + F_{62}\frac{\partial^8\Phi}{\partial x^6\partial s^2} + F_{44}\frac{\partial^8\Phi}{\partial x^4\partial s^4} + F_{26}\frac{\partial^8\Phi}{\partial x^2\partial s^6} + F_{08}\frac{\partial^8\Phi}{\partial s^8} + F_{42}\frac{\partial^6\Phi}{\partial x^4\partial s^2} + F_{24}\frac{\partial^6\Phi}{\partial x^2\partial s^4} +$$

$$F_{06}\frac{\partial^6\Phi}{\partial s^6} + F_{40}\frac{\partial^4\Phi}{\partial x^4} + F_{22}\frac{\partial^4\Phi}{\partial x^2\partial s^2} + F_{04}\frac{\partial^4\Phi}{\partial s^4} = q(x, s) \tag{2.19}$$

The coefficients F_{ij} are

$$F_{80} = \frac{1-v}{2R^2}AD^2 + \frac{1-v}{2}A^2D \qquad (2.20\text{a})$$

$$F_{62} = \frac{(v-1)(v-5)}{4R^2}AD^2 + 2(1-v)A^2D \qquad (2.20\text{b})$$

$$F_{44} = \frac{(v-1)(v+3)}{2R^2}AD^2 + 3(1-v)A^2D \qquad (2.20\text{c})$$

$$F_{26} = \frac{(1-v)^2}{4R^2}AD^2 + 2(1-v)A^2D \qquad (2.20\text{d})$$

$$F_{08} = \frac{1-v}{2}A^2D \qquad (2.20\text{e})$$

$$F_{42} = \frac{(1-v)(v+2)}{R^2}A^2D \qquad (2.20\text{f})$$

$$F_{24} = \frac{(1-v)(v+3)}{R^2}A^2D \qquad (2.20\text{g})$$

$$F_{06} = \frac{(1-v)}{R^2}A^2D \qquad (2.20\text{h})$$

$$F_{40} = \frac{(v-1)^2(v+1)}{2R^4}A^2D + \frac{(v-1)^2(v+1)}{2R^2}A^3 \qquad (2.20\text{i})$$

$$F_{22} = \frac{(1-v)(3v+5)}{4R^4}A^2D \qquad (2.20\text{j})$$

$$F_{04} = \frac{(1-v)}{2R^4}A^2D \qquad (2.20\text{k})$$

Where A and D are the extensional and bending stiffness provided in Eq. (2.3).

2.6.2 Laminated Shells

This section reduces the system of three coupled differential equations for the laminated cylindrical shell into a single eighth-order partial differential equation. For the case of radial loads only, $q_x = q_s = 0$ in Eq. (2.14) reducing the system to

17

$$\begin{bmatrix} L_{11} & L_{12} & L_{13} \\ L_{12} & L_{22} & L_{23} \\ L_{13} & L_{23} & L_{33} \end{bmatrix} \begin{Bmatrix} u_x \\ u_s \\ w \end{Bmatrix} = \begin{Bmatrix} 0 \\ 0 \\ q \end{Bmatrix} \tag{2.21}$$

The displacements in the x, s, and r direction, u_x, u_s, and w, can be written in terms of the potential function $\Phi(x, s)$ (Sharma et al., 1980)

$$u_x = (L_{12}L_{23} - L_{13}L_{22})\Phi(x, s) \tag{2.22a}$$

$$u_s = (L_{13}L_{21} - L_{23}L_{11})\Phi(x, s) \tag{2.22b}$$

$$w = (L_{11}L_{22} - L_{12}L_{21})\Phi(x, s) \tag{2.22c}$$

where the differential operators L_{ij} are presented in Eq. (2.15).

The first two equations in the system of governing differential equations of Eq. (2.21) are identically satisfied by Eq. (2.22). Substituting Eq. (2.22) into the third equation of Eq. (2.21) yields (Sharma et al., 1980)

$$\left(L_{11}L_{22}L_{33} - L_{12}{}^2L_{33} - L_{23}{}^2L_{11} + 2L_{13}L_{12}L_{23} - L_{13}{}^2L_{22}\right)\Phi(x, s) = q(x, s) \tag{2.23}$$

Expansion of Eq. (2.23) gives the eighth-order partial differential equation

$$F_{80}\frac{\partial^8\Phi}{\partial x^8} + F_{71}\frac{\partial^8\Phi}{\partial x^7\partial s} + F_{62}\frac{\partial^8\Phi}{\partial x^6\partial s^2} + F_{53}\frac{\partial^8\Phi}{\partial x^5\partial s^3} + F_{44}\frac{\partial^8\Phi}{\partial x^4\partial s^4} + F_{35}\frac{\partial^8\Phi}{\partial x^3\partial s^5} + F_{26}\frac{\partial^8\Phi}{\partial x^2\partial s^6} +$$

$$F_{17}\frac{\partial^8\Phi}{\partial x\partial s^7} + F_{08}\frac{\partial^8\Phi}{\partial s^8} + F_{60}\frac{\partial^6\Phi}{\partial x^6} + F_{51}\frac{\partial^6\Phi}{\partial x^5\partial s} + F_{42}\frac{\partial^6\Phi}{\partial x^4\partial s^2} + F_{33}\frac{\partial^6\Phi}{\partial x^3\partial s^3} + F_{24}\frac{\partial^6\Phi}{\partial x^2\partial s^4} +$$

$$F_{15}\frac{\partial^6\Phi}{\partial x\partial s^5} + F_{06}\frac{\partial^6\Phi}{\partial s^6} + F_{40}\frac{\partial^4\Phi}{\partial x^4} + F_{31}\frac{\partial^4\Phi}{\partial x^3\partial s} + F_{22}\frac{\partial^4\Phi}{\partial x^2\partial s^2} + F_{13}\frac{\partial^4\Phi}{\partial x\partial s^3} + F_{04}\frac{\partial^4\Phi}{\partial s^4} = q(x, s)$$

$$\tag{2.24}$$

The coefficients F_{ij} for $i, j = 1, 3, 5, 7$ are not presented since they are condensed out of the solution for the analytical strip method; details are presented in Chapter 3. The coefficients F_{ij} for $i, j = 0, 2, 4, 6, 8$ are

$$F_{80} = A_{11}A_{66}D_{11} - A_{16}{}^2D_{11} + 2B_{11}A_{16}B_{16} - B_{16}{}^2A_{11} - B_{11}{}^2A_{66} + \tag{2.25a}$$

$$\frac{2}{R}\left(B_{16}{}^2B_{11} - A_{16}B_{16}D_{11} - D_{16}B_{16}A_{11} + B_{11}A_{16}D_{16} + A_{11}B_{66}D_{11} - \right.$$

$$B_{11}{}^2B_{66}) + \frac{1}{R^2}\left(A_{11}D_{66}D_{11} - B_{16}{}^2D_{11} - D_{16}{}^2A_{11} + 2B_{11}B_{16}D_{16} - B_{11}{}^2D_{66}\right)$$

$$
\begin{aligned}
F_{62} = \ & 2A_{11}A_{66}D_{12} - 2A_{16}{}^2D_{12} - 4A_{16}{}^2D_{66} + 4A_{11}A_{66}D_{66} + A_{11}A_{22}D_{11} + \\
& 8A_{11}A_{26}D_{16} + 2A_{16}A_{26}D_{11} - 2A_{12}A_{66}D_{11} - 8A_{12}A_{16}D_{16} + \\
& 6B_{11}A_{16}B_{26} - 6B_{16}B_{26}A_{11} - 10B_{11}A_{26}B_{16} - A_{12}{}^2D_{11} + 6B_{16}{}^2A_{12} - \\
& 4B_{16}{}^2A_{66} - B_{11}{}^2A_{22} - B_{12}{}^2A_{11} - 4B_{12}B_{66}A_{11} + 2B_{12}B_{11}A_{12} + \\
& 4B_{12}B_{16}A_{16} - 4B_{66}{}^2A_{11} + 8B_{66}B_{16}A_{16} + 4B_{11}A_{12}B_{66} + \\
& \frac{2}{R}\big(A_{12}B_{12}D_{11} + 3B_{26}A_{16}D_{11} + 5A_{11}B_{26}D_{16} + A_{11}B_{22}D_{11} - \\
& 2A_{16}B_{16}D_{66} - A_{12}B_{16}D_{16} - A_{16}B_{16}D_{12} - A_{26}B_{16}D_{11} - \\
& 2A_{66}B_{16}D_{16} - 3D_{26}B_{16}A_{11} + 2B_{11}A_{12}D_{66} + B_{11}A_{12}D_{12} + \\
& 3B_{11}A_{16}D_{26} - 8B_{11}B_{16}B_{26} + B_{11}A_{26}D_{16} + 2B_{11}A_{66}D_{66} + \\
& B_{11}A_{66}D_{12} - B_{11}{}^2B_{22} - 5A_{16}B_{12}D_{16} - A_{66}B_{12}D_{11} + B_{12}{}^2B_{11} + \\
& 7B_{16}{}^2B_{12} + B_{11}B_{12}B_{66} - 2B_{12}A_{11}D_{66} - D_{12}B_{12}A_{11} + 2B_{16}{}^2B_{66} - \\
& A_{12}B_{66}D_{11} + 2A_{16}B_{66}D_{16} - 2B_{66}{}^2B_{11}\big) + \frac{1}{R^2}\big(4B_{16}{}^2D_{12} - \\
& 2B_{26}B_{16}D_{11} - B_{16}{}^2D_{66} - D_{16}{}^2A_{66} - D_{12}{}^2A_{11} + 2A_{11}D_{26}D_{16} - \\
& 2A_{11}D_{66}D_{12} + 4A_{16}D_{26}D_{11} + A_{11}D_{22}D_{11} + A_{66}D_{66}D_{11} - \\
& 4D_{12}D_{16}A_{16} - 6B_{11}B_{16}D_{26} + 2B_{11}B_{26}D_{16} - B_{11}{}^2D_{22} - B_{12}{}^2D_{11} + \\
& 2B_{12}B_{66}D_{11} + 2B_{11}B_{12}D_{66} + 2B_{11}B_{12}D_{12} - B_{66}{}^2D_{11} + \\
& 2B_{11}B_{66}D_{12} + 2B_{16}B_{66}D_{16}\big)
\end{aligned}
$$

$\qquad\qquad\qquad$ (2.25b)

$$
\begin{aligned}
F_{44} = \ & A_{11}A_{66}D_{22} - 4A_{12}{}^2D_{66} - 2A_{12}{}^2D_{12} - A_{16}{}^2D_{22} + 2A_{11}A_{22}D_{12} + \\
& 4A_{11}A_{22}D_{66} + 8A_{16}A_{22}D_{16} + A_{66}A_{22}D_{11} - 4A_{12}A_{66}D_{12} - \\
& 8A_{12}A_{66}D_{66} + 8A_{11}A_{26}D_{26} + A_{16}A_{26}D_{12} + 8A_{16}A_{26}D_{66} - \\
& 8A_{12}A_{26}D_{16} + 8B_{26}B_{16}A_{66} + 2B_{26}B_{11}A_{26} - 8A_{12}A_{16}D_{26} + \\
& 20B_{16}A_{12}B_{26} + 2B_{16}B_{22}A_{16} + 2B_{11}A_{12}B_{22} + 2B_{11}A_{66}B_{22} - \\
& 9B_{16}{}^2A_{22} - A_{26}{}^2D_{11} - 9B_{26}{}^2A_{11} + 2B_{12}{}^2A_{12} - 4B_{26}B_{12}A_{16} - \\
& 2B_{22}B_{12}A_{11} - 4B_{12}A_{26}B_{16} + 8B_{12}A_{12}B_{66} - 2B_{11}B_{12}A_{22} +
\end{aligned}
$$

$\qquad\qquad\qquad$ (2.25c)

$$8B_{66}{}^2A_{12} - 8B_{26}B_{66}A_{16} - 4B_{22}B_{66}A_{11} - 8B_{16}A_{26}B_{66} -$$

$$4B_{11}B_{66}A_{22} + \frac{2}{R}\big(2B_{26}A_{66}D_{16} - B_{26}A_{26}D_{11} - B_{26}{}^2B_{11} - 6B_{16}{}^2B_{22} +$$

$$A_{11}B_{22}D_{12} - A_{11}B_{26}D_{26} + 2A_{11}B_{22}D_{66} + 6A_{16}B_{22}D_{16} +$$

$$A_{66}B_{22}D_{11} + 5A_{12}B_{16}D_{26} + A_{26}B_{16}D_{12} + 2A_{26}B_{16}D_{66} -$$

$$3B_{26}A_{12}D_{16} + 2B_{26}A_{16}D_{66} + B_{26}A_{16}D_{12} + 2A_{66}B_{16}D_{26} +$$

$$B_{11}A_{12}D_{22} + 3B_{11}A_{26}D_{26} + B_{11}A_{66}D_{22} - B_{12}A_{12}D_{12} -$$

$$2B_{12}A_{12}D_{66} - 7B_{12}A_{16}D_{26} - 3B_{12}A_{26}D_{16} - 2B_{12}A_{66}D_{12} -$$

$$4B_{12}A_{66}D_{66} - D_{22}B_{12}A_{11} - B_{11}B_{12}B_{22} + 6B_{12}B_{16}B_{26} + 4B_{12}{}^2B_{66} +$$

$$4B_{66}{}^2B_{12} + B_{12}{}^3 - 2B_{66}A_{16}D_{26} - 2B_{66}A_{26}D_{16} - A_{11}B_{66}D_{22} -$$

$$3B_{11}B_{66}B_{22} - 4B_{16}B_{26}B_{66}\big) + \frac{1}{R^2}\big(4B_{26}B_{16}D_{12} + 2B_{26}B_{16}D_{66} -$$

$$B_{26}{}^2D_{11} - D_{26}{}^2A_{11} - 4B_{16}{}^2D_{22} - D_{12}{}^2A_{66} + A_{11}D_{66}D_{22} -$$

$$4A_{16}D_{26}D_{12} - 2A_{66}D_{66}D_{12} + 4A_{16}D_{22}D_{16} + 2A_{66}D_{26}D_{16} +$$

$$A_{66}D_{22}D_{11} + 2B_{26}B_{11}D_{26} - B_{12}{}^2D_{66} + 4B_{12}B_{16}D_{26} - 4B_{12}B_{26}D_{16} +$$

$$2B_{12}B_{66}D_{12} + 2B_{66}{}^2D_{12} - 2B_{16}B_{66}D_{26} - 2B_{26}B_{66}D_{16} -$$

$$2B_{11}B_{66}D_{22}\big)$$

$$F_{26} = A_{11}A_{22}D_{22} - A_{12}{}^2D_{22} + 2A_{16}A_{26}D_{22} + 8A_{16}A_{22}D_{26} + 2A_{66}A_{22}D_{12} +$$

$$4A_{66}A_{22}D_{66} - 2A_{12}A_{66}D_{22} - 8A_{12}A_{26}D_{26} - 6B_{26}B_{16}A_{22} +$$

$$6B_{16}A_{26}B_{22} - 10B_{26}B_{22}A_{16} + 6B_{26}{}^2A_{12} - 2A_{26}{}^2D_{12} - 4A_{26}{}^2D_{66} -$$

$$4B_{26}{}^2A_{66} - B_{22}{}^2A_{11} - B_{12}{}^2A_{22} + 2B_{12}A_{12}B_{22} + 4B_{12}B_{26}A_{26} -$$

$$4B_{12}B_{66}A_{22} + 8B_{66}B_{26}A_{26} - 4B_{66}{}^2A_{22} + 4B_{66}A_{12}B_{22} +$$

$$\frac{2}{R}\big(2A_{16}B_{22}D_{26} - 2B_{26}A_{16}D_{22} - 2B_{26}A_{26}D_{66} - 2B_{26}A_{66}D_{26} -$$

$$B_{26}A_{26}D_{12} + 2A_{66}B_{22}D_{66} + A_{66}B_{22}D_{12} + 2A_{26}B_{16}D_{22} -$$

$$B_{26}A_{12}D_{26} - 2B_{26}B_{16}B_{22} - A_{66}B_{12}D_{22} - A_{26}B_{12}D_{26} + 3B_{26}{}^2B_{12} -$$

$$B_{12}B_{66}B_{22} + A_{12}B_{66}D_{22} + 2A_{26}B_{66}D_{26} + 2B_{26}{}^2B_{66} - 2B_{66}{}^2B_{22}\big) +$$

$$\frac{1}{R^2}\big(A_{66}D_{66}D_{22} - B_{26}{}^2D_{66} - D_{26}{}^2A_{66} - B_{66}{}^2D_{22} + 2B_{26}B_{66}D_{26}\big)$$

(2.25d)

$$F_{08} = A_{66}A_{22}D_{22} - B_{26}{}^2A_{22} - A_{26}{}^2D_{22} - B_{22}{}^2A_{66} + 2B_{22}B_{26}A_{26} \qquad (2.25e)$$

$$\begin{aligned}
F_{60} = {}& \frac{2}{R}\big(A_{12}B_{11}A_{66} + A_{26}B_{16}A_{11} - B_{11}A_{16}A_{26} - A_{12}A_{16}B_{16} + A_{16}{}^2B_{12} - \\
& A_{11}A_{66}B_{12}\big) + \frac{2}{R^2}\big(B_{26}B_{16}A_{11} + D_{16}A_{26}A_{11} - B_{11}A_{16}B_{26} - \\
& B_{11}B_{16}A_{26} - A_{12}A_{16}D_{16} - B_{16}{}^2A_{12} + 2A_{16}B_{16}B_{12} - 2A_{11}B_{66}B_{12} + \\
& 2B_{11}A_{12}B_{66}\big) + \frac{2}{R^3}\big(A_{12}B_{11}D_{66} + B_{26}D_{16}A_{11} - B_{11}B_{16}B_{26} - \\
& A_{12}B_{16}D_{16} - A_{11}D_{66}B_{12} + B_{16}{}^2B_{12}\big)
\end{aligned} \qquad (2.25f)$$

$$\begin{aligned}
F_{42} = {}& \frac{2}{R}\big(A_{16}{}^2B_{22} + A_{26}{}^2B_{11} + A_{12}B_{16}A_{26} - A_{11}A_{66}B_{22} - A_{11}A_{26}B_{26} + \\
& A_{12}A_{16}B_{26} - A_{22}B_{16}A_{16} - B_{11}A_{66}A_{22} - A_{12}{}^2D_{12} + 2A_{12}A_{66}B_{12} - \\
& 2A_{16}A_{26}B_{12} - 2A_{12}{}^2B_{66} + 2A_{22}B_{66}A_{11}\big) + \frac{2}{R^2}\big(A_{12}B_{11}B_{22} + \\
& 9A_{12}B_{16}B_{26} - 5B_{26}{}^2A_{11} - 3B_{16}{}^2A_{22} + A_{16}B_{16}B_{22} + 2A_{66}B_{16}B_{26} + \\
& A_{22}D_{12}A_{11} + 2A_{22}D_{66}A_{11} + 2A_{22}D_{16}A_{16} + 2D_{66}A_{26}A_{16} + \\
& D_{12}A_{26}A_{16} + 3D_{26}A_{26}A_{11} + 2B_{11}A_{26}B_{26} - B_{11}A_{66}B_{22} - \\
& 3A_{12}A_{16}D_{26} - 2A_{12}A_{66}D_{66} - A_{12}A_{66}D_{12} - 2A_{12}A_{26}D_{16} - \\
& 2A_{12}{}^2D_{66} - A_{12}{}^2D_{12} - 4A_{26}B_{16}B_{12} + 2B_{12}{}^2A_{66} - B_{11}B_{12}A_{22} - \\
& A_{11}B_{22}B_{12} + B_{12}{}^2A_{12} + B_{66}A_{12}B_{12} - B_{26}B_{12}A_{16} + 4B_{66}{}^2A_{12} - \\
& 2A_{16}B_{66}B_{26} - 2B_{66}A_{26}B_{16} - B_{11}B_{66}A_{22}\big) + \frac{2}{R^3}\big(A_{12}B_{11}D_{22} + \\
& 3A_{12}B_{16}D_{26} - 2B_{16}{}^2B_{22} - A_{11}D_{26}B_{26} + A_{11}D_{66}B_{22} + B_{22}D_{12}A_{11} + \\
& 2B_{22}D_{16}A_{16} + 2B_{26}D_{12}A_{16} + B_{26}D_{16}A_{66} - A_{12}B_{26}D_{16} + A_{26}B_{16}D_{66} - \\
& A_{26}B_{16}D_{12} - B_{26}{}^2B_{11} + 2B_{11}A_{26}D_{26} - D_{12}A_{12}B_{12} + B_{12}{}^3 - \\
& B_{12}A_{12}D_{66} - A_{66}D_{66}B_{12} + B_{66}{}^2B_{12} - A_{11}D_{22}B_{12} + 2B_{12}{}^2B_{66} - \\
& 4A_{16}D_{26}B_{12} + 2B_{26}B_{16}B_{12} - D_{16}B_{12}A_{26} - B_{11}B_{12}B_{22} - D_{12}A_{12}B_{66} - \\
& B_{11}B_{66}B_{22} - D_{16}B_{66}A_{26} - B_{16}B_{66}B_{26}\big)
\end{aligned} \qquad (2.25g)$$

$$F_{24} = \frac{2}{R}\big(A_{16}A_{22}B_{26} - A_{12}B_{26}A_{26} - A_{16}A_{26}B_{22} + A_{12}A_{66}B_{22} - A_{66}A_{22}B_{12} + \qquad (2.25h)$$

$$A_{26}{}^2 B_{12}) + \frac{2}{R^2}\big(4B_{26}{}^2 A_{12} - 2B_{26}{}^2 A_{66} - B_{22}{}^2 A_{11} + 4A_{26}B_{16}B_{22} -$$

$$7B_{26}A_{16}B_{22} + A_{22}D_{12}A_{66} + 6A_{22}D_{26}A_{16} + 2A_{22}D_{66}A_{66} +$$

$$A_{22}D_{22}A_{11} + D_{22}A_{26}A_{16} - 4B_{16}B_{26}A_{22} - 6A_{12}A_{26}D_{26} -$$

$$A_{12}A_{66}D_{22} - A_{12}{}^2 D_{22} - A_{26}{}^2 D_{12} - 2A_{26}{}^2 D_{66} + 2A_{12}B_{22}B_{12} +$$

$$3A_{26}B_{12}B_{26} - 3B_{12}B_{66}A_{22} - B_{12}{}^2 A_{22} + 3A_{12}B_{66}B_{22} +$$

$$4A_{26}B_{66}B_{26} - 2B_{66}{}^2 A_{22}\big) + \frac{2}{R^3}\big(2A_{16}D_{26}B_{22} - 2B_{26}B_{16}B_{22} -$$

$$A_{12}B_{26}D_{26} + 2A_{16}D_{26}B_{22} - 2A_{16}D_{22}B_{26} - A_{66}D_{26}B_{26} +$$

$$A_{66}D_{66}B_{22} - B_{26}A_{26}D_{66} + B_{22}D_{12}A_{66} + 2A_{26}B_{16}D_{22} - A_{26}B_{26}D_{12} -$$

$$A_{66}D_{22}B_{12} - B_{12}A_{26}D_{26} + 3B_{26}{}^2 B_{12} - B_{12}B_{66}B_{22} - B_{66}{}^2 B_{22} +$$

$$B_{26}{}^2 B_{66} + D_{26}B_{66}A_{26} + D_{22}A_{12}B_{66}\big)$$

$$F_{06} = \frac{2}{R^2}\big(2B_{26}A_{26}B_{22} - B_{22}{}^2 A_{66} + A_{22}D_{22}A_{66} - A_{26}{}^2 D_{22} - B_{26}{}^2 A_{22}\big) \qquad (2.25\text{i})$$

$$F_{40} = \frac{1}{R^2}\big(A_{11}A_{66}A_{22} - A_{12}{}^2 A_{66} - A_{16}{}^2 A_{22} - A_{26}{}^2 A_{11} + 2A_{12}A_{16}A_{26}\big) +$$

$$\frac{2}{R^3}\big(A_{12}A_{16}B_{26} - A_{16}B_{16}A_{22} - B_{26}A_{26}A_{11} + A_{12}B_{16}A_{26} +$$

$$A_{11}B_{66}A_{22} - A_{12}{}^2 B_{66}\big) + \frac{1}{R^4}\big(A_{11}D_{66}A_{22} - A_{12}{}^2 D_{66} - B_{16}{}^2 A_{22} -$$

$$B_{26}{}^2 A_{11} + 2A_{12}B_{16}B_{26}\big) \qquad (2.25\text{j})$$

$$F_{22} = \frac{2}{R^3}\big(B_{26}A_{16}A_{22} - A_{12}A_{26}B_{26} - B_{22}A_{26}A_{16} + A_{12}A_{66}B_{22} -$$

$$A_{66}B_{12}A_{22} + A_{26}{}^2 B_{12}\big) + \frac{1}{R^4}\big(A_{11}D_{22}A_{22} - 2B_{26}B_{16}A_{22} - A_{12}{}^2 D_{22} -$$

$$B_{22}{}^2 A_{11} - B_{26}{}^2 A_{66} - 4A_{12}A_{26}D_{26} + 4A_{16}D_{26}A_{22} + A_{66}D_{66}A_{22} -$$

$$4B_{26}B_{22}A_{16} + 2A_{26}B_{16}B_{22} + 2B_{26}{}^2 A_{12} - A_{26}{}^2 D_{66} + 2B_{22}A_{12}B_{12} +$$

$$2B_{26}A_{26}B_{12} - B_{12}{}^2 A_{22} - 2B_{12}B_{66}A_{22} + 2B_{26}A_{26}B_{66} +$$

$$2B_{22}A_{12}B_{66} - B_{66}{}^2 A_{22}\big) \qquad (2.25\text{k})$$

$$F_{04} = \frac{1}{R^4}\big(A_{66}D_{22}A_{22} - B_{22}{}^2 A_{66} + 2A_{26}B_{26}B_{22} - A_{26}{}^2 D_{22} - B_{26}{}^2 A_{22}\big) \qquad (2.25\text{l})$$

where A_{ij} are the extensional stiffnesses, B_{ij} are the bending-extensional coupling stiffnesses, and D_{ij} are the bending stiffnesses given by Eq. (2.8)

2.7 Displacement Equations

2.7.1 Isotropic Shells

The displacement equations of Eq. (2.17) can be expressed in terms of the potential function $\Phi(x, s)$. The longitudinal displacement is

$$u_x = a_3 \frac{\partial^5 \Phi(x,s)}{\partial x^3 \partial s^2} + a_5 \frac{\partial^5 \Phi(x,s)}{\partial x \partial s^4} + a_7 \frac{\partial^3 \Phi(x,s)}{\partial x^3} + a_9 \frac{\partial^3 \Phi(x,s)}{\partial x \partial s^2} \qquad (2.26)$$

where

$$a_3 = -\frac{(1+v)}{2R} AD \qquad (2.27a)$$

$$a_5 = -\frac{2(1+v)}{R} AD \qquad (2.27b)$$

$$a_7 = -\frac{v(1-v)}{2R} A^2 - \frac{v(1-v)}{2R^3} AD \qquad (2.27c)$$

$$a_9 = \frac{(1-v)}{2R} A^2 - \frac{v}{R^3} AD \qquad (2.27d)$$

The circumferential displacement is

$$u_s = a_{12} \frac{\partial^5 \Phi(x,s)}{\partial x^4 \partial s} + a_{14} \frac{\partial^5 \Phi(x,s)}{\partial x^2 \partial s^3} + a_{16} \frac{\partial^5 \Phi(x,s)}{\partial s^5} + a_{18} \frac{\partial^3 \Phi(x,s)}{\partial x^2 \partial s} + a_{20} \frac{\partial^3 \Phi(x,s)}{\partial s^3} \qquad (2.28)$$

where

$$a_{12} = \frac{1}{R} AD \qquad (2.29a)$$

$$a_{14} = \frac{(3-v)}{2R} AD \qquad (2.29b)$$

$$a_{16} = \frac{(1-v)}{2R} AD \qquad (2.29c)$$

$$a_{18} = -\frac{(1-v)}{R}A^2 \tag{2.29d}$$

$$a_{20} = -\frac{(1-v)}{2R}A^2 \tag{2.29e}$$

The radial displacement is

$$w = a_{21}\frac{\partial^4\Phi(x,s)}{\partial x^4} + a_{23}\frac{\partial^4\Phi(x,s)}{\partial x^2\partial s^2} + a_{25}\frac{\partial^4\Phi(x,s)}{\partial s^4} \tag{2.30}$$

where

$$a_{21} = \frac{(1-v)}{2}A^2 + \frac{(1-v)}{2R^2}AD \tag{2.31a}$$

$$a_{23} = (1-v)A^2 + \frac{4+(1-v)^2}{4R^2}AD \tag{2.31b}$$

$$a_{25} = \frac{(1-v)}{2}A^2 + \frac{(1-v)}{2R^2}AD \tag{2.31c}$$

The extensional and bending stiffness, A and D, are provided in Eq. (2.3).

2.7.2 Laminated Shells

The displacement equations of Eq. (2.22) can be expressed in terms of the potential function $\Phi(x,s)$. The longitudinal displacement is

$$u_x = a_1\frac{\partial^5\Phi(x,s)}{\partial x^5} + a_2\frac{\partial^5\Phi(x,s)}{\partial x^4\partial s} + a_3\frac{\partial^5\Phi(x,s)}{\partial x^3\partial s^2} + a_4\frac{\partial^5\Phi(x,s)}{\partial x^2\partial s^3} + a_5\frac{\partial^5\Phi(x,s)}{\partial x\partial s^4} + a_6\frac{\partial^5\Phi(x,s)}{\partial s^5} +$$
$$a_7\frac{\partial^3\Phi(x,s)}{\partial x^3} + a_8\frac{\partial^3\Phi(x,s)}{\partial x^2\partial s} + a_9\frac{\partial^3\Phi(x,s)}{\partial x\partial s^2} + a_{10}\frac{\partial^3\Phi(x,s)}{\partial s^3} \tag{2.32}$$

where

$$a_1 = B_{11}A_{66} + \frac{1}{R^2}B_{11}D_{66} - A_{16}B_{16} - \frac{1}{R}A_{16}D_{16} - \frac{1}{R^2}B_{16}D_{16} - \frac{1}{R}B_{16}{}^2 +$$
$$\frac{2}{R}B_{11}B_{66} \tag{2.33a}$$

24

$$a_2 = 2B_{11}A_{26} - \frac{1}{R}A_{12}D_{16} - \frac{2}{R}A_{16}D_{66} - \frac{1}{R}A_{16}D_{12} + \frac{1}{R^2}B_{16}D_{66} - \frac{1}{R^2}B_{16}D_{12} -$$

$$\frac{1}{R}A_{66}D_{16} + \frac{2}{R^2}B_{11}D_{26} + \frac{4}{R}B_{11}B_{26} - A_{12}B_{16} + 2A_{66}B_{16} + \frac{2}{R}B_{12}B_{16} - \qquad (2.33\text{b})$$

$$A_{16}B_{12} - \frac{1}{R^2}B_{66}D_{16} - \frac{1}{R^2}B_{12}D_{16} + \frac{3}{R}B_{16}B_{66} - 2A_{16}B_{66}$$

$$a_3 = 5A_{26}B_{16} - \frac{2}{R}A_{12}D_{66} - \frac{1}{R}A_{12}D_{12} - \frac{2}{R}A_{66}D_{66} - \frac{1}{R}A_{66}D_{12} + B_{11}A_{22} +$$

$$\frac{2}{R}B_{11}B_{22} + \frac{1}{R^2}B_{11}D_{22} - \frac{6}{R}A_{16}D_{26} + \frac{8}{R}B_{16}B_{26} + \frac{3}{R^2}B_{16}D_{26} -$$

$$\frac{1}{R}A_{26}D_{16} - \frac{1}{R^2}B_{26}D_{16} - 3A_{16}B_{26} - \frac{1}{R^2}B_{12}D_{12} - \frac{1}{R^2}B_{12}D_{66} - \qquad (2.33\text{c})$$

$$\frac{1}{R}B_{12}B_{66} - \frac{1}{R}{B_{12}}^2 - \frac{1}{R^2}B_{66}D_{12} + \frac{2}{R}{B_{66}}^2 - A_{12}B_{12} - 2A_{12}B_{66}$$

$$a_4 = 3B_{16}A_{22} - \frac{3}{R}A_{12}D_{26} - \frac{1}{R}A_{16}D_{22} + \frac{5}{R}B_{16}B_{22} + \frac{2}{R^2}B_{16}D_{22} - \frac{2}{R}A_{26}D_{66} -$$

$$\frac{1}{R}A_{26}D_{12} - \frac{3}{R}A_{66}D_{26} - \frac{1}{R^2}B_{26}D_{66} - \frac{1}{R^2}B_{26}D_{12} - 3A_{12}B_{26} - A_{16}B_{22} - \qquad (2.33\text{d})$$

$$2A_{66}B_{26} + 2A_{26}B_{66} + \frac{1}{R^2}B_{66}D_{26} - \frac{1}{R^2}B_{12}D_{26} + A_{26}B_{12} + \frac{5}{R}B_{26}B_{66}$$

$$a_5 = \frac{1}{R}{B_{26}}^2 - A_{12}B_{22} - \frac{1}{R}A_{12}D_{22} - A_{66}B_{22} - \frac{1}{R}A_{66}D_{22} - \frac{3}{R}A_{26}D_{26} -$$

$$\frac{1}{R^2}B_{26}D_{26} - A_{26}B_{26} + B_{12}A_{22} + 2B_{66}A_{22} + \frac{3}{R}B_{66}B_{22} + \frac{1}{R}B_{12}B_{22} + \qquad (2.33\text{e})$$

$$\frac{1}{R^2}B_{66}D_{22}$$

$$a_6 = B_{26}A_{22} - \frac{1}{R}A_{26}D_{22} + \frac{1}{R}B_{26}B_{22} - A_{26}B_{22} \qquad (2.33\text{f})$$

$$a_7 = \frac{1}{R^2}B_{16}A_{26} - \frac{1}{R}A_{12}A_{66} - \frac{1}{R^3}A_{12}D_{66} + \frac{1}{R^2}A_{16}B_{26} + \frac{1}{R}A_{16}A_{26} +$$

$$\frac{1}{R^3}B_{16}B_{26} - \frac{2}{R^2}A_{12}B_{66} \qquad (2.33\text{g})$$

$$a_8 = \frac{1}{R}A_{16}A_{22} - \frac{3}{R^2}A_{12}B_{26} - \frac{1}{R}A_{12}A_{26} + \frac{1}{R^2}A_{16}B_{22} + \frac{1}{R^2}B_{16}A_{22} +$$

$$\frac{1}{R^3}B_{16}B_{22} + \frac{1}{R^2}A_{66}B_{26} - \frac{2}{R^3}A_{12}D_{26} - \frac{1}{R^3}A_{26}D_{66} + \frac{1}{R^3}B_{12}B_{26} + \qquad (2.33\text{h})$$

$$\frac{1}{R^2}B_{12}A_{26} + \frac{1}{R^3}B_{66}B_{26} - \frac{1}{R^2}B_{66}A_{26}$$

$$a_9 = \frac{1}{R^3}B_{26}{}^2 - \frac{1}{R^2}A_{12}B_{22} + \frac{1}{R}A_{66}A_{22} + \frac{1}{R^2}A_{66}B_{22} - \frac{1}{R^3}A_{12}D_{22} -$$
$$\frac{2}{R^2}A_{26}B_{26} - \frac{1}{R^3}A_{26}D_{26} - \frac{1}{R}A_{26}{}^2 + \frac{1}{R^2}B_{66}A_{22} + \frac{1}{R^3}B_{66}B_{22} + \qquad (2.33\text{i})$$
$$\frac{1}{R^2}B_{12}A_{22} + \frac{1}{R^3}B_{12}B_{22}$$

$$a_{10} = \frac{1}{R^2}B_{26}A_{22} - \frac{1}{R^2}A_{26}B_{22} + \frac{1}{R^3}B_{26}B_{22} - \frac{1}{R^3}A_{26}D_{22} \qquad (2.33\text{j})$$

The circumferential displacement is

$$u_s = a_{11}\frac{\partial^5\Phi(x,s)}{\partial x^5} + a_{12}\frac{\partial^5\Phi(x,s)}{\partial x^4\partial s} + a_{13}\frac{\partial^5\Phi(x,s)}{\partial x^3\partial s^2} + a_{14}\frac{\partial^5\Phi(x,s)}{\partial x^2\partial s^3} + a_{15}\frac{\partial^5\Phi(x,s)}{\partial x\partial s^4} +$$
$$a_{16}\frac{\partial^5\Phi(x,s)}{\partial s^5} + a_{17}\frac{\partial^3\Phi(x,s)}{\partial x^3} + a_{18}\frac{\partial^3\Phi(x,s)}{\partial x^2\partial s} + a_{19}\frac{\partial^3\Phi(x,s)}{\partial x\partial s^2} + a_{20}\frac{\partial^3\Phi(x,s)}{\partial s^3} \qquad (2.34)$$

where

$$a_{11} = B_{16}A_{11} - \frac{1}{R}B_{11}B_{16} + \frac{1}{R}D_{16}A_{11} - B_{11}A_{16} \qquad (2.35\text{a})$$

$$a_{12} = \frac{1}{R}D_{12}A_{11} - B_{11}A_{12} - B_{11}A_{66} + \frac{2}{R}D_{66}A_{11} + \frac{2}{R}D_{16}A_{16} - B_{16}A_{16} -$$
$$\frac{3}{R}B_{16}{}^2 - \frac{1}{R}B_{11}B_{12} + B_{12}A_{11} + 2B_{66}A_{11} - \frac{1}{R}B_{11}B_{66} \qquad (2.35\text{b})$$

$$a_{13} = 3B_{26}A_{11} - \frac{1}{R}B_{11}B_{26} + \frac{4}{R}D_{66}A_{16} + \frac{2}{R}D_{12}A_{16} + \frac{1}{R}D_{16}A_{66} +$$
$$\frac{3}{R}D_{26}A_{11} - B_{11}A_{26} - 3B_{16}A_{12} - 2B_{16}A_{66} - \frac{5}{R}B_{16}B_{66} + B_{12}A_{16} - \qquad (2.35\text{c})$$
$$\frac{4}{R}B_{12}B_{16} + 2B_{66}A_{16}$$

$$a_{14} = B_{22}A_{11} + \frac{2}{R}D_{66}A_{66} + \frac{1}{R}D_{12}A_{66} + \frac{1}{R}D_{22}A_{11} - \frac{4}{R}B_{16}B_{26} + \frac{6}{R}D_{26}A_{16} - \qquad (2.35\text{d})$$
$$3B_{16}A_{26} + 5B_{26}A_{16} - B_{12}A_{12} - \frac{3}{R}B_{12}B_{66} - 2B_{66}A_{12} - \frac{2}{R}B_{66}{}^2 -$$

$$\frac{1}{R}B_{12}{}^2$$

$$a_{15} = \frac{2}{R}D_{22}A_{16} + \frac{3}{R}D_{26}A_{66} - B_{26}A_{12} + 2B_{26}A_{66} + 2B_{22}A_{16} - B_{12}A_{26} -$$

$$\frac{2}{R}B_{12}B_{26} - 2B_{66}A_{26} - \frac{3}{R}B_{26}B_{66}$$

(2.35e)

$$a_{16} = B_{22}A_{66} + \frac{1}{R}D_{22}A_{66} - B_{26}A_{26} - \frac{1}{R}B_{26}{}^2$$

(2.35f)

$$a_{17} = \frac{1}{R}A_{12}A_{16} + \frac{1}{R^2}A_{12}B_{16} - \frac{1}{R^2}B_{26}A_{11} - \frac{1}{R}A_{26}A_{11}$$

(2.35g)

$$a_{18} = \frac{1}{R}A_{12}{}^2 + \frac{1}{R}A_{12}A_{66} - \frac{1}{R}A_{22}A_{11} - \frac{1}{R^2}B_{22}A_{11} - \frac{1}{R}A_{26}A_{16} + \frac{1}{R^2}A_{26}B_{16} -$$

$$\frac{2}{R^2}B_{26}A_{16} + \frac{1}{R^2}A_{12}B_{66} + \frac{1}{R^2}A_{12}B_{12}$$

(2.35h)

$$a_{19} = \frac{2}{R}A_{12}A_{26} + \frac{1}{R^2}A_{12}B_{26} - \frac{2}{R}A_{22}A_{16} - \frac{1}{R^2}B_{26}A_{66} - \frac{2}{R^2}B_{22}A_{16} +$$

$$\frac{1}{R^2}A_{26}B_{12} + \frac{1}{R^2}A_{26}B_{66}$$

(2.35i)

$$a_{20} = \frac{1}{R}A_{26}{}^2 - \frac{1}{R}A_{22}A_{66} - \frac{1}{R^2}B_{22}A_{66} + \frac{1}{R^2}A_{26}B_{26}$$

(2.35j)

The radial displacement is

$$w = a_{21}\frac{\partial^4\Phi(x,s)}{\partial x^4} + a_{22}\frac{\partial^4\Phi(x,s)}{\partial x^3\partial s} + a_{23}\frac{\partial^4\Phi(x,s)}{\partial x^2\partial s^2} + a_{24}\frac{\partial^4\Phi(x,s)}{\partial x\partial s^3} + a_{25}\frac{\partial^4\Phi(x,s)}{\partial s^4}$$

(2.36)

where

$$a_{21} = A_{11}A_{66} + \frac{1}{R^2}A_{11}D_{66} - \frac{2}{R}A_{16}B_{16} - \frac{1}{R^2}B_{16}{}^2 - A_{16}{}^2 + \frac{2}{R}A_{11}B_{66}$$

(2.37a)

$$a_{22} = \frac{2}{R^2}A_{11}D_{26} + \frac{4}{R}A_{11}B_{26} + \frac{2}{R^2}A_{16}D_{66} - \frac{2}{R}A_{12}B_{16} - \frac{2}{R}B_{16}A_{66} +$$

(2.37b)

$$2A_{11}A_{26} - 2A_{12}A_{16} - \frac{2}{R}A_{16}B_{12} - \frac{2}{R^2}B_{12}B_{16} + \frac{2}{R}A_{16}B_{33} - \frac{2}{R^2}B_{16}B_{66}$$

$$a_{23} = A_{11}A_{22} + \frac{2}{R}A_{11}B_{22} + \frac{1}{R^2}A_{11}D_{22} + \frac{1}{R^2}A_{66}D_{66} - A_{12}{}^2 - 2A_{12}A_{66} +$$

$$\frac{4}{R^2}A_{16}D_{26} + \frac{6}{R}A_{16}B_{26} - \frac{2}{R}B_{16}A_{26} - \frac{2}{R^2}B_{16}B_{26} + 2A_{16}A_{26} - \qquad (2.37c)$$

$$\frac{2}{R}A_{12}B_{12} - \frac{2}{R^2}B_{12}B_{66} - \frac{2}{R}B_{12}A_{66} - \frac{1}{R^2}B_{12}{}^2 - \frac{1}{R^2}B_{66}{}^2 - \frac{2}{R}A_{12}B_{66}$$

$$a_{24} = \frac{4}{R}A_{16}B_{22} + \frac{2}{R^2}A_{16}D_{22} + \frac{2}{R^2}A_{66}D_{26} + \frac{2}{R}A_{66}B_{26} - \frac{2}{R}A_{12}B_{26} -$$

$$2A_{12}A_{26} + 2A_{16}A_{22} - \frac{2}{R}B_{12}A_{26} - \frac{2}{R^2}B_{12}B_{26} - \frac{2}{R}A_{26}B_{66} - \frac{2}{R^2}B_{26}B_{66} \qquad (2.37d)$$

$$a_{25} = A_{66}A_{22} + \frac{2}{R}A_{66}B_{22} + \frac{1}{R^2}A_{66}D_{22} - \frac{2}{R}A_{26}B_{26} - \frac{1}{R^2}B_{26}{}^2 - A_{26}{}^2 \qquad (2.37e)$$

The extensional stiffnesses A_{ij}, extensional-bending coupling stiffnesses B_{ij}, and the bending stiffnesses D_{ij} are provided in Eq. (2.8).

2.8 Force Equations

2.8.1 Isotropic Shells

The force equations are derived by substituting the strain-displacement equations of Eq. (2.1) into the constitutive relations of Eq. (2.2). This produces the following equations for the membrane and bending force components

$$\begin{Bmatrix} N_x \\ N_s \\ N_{xs} \end{Bmatrix} = \begin{bmatrix} A & \nu A & 0 \\ \nu A & A & 0 \\ 0 & 0 & \frac{1-\nu}{2}A \end{bmatrix} \begin{Bmatrix} \frac{\partial u_x}{\partial x} \\ \frac{\partial u_s}{\partial s} + \frac{w}{R} \\ \frac{\partial u_s}{\partial x} + \frac{\partial u_x}{\partial s} \end{Bmatrix} \qquad (2.38a)$$

$$
\begin{Bmatrix} M_x \\ M_s \\ M_{xs} \end{Bmatrix} = \begin{bmatrix} D & vD & 0 \\ vD & D & 0 \\ 0 & 0 & \frac{1-v}{2}D \end{bmatrix} \begin{Bmatrix} -\dfrac{\partial^2 w}{\partial x^2} \\ \dfrac{\partial}{\partial s}\left(\dfrac{u_s}{R} - \dfrac{\partial w}{\partial s}\right) \\ \dfrac{1}{R}\dfrac{\partial u_s}{\partial x} - 2\dfrac{\partial^2 w}{\partial x \partial s} \end{Bmatrix}
\tag{2.38b}
$$

The shearing forces are derived from Eq. (2.10d) and Eq. (2.10e)

$$
Q_x = \left\{ \frac{\partial}{\partial x} \quad \frac{\partial}{\partial s} \right\} \begin{bmatrix} D & vD & 0 \\ 0 & 0 & \frac{1-v}{2}D \end{bmatrix} \begin{Bmatrix} -\dfrac{\partial^2 w}{\partial x^2} \\ \dfrac{\partial}{\partial s}\left(\dfrac{u_s}{R} - \dfrac{\partial w}{\partial s}\right) \\ \dfrac{1}{R}\dfrac{\partial u_s}{\partial x} - 2\dfrac{\partial^2 w}{\partial x \partial s} \end{Bmatrix}
\tag{2.39a}
$$

$$
Q_s = \left\{ \frac{\partial}{\partial x} \quad \frac{\partial}{\partial s} \right\} \begin{bmatrix} 0 & 0 & \frac{1-v}{2}D \\ vD & D & 0 \end{bmatrix} \begin{Bmatrix} -\dfrac{\partial^2 w}{\partial x^2} \\ \dfrac{\partial}{\partial s}\left(\dfrac{u_s}{R} - \dfrac{\partial w}{\partial s}\right) \\ \dfrac{1}{R}\dfrac{\partial u_s}{\partial x} - 2\dfrac{\partial^2 w}{\partial x \partial s} \end{Bmatrix}
\tag{2.39b}
$$

The extensional and bending stiffness, A and D, are provided in Eq. (2.3). The displacements, u_x, u_s, and w, are presented in terms of the potential function, $\Phi(x, s)$, in Eq. (2.26), Eq. (2.28), and Eq. (2.30).

2.8.2 Laminated Shells

The force equations are derived by substituting the strain-displacement equations of Eq. (2.1) into the constitutive relations of Eq. (2.9). This produces the following equations for the membrane and bending force components

$$
\begin{Bmatrix} N_x \\ N_s \\ N_{xs} \end{Bmatrix} = \begin{bmatrix} A_{11} & A_{12} & A_{16} \\ A_{12} & A_{22} & A_{26} \\ A_{16} & A_{26} & A_{66} \end{bmatrix} \begin{Bmatrix} \dfrac{\partial u_x}{\partial x} \\ \dfrac{\partial u_s}{\partial s} + \dfrac{w}{R} \\ \dfrac{\partial u_s}{\partial x} + \dfrac{\partial u_x}{\partial s} \end{Bmatrix} + \begin{bmatrix} B_{11} & B_{12} & B_{16} \\ B_{12} & B_{22} & B_{26} \\ B_{16} & B_{26} & B_{66} \end{bmatrix} \begin{Bmatrix} -\dfrac{\partial^2 w}{\partial x^2} \\ \dfrac{\partial}{\partial s}\left(\dfrac{u_s}{R} - \dfrac{\partial w}{\partial s}\right) \\ \dfrac{1}{R}\dfrac{\partial u_s}{\partial x} - 2\dfrac{\partial^2 w}{\partial x \partial s} \end{Bmatrix}
\tag{2.40a}
$$

$$\begin{Bmatrix} M_x \\ M_s \\ M_{xs} \end{Bmatrix} = \begin{bmatrix} B_{11} & B_{12} & B_{16} \\ B_{12} & B_{22} & B_{26} \\ B_{16} & B_{26} & B_{66} \end{bmatrix} \begin{Bmatrix} \dfrac{\partial u_x}{\partial x} \\ \dfrac{\partial u_s}{\partial s} + \dfrac{w}{R} \\ \dfrac{\partial u_s}{\partial x} + \dfrac{\partial u_x}{\partial s} \end{Bmatrix} + \begin{bmatrix} D_{11} & D_{12} & D_{16} \\ D_{12} & D_{22} & D_{26} \\ D_{16} & D_{26} & D_{66} \end{bmatrix} \begin{Bmatrix} -\dfrac{\partial^2 w}{\partial x^2} \\ \dfrac{\partial}{\partial s}\left(\dfrac{u_s}{R} - \dfrac{\partial w}{\partial s}\right) \\ \dfrac{1}{R}\dfrac{\partial u_s}{\partial x} - 2\dfrac{\partial^2 w}{\partial x \partial s} \end{Bmatrix} \qquad (2.40\text{b})$$

The shearing forces are derived from Eq. (2.10d) and Eq. (2.10e)

$$Q_x = \begin{Bmatrix} \dfrac{\partial}{\partial x} & \dfrac{\partial}{\partial s} \end{Bmatrix}\left(\begin{bmatrix} B_{11} & B_{12} & B_{16} \\ B_{16} & B_{26} & B_{66} \end{bmatrix} \begin{Bmatrix} \dfrac{\partial u_x}{\partial x} \\ \dfrac{\partial u_s}{\partial s} + \dfrac{w}{R} \\ \dfrac{\partial u_s}{\partial x} + \dfrac{\partial u_x}{\partial s} \end{Bmatrix} + \begin{bmatrix} D_{11} & D_{12} & D_{16} \\ D_{16} & D_{26} & D_{66} \end{bmatrix} \begin{Bmatrix} -\dfrac{\partial^2 w}{\partial x^2} \\ \dfrac{\partial}{\partial s}\left(\dfrac{u_s}{R} - \dfrac{\partial w}{\partial s}\right) \\ \dfrac{1}{R}\dfrac{\partial u_s}{\partial x} - 2\dfrac{\partial^2 w}{\partial x \partial s} \end{Bmatrix} \right)$$

$$(2.41\text{a})$$

$$Q_s = \begin{Bmatrix} \dfrac{\partial}{\partial x} & \dfrac{\partial}{\partial s} \end{Bmatrix}\left(\begin{bmatrix} B_{16} & B_{26} & B_{66} \\ B_{12} & B_{22} & B_{26} \end{bmatrix} \begin{Bmatrix} \dfrac{\partial u_x}{\partial x} \\ \dfrac{\partial u_s}{\partial s} + \dfrac{w}{R} \\ \dfrac{\partial u_s}{\partial x} + \dfrac{\partial u_x}{\partial s} \end{Bmatrix} + \begin{bmatrix} D_{16} & D_{26} & D_{66} \\ D_{12} & D_{22} & D_{26} \end{bmatrix} \begin{Bmatrix} -\dfrac{\partial^2 w}{\partial x^2} \\ \dfrac{\partial}{\partial s}\left(\dfrac{u_s}{R} - \dfrac{\partial w}{\partial s}\right) \\ \dfrac{1}{R}\dfrac{\partial u_s}{\partial x} - 2\dfrac{\partial^2 w}{\partial x \partial s} \end{Bmatrix} \right)$$

$$(2.41\text{b})$$

The extensional stiffnesses A_{ij}, extensional-bending coupling stiffnesses B_{ij}, and the bending stiffnesses D_{ij} are provided in Eq. (2.8). The displacements, u_x, u_s, and w, are presented in terms of the potential function, $\Phi(x, s)$, in Eq. (2.32), Eq. (2.34), and Eq. (2.36).
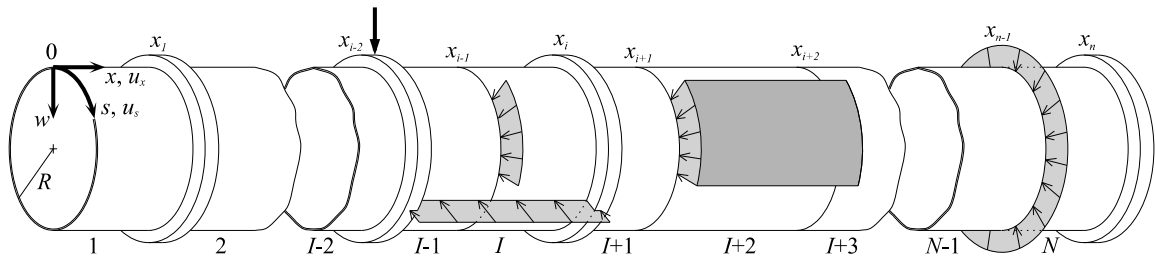
Figure 2.1. Stiffened cylindrical shell with strip and edge loadings
Note: The stiffeners are concentric with the shell

CHAPTER 3

DERIVATION OF THE ANALYTICAL STRIP METHOD

3.1 Introduction

This chapter presents the derivation of the Analytical Strip Method for stiffened and unstiffened cylindrical shells. The shells may be isotropic, generally orthotropic, or laminated with any generalized layer configuration and ply-angle scheme, such that the shell behaves anisotropically. In addition to the assumptions made in the derivation of the equations in Chapter 2, the derivation of the solution is based on the following assumptions:

- Stiffeners consist of isotropic beams and are concentric with the middle surface of the shell.

- Changes in thickness of the shell wall occur at a discrete location, such that the structure can be divided in to a finite number of strips, where the wall thickness is constant within a strip.

- Adjacent strips have a coincident middle surface, even in the case where the wall thickness changes.

- Loads are applied in the radial direction.

3.2 Governing Differential Equation

Since the governing equation for isotropic shells is a reduced case of the laminated shell equation, the solution method will be derived based on the laminated shell equation. The governing differential equation for laminated shells subjected to a radial load, $q(x,s)$, is given in Eq. (2.24).

$$F_{80}\frac{\partial^8\Phi}{\partial x^8} + F_{71}\frac{\partial^8\Phi}{\partial x^7\partial s} + F_{62}\frac{\partial^8\Phi}{\partial x^6\partial s^2} + F_{53}\frac{\partial^8\Phi}{\partial x^5\partial s^3} + F_{44}\frac{\partial^8\Phi}{\partial x^4\partial s^4} + F_{35}\frac{\partial^8\Phi}{\partial x^3\partial s^5} + F_{26}\frac{\partial^8\Phi}{\partial x^2\partial s^6} +$$

$$F_{17}\frac{\partial^8\Phi}{\partial x\partial s^7} + F_{08}\frac{\partial^8\Phi}{\partial s^8} + F_{60}\frac{\partial^6\Phi}{\partial x^6} + F_{51}\frac{\partial^6\Phi}{\partial x^5\partial s} + F_{42}\frac{\partial^6\Phi}{\partial x^4\partial s^2} + F_{33}\frac{\partial^6\Phi}{\partial x^3\partial s^3} + F_{24}\frac{\partial^6\Phi}{\partial x^2\partial s^4} +$$

$$F_{15}\frac{\partial^6\Phi}{\partial x\partial s^5} + F_{06}\frac{\partial^6\Phi}{\partial s^6} + F_{40}\frac{\partial^4\Phi}{\partial x^4} + F_{31}\frac{\partial^4\Phi}{\partial x^3\partial s} + F_{22}\frac{\partial^4\Phi}{\partial x^2\partial s^2} + F_{13}\frac{\partial^4\Phi}{\partial x\partial s^3} + F_{04}\frac{\partial^4\Phi}{\partial s^4} = q(x,s)$$

$$(2.24)$$

3.3 Analytical Strip Method

The ASM was first developed by Harik and Salamoun (1986, 1988) for the analysis of thin orthotropic and stiffened rectangular plates subjected to uniform, partial uniform, patch, line, partial line and point loads, or any combination thereof. The solution procedure requires that the structure be divided into strips based on the geometric discontinuities and applied loads (Figure 3.1). The governing differential equation for each strip is solved analytically and the applicable continuity and boundary conditions are used to combine the solutions for the strips.

The solution of the differential equation for a general strip I assumes that the form for the potential function, Φ_I, satisfies continuity at the surface coordinates $s = 0$ and $s = 2\pi R$. Let

$$\Phi_I(x,s) = \sum_n^\infty \phi_{nI}(x)\cos(\beta_n s) \tag{3.1}$$

Where

$$\beta_n = \frac{n}{R} \tag{3.2}$$

Hereinafter, the subscript I, denoting the Ith strip, will be excluded in the derivation.

Substituting Eq. (3.1) into the governing differential equation, Eq. (2.24), yields

$$F_{80} \sum_n^\infty \frac{d^8\phi_n(x)}{dx^8} \cos(\beta_n s) - F_{71} \sum_n^\infty \frac{d^7\phi_n(x)}{dx^7} \beta_n \sin(\beta_n s) - F_{62} \sum_n^\infty \frac{d^6\phi_n(x)}{dx^6} \beta_n{}^2 \cos(\beta_n s) +$$

$$F_{53} \sum_n^\infty \frac{d^5\phi_n(x)}{dx^5} \beta_n{}^3 \sin(\beta_n s) + F_{44} \sum_n^\infty \frac{d^4\phi_n(x)}{dx^4} \beta_n{}^4 \cos(\beta_n s) -$$

$$F_{35} \sum_n^\infty \frac{d^3\phi_n(x)}{dx^3} \beta_n{}^5 \sin(\beta_n s) - F_{26} \sum_n^\infty \frac{d^2\phi_n(x)}{dx^2} \beta_n{}^6 \cos(\beta_n s) +$$

$$F_{17} \sum_n^\infty \frac{d\phi_n(x)}{dx} \beta_n{}^7 \sin(\beta_n s) + F_{08} \sum_n^\infty \phi_n(x) \beta_n{}^8 \cos(\beta_n s) + F_{60} \sum_n^\infty \frac{d^6\phi_n(x)}{dx^6} \cos(\beta_n s) -$$

$$F_{51} \sum_n^\infty \frac{d^5\phi_n(x)}{dx^5} \beta_n \sin(\beta_n s) - F_{42} \sum_n^\infty \frac{d^4\phi_n(x)}{dx^4} \beta_n{}^2 \cos(\beta_n s) +$$

$$F_{33} \sum_n^\infty \frac{d^3\phi_n(x)}{dx^3} \beta_n{}^3 \sin(\beta_n s) + F_{24} \sum_n^\infty \frac{d^2\phi_n(x)}{dx^2} \beta_n{}^4 \cos(\beta_n s) -$$

$$F_{15} \sum_n^\infty \frac{d\phi_n(x)}{dx} \beta_n{}^5 \sin(\beta_n s) - F_{06} \sum_n^\infty \phi_n(x) \beta_n{}^6 \cos(\beta_n s) + F_{40} \sum_n^\infty \frac{d^4\phi_n(x)}{dx^4} \cos(\beta_n s) -$$

$$F_{31} \sum_n^\infty \frac{d^3\phi_n(x)}{dx^3} \beta_n \sin(\beta_n s) - F_{22} \sum_n^\infty \frac{d^2\phi_n(x)}{dx^2} \beta_n{}^2 \cos(\beta_n s) +$$

$$F_{13} \sum_n^\infty \frac{d\phi_n(x)}{dx} \beta_n{}^3 \sin(\beta_n s) + F_{04} \sum_n^\infty \phi_n(x) \beta_n{}^4 \cos(\beta_n s) = q(x,s) \tag{3.3}$$

Eq. (3.3) is multiplied by $\cos(\beta_m s)$, integrated from $s = 0$ to $s = 2\pi R$, and summed from $m = 0$ to $m = \infty$. Due to orthogonality of the trigonometric functions, $\int_0^{2\pi R} \sin(\beta_n s) \cos(\beta_m s) = 0$ for all values of m and n when $m \neq n$. The term $\int_0^{2\pi R} \cos(\beta_n s) \cos(\beta_m s) = 2\pi R$ for $m = n = 0$, and $\int_0^{2\pi R} \cos(\beta_n s) \cos(\beta_m s) = \pi R$ for $m = n \neq 0$. Implementing these relations leads to

$$\sum_m^\infty \left\{ F_{8m}^* \frac{d^8\phi_m(x)}{dx^8} + F_{6m}^* \frac{d^6\phi_m(x)}{dx^6} + F_{4m}^* \frac{d^4\phi_m(x)}{dx^4} + F_{2m}^* \frac{d^2\phi_m(x)}{dx^2} + F_{0m}^* \phi_m(x) \right\} =$$
$$\frac{1}{2\pi R} \int_0^{2\pi R} q(x,s)ds + \sum_{m=1}^\infty \frac{1}{\pi R} \int_0^{2\pi R} q(x,s) \cos(\beta_m s)\, ds \tag{3.4}$$

Where:

$$F_{8m}^* = F_{80} \tag{3.5a}$$

$$F_{6m}^* = -F_{62}\beta_m{}^2 \tag{3.5b}$$

$$F_{4m}^* = F_{44}\beta_m{}^4 - F_{42}\beta_m{}^2 + F_{40} \tag{3.5c}$$

$$F_{2m}^* = -F_{26}\beta_m{}^6 + F_{24}\beta_m{}^4 - F_{22}\beta_m{}^2 \tag{3.6d}$$

$$F_{0m}^* = F_{08}\beta_m{}^8 - F_{06}\beta_m{}^6 + F_{04}\beta_m{}^4 \tag{3.6e}$$

For $m = 0$, $F_{20}^* = F_{00}^* = 0$ and for $m = 1$, $F_{01}^* = 0$. The coefficients F_{ij} are provided in equations Eq. (2.20) for isotropic shells and Eq. (2.25) for laminated shells.

Eq. (3.4) is an infinite set of linear eighth-order ordinary differential equations for $\phi_m(x)$ with $m = 0, 1, 2, \ldots, \infty$. The solution is obtained by superposition of the associated homogeneous and particular solutions.

$$\Phi(x, s) = \Phi_H(x, s) + \Phi_P(x, s) \tag{3.7}$$

where the homogeneous solution

$$\Phi_H(x, s) = \sum_m^\infty \phi_{Hm}(x) \cos(\beta_m s) \tag{3.8}$$

and the particular solution

$$\Phi_P(x, s) = \sum_m^\infty \phi_{Pm}(x) \cos(\beta_m s) \tag{3.9}$$

3.3.1 Homogeneous Solution

The homogeneous solution for mode m, $\phi_{Hm}(x)$, is expressed as

$$\phi_{Hm}(x) = e^{\gamma_m \beta_m x} \tag{3.10}$$

Substituting Eq. (3.10) into Eq. (3.4) yields the characteristic equation for mode $m = 0$.

$$F_8^* \gamma_0{}^8 + F_6^* \gamma_0{}^6 + F_4^* \gamma_0{}^4 = 0 \tag{3.11}$$

Setting $\gamma_0{}^2 = \xi_0$ reduces Eq. (3.11) to

$$\left(F_8^* \xi_0{}^2 + F_6^* \xi_0 + F_4^*\right)\xi_0{}^2 = 0 \tag{3.12}$$

Two roots of Eq. (3.12) are $\xi_0 = 0$ with a multiplicity of two and the other two roots are given by the quadratic formula (Stewart, 1995). Substituting the roots of the

characteristic equation Eq. (3.11) into Eq. (3.10) leads to the homogenous solution for mode $m = 0$

$$\Phi_{H0}(x,s) = C_{10} + C_{20}x + C_{30}x^2 + C_{40}x^3 + [C_{50}\cosh(\gamma_{30}x) +$$
$$C_{60}\sinh(\gamma_{30}x)]\cos(\gamma_{40}x) + [C_{70}\cosh(\gamma_{30}x) + C_{80}\sinh(\gamma_{30}x)]\sin(\gamma_{40}x)$$

(3.13)

where

$$\gamma_{30} = \sqrt{\frac{-F_6^* + \sqrt{F_6^{*2} - 4F_8^*F_4^*}}{2F_8^*}}$$

(3.14a)

$$\gamma_{40} = \sqrt{\frac{-F_6^* - \sqrt{F_6^{*2} - 4F_8^*F_4^*}}{2F_8^*}}$$

(3.14b)

and coefficients C_{d0} for $d = 1, 2, ..., 8$ are constants determined by the boundary conditions at $x = 0$ and $x = x_n$ and the continuity conditions at $x = x_i$ ($i = 1,2, ..., n - 1$), see Figure 3.1.

The characteristic equation for mode $m = 1$ is

$$F_8^* \gamma_m^{\ 8} + F_6^* \gamma_m^{\ 6} + F_4^* \gamma_m^{\ 4} + F_2^* \gamma_m^{\ 2} = 0$$

(3.15)

and for all other modes ($m = 2, 3, ..., \infty$)

$$F_8^* \gamma_m^{\ 8} + F_6^* \gamma_m^{\ 6} + F_4^* \gamma_m^{\ 4} + F_2^* \gamma_m^{\ 2} + F_0^* = 0$$

(3.16)

The characteristic equation of Eq. (3.15) may be considered a special case of Eq. (3.16) with $F_0^* = 0$ and two of the roots taken as $\gamma_m = 0$ with a multiplicity of two.

Dividing Eq. (3.16) by F_0^* and setting $\gamma_m^{\ 2} = \xi_m$ leads to

$$\xi_m^{\ 4} + b\xi_m^{\ 3} + c\xi_m^{\ 2} + d\xi_m + e = 0$$

(3.17)

where

$$b = \frac{F_6^*}{F_8^*}, \quad c = \frac{F_4^*}{F_8^*}, \quad d = \frac{F_2^*}{F_8^*}, \quad e = \frac{F_0^*}{F_8^*} \tag{3.18}$$

Eq. (3.17) is a quartic equation that can be solved analytically (Editing Group of the Manual of Mathematics, 1979; Sun, 2009). The four roots for Eq. (3.17) are the same as the four roots in the following two equations

$$\xi_n{}^2 + \left(b + \sqrt{8s + b^2 - 4c}\right)\frac{\xi_n}{2} + \left(s + \frac{bs-d}{\sqrt{8s+b^2-4c}}\right) = 0 \tag{3.19a}$$

$$\xi_n{}^2 + \left(b - \sqrt{8s + b^2 - 4c}\right)\frac{\xi_n}{2} + \left(s - \frac{bs-d}{\sqrt{8s+b^2-4c}}\right) = 0 \tag{3.19b}$$

Where s is any real root for the following equation

$$8s^3 - 4cs^2 + (2bd - 8e)s + e(4c - b^2) - d^2 = 0 \tag{3.20}$$

Eq. (3.20) can be reduced to

$$s^3 + fs^2 + gs + h = 0 \tag{3.21}$$

where,

$$f = -\frac{c}{2} \tag{3.22a}$$

$$g = \frac{2bd - 8e}{8} \tag{3.22b}$$

$$h = \frac{e(4c - b^2) - d^2}{8} \tag{3.22c}$$

Let

$$s = t - \frac{f}{3} \tag{3.23}$$

Then, substitute into Eq. (3.21)

$$\left(t - \frac{f}{3}\right)^3 + f\left(t - \frac{f}{3}\right)^2 + g\left(t - \frac{f}{3}\right) + h = t^3 + \left(-\frac{f^2}{3} + g\right)t + \left(\frac{2f^3}{27} - \frac{fg}{3} + h\right) \tag{3.24}$$

Eq. (3.24) becomes

37

$$t^3 + pt + q = 0 \tag{3.25}$$

in which,

$$p = -\frac{f^2}{3} + g \tag{3.26a}$$

$$q = \frac{2f^3}{27} - \frac{fg}{3} + h \tag{3.26b}$$

Let,

$$\Delta = \left(\frac{q}{2}\right)^2 + \left(\frac{p}{3}\right)^3 \tag{3.27}$$

$$t_1 = \sqrt[3]{-\frac{q}{2} + \sqrt{\Delta}} + \sqrt[3]{-\frac{q}{2} - \sqrt{\Delta}} \qquad \text{when} \quad \Delta > 0 \tag{3.28}$$

$$t_1 = 2\sqrt[3]{r} \cos\theta \qquad \text{when} \quad \Delta < 0 \tag{3.29}$$

where,

$$r = \sqrt{-\left(\frac{p}{3}\right)^3} \tag{3.30a}$$

$$\theta = \frac{1}{3}\cos^{-1}\left(-\frac{q}{2r}\right) \tag{3.30b}$$

Substituting t_1 into Eq. (3.23) gives

$$s = t_1 - \frac{f}{3} \tag{3.31}$$

Substituting the results from Eq. (3.31) into Eq. (3.19), and carrying out the solution, produces four roots to Eq. (3.17). From the relation of $\gamma_m^2 = \xi_m$, γ_m is solved for the characteristic equation of Eq. (3.15) and Eq. (3.16).

The homogeneous solution for mode $m = 1$ is

$$\Phi_{H1}(x,s) = \begin{cases} C_{11} + C_{21}x + C_{31}e^{\gamma_{31}x} + C_{41}e^{-\gamma_{31}x} \\ +[C_{51}\cosh(\gamma_{11}x) + C_{61}\sinh(\gamma_{11}x)]\cos(\gamma_{21}x) \\ +[C_{71}\cosh(\gamma_{11}x) + C_{81}\sinh(\gamma_{11}x)]\sin(\gamma_{21}x) \end{cases} \cos(\beta_1 s) \quad (3.32)$$

where γ_{j1} (j = 1, 2, 3) are the non-zero roots to the characteristic equation [Eq. (3.15)]. The coefficients C_{d1} (d = 1, 2, …, 8) are constants determined from the applicable boundary and continuity conditions at the ends of the strip.

The homogeneous solution for all other modes (m = 2, 3, …, ∞) is

$$\Phi_{Hm}(x,s) = \begin{cases} [C_{1m}\cosh(\gamma_{1m}x) + C_{2m}\sinh(\gamma_{1m}x)]\cos(\gamma_{2m}x) \\ +[C_{3m}\cosh(\gamma_{1m}x) + C_{4m}\sinh(\gamma_{1m}x)]\sin(\gamma_{2m}x) \\ +[C_{5m}\cosh(\gamma_{3m}x) + C_{6m}\sinh(\gamma_{3m}x)]\cos(\gamma_{4m}x) \\ +[C_{7m}\cosh(\gamma_{3m}x) + C_{8m}\sinh(\gamma_{3m}x)]\sin(\gamma_{4m}x) \end{cases} \cos(\beta_m s) \quad (3.33)$$

where γ_{jm} (j = 1, 2, 3, 4) are the non-zero roots to the characteristic equation [Eq. (3.16)] for mode m = 2, 3, …, ∞. The coefficients C_{dm} (d = 1, 2, …, 8) are constants determined from the boundary conditions at $x = 0$ and $x = x_n$ and the continuity conditions at $x = x_i$ [$i = 1, 2, …, n - 1$ (Figure 3.1)].

3.3.2 Particular Solution

The particular solution is dependent upon the load distribution applied to the strip. For a given strip loading, the load distribution function, $q(x, s)$, is expressed as

$$q(x,s) = q_0 f(x)g(s) \tag{3.34}$$

where q_0 is the load amplitude and $f(x)$ and $g(s)$ are the load distribution functions in the x and s directions.

Substituting into the right hand side of Eq. (3.4) yields,

$$\frac{q_0 f(x)}{2\pi R} \int_0^{2\pi R} g(s)ds \qquad \text{for } m = 0 \tag{3.35}$$

and

39

$$\frac{q_0 f(x)}{\pi R} \int_0^{2\pi R} g(s) \cos(\beta_m s) \, ds \qquad \text{for } m = 1, 2, \ldots, \infty \qquad (3.36)$$

The potential function, $\phi_{pm}(x)$, can be derived for a wide range of commonly encountered load distributions. The particular solution for most common strip loadings are presented in Table 3.1.

When a strip is subjected to more than one load, the method of superposition is employed to determine the particular solution.

3.3.3 Edge Loading

For cylinders subjected to point loads and radial line loads distributed along the circumferential direction, the cylinder is divided into strips such that the loads coincide with the edges of the strips (Figure 3.1). These loads are expressed as a Fourier series and incorporated into the solution as shear force discontinuities between strips. Table 3.2 presents the edge loading function, $\psi_i(s)$, for several common loadings.

When an edge is subjected to a combination of loads, the method of superposition is employed to determine the edge loading function.

3.3.4 Isotropic Beam Equations

For cylinders with ring stiffeners along the circumferential direction, the structure is divided into strips such that the stiffeners coincide with the edges of the strips (Figure 3.1). The stiffeners are incorporated into the solution as part of the boundary and continuity conditions. The solution method assumes that the ring stiffeners are isotropic beams and are concentric with the middle surface of the shell.

The following differential equations can be derived from the equilibrium of an isotropic curved beam element (Vlasov, 1961)

$$q_{xb} = E_b I_r \left(\frac{d^4 u_{xb}}{ds^4} - \frac{1}{R} \frac{d^2 \phi_b}{ds^2} \right) + \frac{E_b C_w}{R} \left(\frac{d^4 \phi_b}{ds^4} + \frac{1}{R} \frac{d^4 u_{xb}}{ds^4} \right) - \frac{G_b J_b}{R} \left(\frac{d^2 \phi_b}{ds^2} + \frac{1}{R} \frac{d^2 u_{xb}}{ds^2} \right) \qquad (3.37a)$$

$$q_{rb} = E_b I_x \left(\frac{d^4 w_b}{ds^4} - \frac{1}{R} \frac{d^3 u_{sb}}{ds^3} \right) + \frac{E_b A_b}{R} \left(\frac{d u_{sb}}{ds} + \frac{1}{R} w_b \right) \qquad (3.37b)$$

$$q_{sb} = \frac{E_b I_x}{R} \left(\frac{d^3 w_b}{ds^3} - \frac{1}{R} \frac{d^2 u_{sb}}{ds^2} \right) - E_b A_b \left(\frac{d^2 u_{sb}}{ds^2} + \frac{1}{R} \frac{d w_b}{ds} \right) \qquad (3.37c)$$

$$m_{xb} = \frac{E_b I_r}{R} \left(- \frac{d^2 u_{xb}}{ds^2} + \frac{1}{R} \phi_b \right) + E_b C_w \left(\frac{d^4 \phi_b}{ds^4} + \frac{1}{R} \frac{d^4 u_{xb}}{ds^4} \right) - G_b J_b \left(\frac{d^2 \phi_b}{ds^2} + \frac{1}{R} \frac{d^2 u_{xb}}{ds^2} \right) \qquad (3.37d)$$

The terms q_{xb}, q_{rb}, and q_{sb} are the distributed forces per unit length applied to the beam in the x, r, and s directions (Figure 3.2); m_{xb} is the twisting moment per unit length applied to the beam; u_{xb}, u_{sb}, and w_b are the deflections of the beam in the x, r, and s directions (Figure 3.2); ϕ_b is the twist angle of the beam; R is the radius measured to the centroid of the beam; $E_b I_r$ = flexural rigidity about the r-axis (Figure 3.2); $E_b I_x$ = flexural rigidity about the x-axis (Figure 3.2); $E_b A_b$ = axial stiffness of the beam; $G_b J_b$ = torsional rigidity of the beam; $E_b C_w$ = warping rigidity of the beam.

3.3.5 Boundary Conditions

The boundary conditions along the edges $x = 0$ and $x = x_n$ are:

For simply supported edges: $u_x = 0, \quad u_s = 0, \quad w = 0, \quad M_x = 0$ $\qquad$ (3.38a, b, c, d)

For clamped edges: $u_x = 0, \quad u_s = 0, \quad w = 0, \quad \frac{\partial w}{\partial x} = 0,$ $\qquad$ (3.38a, b, c, d)

For free edges: $Q_x = \psi, \quad N_x = 0, \quad N_{xs} = 0, \quad M_x = 0,$ $\qquad$ (3.38a, b, c, d)

For beam support: $w = w_b, \quad \frac{dw}{dx} = \phi_b, \quad Q_x = q_{rb} + \psi, \quad M_x = m_{tb}$ $\quad$ (3.38a, b, c, d)

Where ϕ_b is the twist angle of the beam and m_{tb} is the twisting moment per unit length applied to the beam from Eq. (3.37d).

Difficulties arise when the coefficients on the odd derivatives of the s terms in Eq. 2.32, Eq. 2.34, and Eq. 2.36 are non-zero. Expansion of these equations lead to both $\cos(\beta_m s)$ and $\sin(\beta_m s)$ in the expressions for u_x, u_s, and w when $m = 1, 2, \ldots, \infty$. This necessitates two constraint equations to impose any one of the boundary conditions in Eq. 3.38. For these cases, only four boundary conditions can be assigned per strip, in contrast to the eight conditions allowed for the alternative case.

3.3.6 Continuity Conditions

The following continuity conditions are applied along the shared edge between strips I and $I + 1$ at $x = x_i$ when there is no stiffener present

$$u_{xI} = u_{x(I+1)}, \quad u_{sI} = u_{s(I+1)}, \quad w_I = w_{(I+1)}, \quad \frac{\partial w_I}{\partial x} = \frac{\partial w_{(I+1)}}{\partial x} \qquad \text{(3.39a, b, c, d)}$$

and

$$M_{xI} = M_{x(I+1)}, \quad N_{xI} = N_{x(I+1)}, \quad Q_{xI} = Q_{x(I+1)} + \psi_i, \quad N_{xsI} = N_{xs(I+1)} \qquad \text{(3.40a, b, c, d)}$$

When a beam is present at $x = x_i$, the following continuity conditions are imposed along the common edge $x = x_i$, between strips I and $I+1$.

$$u_{xI} = u_{x(I+1)}, \quad u_{sI} = u_{s(I+1)}, \quad w_I = w_{(I+1)}, \quad \frac{\partial w_I}{\partial x} = \frac{\partial w_{(I+1)}}{\partial x} = \phi_b \qquad \text{(3.41a, b, c, d)}$$

and

$$m_{tb} = M_{x(I+1)} - M_{xI}, \quad q_{xb} = N_{x(I+1)} - N_{xI}, \qquad \text{(3.42a, b)}$$

$$q_{rb} = Q_{x(I+1)} - Q_{xI} + \psi_i, \quad q_{sb} = N_{xs(I+1)} - N_{xsI} \qquad \text{(3.43c, d)}$$

Where ψ_i is the edge loading function, ϕ_b is the twist angle of the beam, m_{tb} is the twisting moment per unit length applied to the beam from Eq. (3.37d), and q_{xb}, q_{rb}, and q_{sb} are the distributed forces per unit length applied to the beam in the x, r, and s directions from Eq. (3.37a,b,c).

3.3.7 Solution

A cylindrical shell is divided into N-strips (Figure 3.1) depending on the number of loading and geometric discontinuities and the locations of the ring stiffeners. For each of the N-strips, eight equations are generated from the boundary and continuity conditions. This yields a unique $8N$ system of equations for each mode m (m = 0, 1, 2, …, ∞). Solution of these systems of equations provide the constants C_{dmI} (d = 1, 2, …, 8) in the homogeneous solution. The potential function Φ_I for each strip I (I = 1, 2, …, N) is derived by summing the homogeneous and particular solutions. The potential function is then back-substituted into the relevant equations to yield the desired forces and displacements.

3.3.8 Convergence
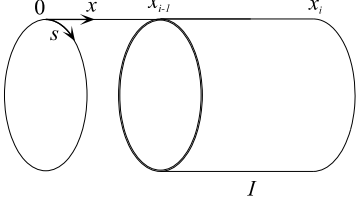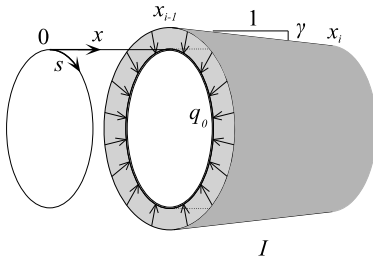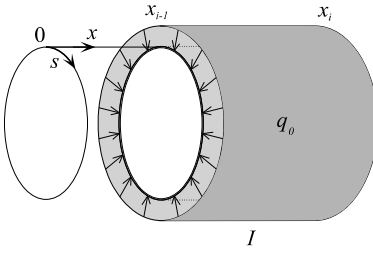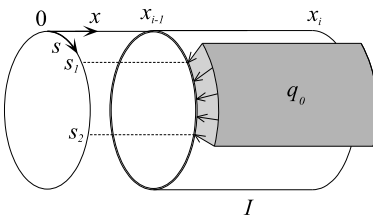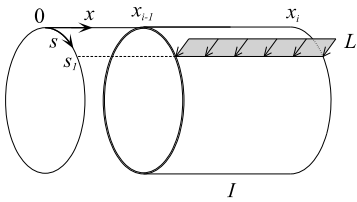
The ASM results are derived from the summation of modes in the infinite series solution. The number of modes required for the convergence of the solution is dependent on the geometry of the structure and the applied loading. In practice, the summation continues until the modal contribution is significantly less than the required accuracy of the results. Typically, 50 modes are adequate to obtain deflection and force results accurate to four significant digits.

3.3.9 Implementation
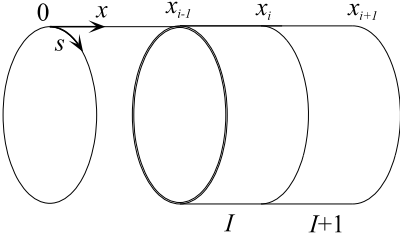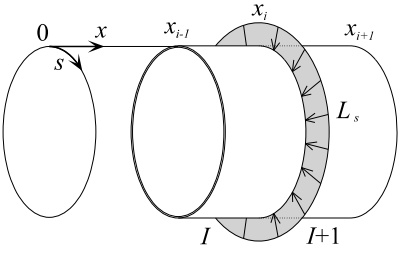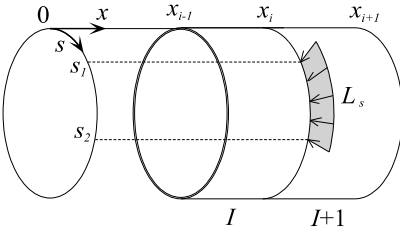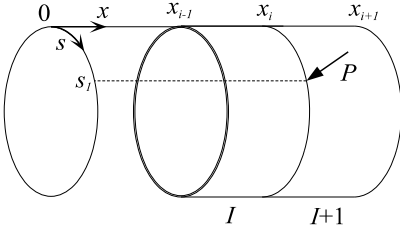
The ASM is easily programmable. For the examples considered in Chapter 4 and Chapter 5, a MATLAB (Mathworks, 2017) program was developed to compute the results. Due to the ill-conditioned nature of the solution, the ASM is susceptible to numerical instabilities when computing solutions using double precision floating point format. This required the use of an arbitrary-precision package, which solved the problem with overflow/underflow and allowed for the storage of an arbitrary number of digits in the solution.

Solution times vary depending on the number of strips required, shell wall material, loading complexity, and number of modes. For simple cases with isotropic shells and axisymmetric loading, the computation time required for the solution is seconds. A laminated shell with four strips, non-axisymmetric loading, and 50 modes required for the solution would have a computational time of approximately 20 minutes.

Table 3.1. Particular solution $\Phi_{PI}(x,s)$ for cylindrical strip I

Load Case	$\Phi_{PI}(x,s)$

Case 1 - Zero load

$$\Phi_{PI}(x,s) = 0$$

Case 2 - Linearly varying load (hydrostatic load)

$$q(x,s) = q_0 - \gamma(x - x_{i-1})$$

$$\Phi_{PIm=0}(x,s) = \frac{q_0}{24A_{40}^*}x^4 - \frac{\gamma}{120A_{40}^*}x^5$$

$$\Phi_{PIm=1,2,\dots,\infty}(x,s) = 0$$

Case 3 - Uniform load q_0

$$\Phi_{PIm=0}(x,s) = \frac{q_0}{24A_{40}^*}x^4$$

$$\Phi_{PIm=1,2,\dots,\infty}(x,s) = 0$$

Case 4 - Partial uniform load q_0

$$\Phi_{PIm=0}(x,s) = \frac{q_0}{48\pi RA_{40}^*}(s_2 - s_1)x^4$$

$$\Phi_{PIm=1}(x,s) = \frac{q_0}{2\pi RA_{21}^*}\left[\sin\left(\frac{s_2}{R}\right) - \sin\left(\frac{s_1}{R}\right)\right]x^2 \cos\left(\frac{s}{R}\right)$$

$$\Phi_{PIm=2,3,\dots,\infty}(x,s) = \frac{q_0}{m\pi RA_{0m}^*}\left[\sin\left(\frac{m}{R}s_2\right) - \sin\left(\frac{m}{R}s_1\right)\right]\cos\left(\frac{m}{R}s\right)$$

Case 5 - Line load L_x

$$\Phi_{PIm=0}(x,s) = \frac{L_x}{48\pi RA_{40}^*}x^4$$

$$\Phi_{PIm=1}(x,s) = \frac{L_x}{2\pi RA_{21}^*}\cos\left(\frac{s_1}{R}\right)x^2 \cos\left(\frac{s}{R}\right)$$

$$\Phi_{PIm=2,3,\dots,\infty}(x,s) = \frac{L_x}{\pi RA_{0m}^*}\cos\left(\frac{m}{R}s_1\right)\cos\left(\frac{m}{R}s\right)$$

Table 3.2. Edge loading function $\psi_i(s)$ along the edge $x = x_i$

Load Case	$\psi_i(s)$

Case 1 - Zero load

$$\psi_i(s) = 0$$

Case 2 - Line load L_s in s direction

$$\psi_{im=0}(s) = L_s$$

$$\psi_{im=1,2,\dots,\infty}(s) = 0$$

Case 3 - Partial line load L_y

$$\psi_{im=0}(s) = \frac{L_s(s_2 - s_1)}{2\pi R}$$

$$\psi_{im=1,2,\dots,\infty}(s) = \frac{2L_s}{m\pi} \sin\left[\frac{m}{2R}(s_2 - s_1)\right] \cos\left[\frac{m}{R}\left(s - \frac{s_1 + s_2}{2}\right)\right]$$

Case 4 - Concentrated point load P

$$\psi_{im=0}(s) = \frac{P}{2\pi R}$$

$$\psi_{im=1,2,\dots,\infty}(s) = \frac{P}{\pi R} \cos\left[\frac{m}{R}(s - s_1)\right]$$

Figure 3.1. Stiffened cylindrical shell with strip and edge loadings
Note: The stiffeners are concentric with the shell
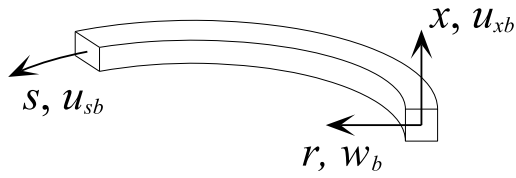
Figure 3.2. Coordinate system for the ring stiffener

CHAPTER 4
ANALYTICAL STRIP METHOD FOR THIN ISOTROPIC CYLINDRICAL SHELLS

4.1 Introduction

Cylindrical Shells are important structural elements with widespread applications in various fields such as civil, environmental, mechanical, and aerospace engineering. Much effort has been dedicated to understanding the behavior of these structures. Several shell theories have been developed to simplify complex three-dimensional elasticity based solutions. These theories are roughly divided into two categories, thin shell theories which adopt Love's assumptions and higher order shell theories that relax one or more of the Love's assumptions (Kraus, 1967). Due to the complexity of the governing equations for cylindrical shells, many of the existing analytical solutions are based on thin shell theory. Leissa (1973) provides an excellent review of available thin shell theories.

Analytical solutions to cylindrical shells subjected to axisymmetric loads are widely available. Timoshenko and Woinowsky-Krieger (1959) provide solutions for cylindrical shells with uniform internal pressure as well as cylindrical tanks subjected to hydrostatic loads. Due to the introduction of a second variable in the circumferential direction, non-axisymmetric type loadings are difficult to incorporate in the solution. Bijlaard (1955) developed a double series solution for cylindrical shells subjected to a patch load as well as a similar solution for points. Odqvist (1946), Hoff et al. (1954), Cooper (1957), and Naghdi (1968) have developed unique solutions for cylindrical shells subjected to a uniform line load along a generator. Meck (1961) presented a solution for line loads applied along the circumferential direction.

The objective of this paper is to develop an analytical strip method (ASM) of solution for stiffened isotropic thin cylindrical shells. The ASM was first developed by Harik and Salamoun (1986, 1988) for the analysis of thin orthotropic and stiffened rectangular plates subjected to uniform, partial uniform, patch, line, partial line and point loads or any

combination thereof. The solution procedure requires that the structure be divided into strips based on the geometric discontinuities and applied loads (Figure 4.1). The governing differential equation for each strip is solved analytically and the applicable continuity and boundary conditions are used to combine the solutions for the strips.

The primary contribution of the ASM is in its ability to handle a wide variety of loading and geometric configurations. At present, analytical solutions are limited to axisymmetric and simple non-axisymmetric loadings applied to cylindrical shells of basic geometry. Other more complex cases must utilize numerical or semi-numerical techniques. Unlike numerical based solutions, the accuracy of the ASM does not depend on the number of strips within the structure, but rather the number of modes considered in the series solution.

4.2 Governing Differential Equation for Isotropic Cylindrical Shells

The surface coordinate system used in the derivation of the governing equation for a cylindrical strip is shown in Figure 4.1. The strain-displacement equations associated with thin shell theory are given as (Kraus, 1967)

$$\epsilon_x = \frac{\partial u_x}{\partial x} \tag{4.1a}$$

$$\epsilon_s = \frac{\partial u_s}{\partial s} + \frac{w}{R} \tag{4.1b}$$

$$\gamma_{xs} = \frac{\partial u_s}{\partial x} + \frac{\partial u_x}{\partial s} \tag{4.1c}$$

$$\kappa_x = -\frac{\partial^2 w}{\partial x^2} \tag{4.1d}$$

$$\kappa_s = \frac{\partial}{\partial s}\left(\frac{u_s}{R} - \frac{\partial w}{\partial s}\right) \tag{4.1e}$$

$$\kappa_{xs} = \frac{1}{R}\frac{\partial u_s}{\partial x} - 2\frac{\partial^2 w}{\partial x \partial s} \tag{4.1f}$$

And the equilibrium equations are (Kraus, 1967)

$$\frac{\partial N_x}{\partial x} + \frac{\partial N_{sx}}{\partial s} + q_x = 0 \qquad (4.2a)$$

$$\frac{\partial N_{xs}}{\partial x} + \frac{\partial N_s}{\partial s} + \frac{Q_s}{R} + q_s = 0 \qquad (4.2b)$$

$$\frac{\partial Q_x}{\partial x} + \frac{\partial Q_s}{\partial s} - \frac{N_s}{R} + q = 0 \qquad (4.2c)$$

$$\frac{\partial M_x}{\partial x} + \frac{\partial M_{xs}}{\partial s} - Q_x = 0 \qquad (4.2d)$$

$$\frac{\partial M_{xs}}{\partial x} + \frac{\partial M_s}{\partial s} - Q_s = 0 \qquad (4.2e)$$

The five equilibrium equations are reduced to three by substituting Eq. (4.2d) and Eq. (4.2e) into Eq. (4.2c). Substitution of the strain-displacement equations into the equilibrium equations yield a system of three differential equations that may be presented as

$$\begin{bmatrix} L_{11} & L_{12} & L_{13} \\ L_{12} & L_{22} & L_{23} \\ L_{13} & L_{23} & L_{33} \end{bmatrix} \begin{Bmatrix} u_x \\ u_s \\ w \end{Bmatrix} = \begin{Bmatrix} q_x \\ q_s \\ q \end{Bmatrix} \qquad (4.3)$$

where L_{ij} are differential operators

$$L_{11} = A\frac{\partial^2}{\partial x^2} + \frac{1-\nu}{2}A\frac{\partial^2}{\partial s^2} \qquad (4.4a)$$

$$L_{12} = \frac{1+\nu}{2}A\frac{\partial^2}{\partial x \partial s} \qquad (4.4b)$$

$$L_{13} = \frac{\nu}{R}A\frac{\partial}{\partial x} \qquad (4.4c)$$

$$L_{22} = \left(\frac{1-\nu}{2}A + \frac{1-\nu}{2R^2}D\right)\frac{\partial^2}{\partial x^2} + (A+D)\frac{\partial^2}{\partial s^2} \qquad (4.4d)$$

$$L_{23} = \frac{1}{R}A\frac{\partial}{\partial s} - \frac{1}{R}D\frac{\partial^3}{\partial x^2 \partial s} - \frac{1}{R}D\frac{\partial^3}{\partial s^3} \qquad (4.4e)$$

$$L_{33} = \frac{1}{R^2}A + D\frac{\partial^4}{\partial x^4} + 2D\frac{\partial^4}{\partial x^2 \partial s^2} + D\frac{\partial^4}{\partial s^4} \tag{4.4f}$$

A and D are the extensional and bending stiffness of the shell

$$A = \frac{Et}{1-v^2} \tag{4.5a}$$

$$D = \frac{Et^3}{12(1-v^2)} \tag{4.5b}$$

Where t is the thickness, E is the elastic modulus, and v is Poisson's ratio.

The displacements in the x, s, and r direction, u_x, u_s, and w, are presented in terms of the potential function $\Phi(x,s)$ (Sharma et al., 1980)

$$u_x = (L_{12}L_{23} - L_{13}L_{22})\Phi(x,s) \tag{4.6a}$$

$$u_s = (L_{13}L_{21} - L_{23}L_{11})\Phi(x,s) \tag{4.6b}$$

$$w = (L_{11}L_{22} - L_{12}L_{21})\Phi(x,s) \tag{4.6c}$$

For the case of radial loads only, the three equations can be combined into a single eighth order differential equation expressed in terms of the potential function Φ (Sharma et al., 1980).

$$F_{80}\frac{\partial^8\Phi}{\partial x^8} + F_{62}\frac{\partial^8\Phi}{\partial x^6 \partial s^2} + F_{44}\frac{\partial^8\Phi}{\partial x^4 \partial s^4} + F_{26}\frac{\partial^8\Phi}{\partial x^2 \partial s^6} + F_{08}\frac{\partial^8\Phi}{\partial s^8} + F_{42}\frac{\partial^6\Phi}{\partial x^4 \partial s^2} + F_{24}\frac{\partial^6\Phi}{\partial x^2 \partial s^4} +$$

$$F_{06}\frac{\partial^6\Phi}{\partial s^6} + F_{40}\frac{\partial^4\Phi}{\partial x^4} + F_{22}\frac{\partial^4\Phi}{\partial x^2 \partial s^2} + F_{04}\frac{\partial^4\Phi}{\partial s^4} = q(x,s) \tag{4.7}$$

The coefficients F_{ij} are

$$F_{80} = \frac{1-v}{2R^2}AD^2 + \frac{1-v}{2}A^2D \tag{4.8a}$$

$$F_{62} = \frac{(v-1)(v-5)}{4R^2}AD^2 + 2(1-v)A^2D \tag{4.8b}$$

$$F_{44} = \frac{(v-1)(v+3)}{2R^2}AD^2 + 3(1-v)A^2D \tag{4.8c}$$

$$F_{26} = \frac{(1-v)^2}{4R^2}AD^2 + 2(1-v)A^2D \qquad (4.8d)$$

$$F_{08} = \frac{1-v}{2}A^2D \qquad (4.8e)$$

$$F_{42} = \frac{(1-v)(v+2)}{R^2}A^2D \qquad (4.8f)$$

$$F_{24} = \frac{(1-v)(v+3)}{R^2}A^2D \qquad (4.8g)$$

$$F_{06} = \frac{(1-v)}{R^2}A^2D \qquad (4.8h)$$

$$F_{40} = \frac{(v-1)^2(v+1)}{2R^4}A^2D + \frac{(v-1)^2(v+1)}{2R^2}A^3 \qquad (4.8i)$$

$$F_{22} = \frac{(1-v)(3v+5)}{4R^4}A^2D \qquad (4.8j)$$

$$F_{04} = \frac{(1-v)}{2R^4}A^2D \qquad (4.8k)$$

Where A and D are the extensional and bending stiffness provided in Eq. (4.5).

4.3 Isotropic Beam Equations

The following differential equations can be derived from the equilibrium of an isotropic curved beam element (Vlasov, 1961)

$$q_{xb} = E_b I_r \left(\frac{d^4 u_{xb}}{ds^4} - \frac{1}{R}\frac{d^2 \phi_b}{ds^2}\right) + \frac{E_b C_w}{R}\left(\frac{d^4 \phi_b}{ds^4} + \frac{1}{R}\frac{d^4 u_{xb}}{ds^4}\right) - \frac{G_b J_b}{R}\left(\frac{d^2 \phi_b}{ds^2} + \frac{1}{R}\frac{d^2 u_{xb}}{ds^2}\right) \qquad (4.9)$$

$$q_{rb} = E_b I_x \left(\frac{d^4 w_b}{ds^4} - \frac{1}{R}\frac{d^3 u_{sb}}{ds^3}\right) + \frac{E_b A_b}{R}\left(\frac{d u_{sb}}{ds} + \frac{1}{R}w_b\right) \qquad (4.10)$$

$$q_{sb} = \frac{E_b I_x}{R}\left(\frac{d^3 w_b}{ds^3} - \frac{1}{R}\frac{d^2 u_{sb}}{ds^2}\right) - E_b A_b \left(\frac{d^2 u_{sb}}{ds^2} + \frac{1}{R}\frac{d w_b}{ds}\right) \qquad (4.11)$$

$$m_{xb} = \frac{E_b I_r}{R}\left(-\frac{d^2 u_{xb}}{ds^2} + \frac{1}{R}\phi_b\right) + E_b C_w \left(\frac{d^4 \phi_b}{ds^4} + \frac{1}{R}\frac{d^4 u_{xb}}{ds^4}\right) - G_b J_b \left(\frac{d^2 \phi_b}{ds^2} + \frac{1}{R}\frac{d^2 u_{xb}}{ds^2}\right) \qquad (4.12)$$

The terms q_{xb}, q_{rb}, and q_{sb} are the distributed forces per unit length applied to the beam in the x, r, and s directions (Figure 4.2); m_{xb} is the twisting moment per unit length applied to the beam; u_{xb}, u_{sb}, and w_b are the deflections of the beam in the x, r, and s directions (Figure 4.2); ϕ_b is the twist angle of the beam; R is the radius measured to the centroid of the beam; E_bI_r = flexural rigidity about the r-axis (Figure 4.2); E_bI_x = flexural rigidity about the x-axis (Figure 4.2); E_bA_b = axial stiffness of the beam; G_bJ_b = torsional rigidity of the beam; E_bC_w = warping rigidity of the beam.

4.4 Analytical Strip Method

The solution of the differential equation for a general strip I is based on the assumption that the form for the potential function, Φ_I, satisfies continuity at the surface coordinate $s = 0$ and $s = 2\pi R$. Let

$$\Phi = \sum_{n}^{\infty} \phi_n(x) \cos(\beta_n s) \tag{4.13}$$

Where

$$\beta_n = \frac{n}{R} \tag{4.14}$$

Substituting Eq. (4.13) into the governing differential equation [Eq. (4.7)], multiplying both sides of the equation by $\cos(\beta_m s)$, integrating from $s = 0$ to $s = 2\pi R$, and summing from $m = 0$ to $m = \infty$ yields the following equation by orthogonality

$$\sum_{m}^{\infty} \left\{ F_{8m}^* \frac{d^8\phi_m(x)}{dx^8} + F_{6m}^* \frac{d^6\phi_m(x)}{dx^6} + F_{4m}^* \frac{d^4\phi_m(x)}{dx^4} + F_{2m}^* \frac{d^2\phi_m(x)}{dx^2} + F_{0m}^* \phi_m(x) \right\} =$$

$$\frac{1}{2\pi R} \int_0^{2\pi R} q(x,s)ds + \sum_{m=1}^{\infty} \frac{1}{\pi R} \int_0^{2\pi R} q(x,s) \cos(\beta_m s)\, ds \tag{4.15}$$

Where:

$$F_{8m}^* = F_{80} \tag{4.16a}$$

$$F_{6m}^* = -F_{62}\beta_m^{\,2} \tag{4.16b}$$

$$F_{4m}^* = F_{44}\beta_m{}^4 - F_{42}\beta_m{}^2 + F_{40} \qquad (4.16\text{c})$$

$$F_{2m}^* = -F_{26}\beta_m{}^6 + F_{24}\beta_m{}^4 - F_{22}\beta_m{}^2 \qquad (4.16\text{d})$$

$$F_{0m}^* = F_{08}\beta_m{}^8 - F_{06}\beta_m{}^6 + F_{04}\beta_m{}^4 \qquad (4.16\text{e})$$

For $m = 0$, $F_{20}^* = F_{00}^* = 0$ and for $m = 1$, $F_{01}^* = 0$.

Eq. (4.15) is an infinite set of linear 8th order ordinary differential equations for $\phi_m(x)$ with $m = 0, 1, 2, \ldots, \infty$. The solution is obtained by superposition of the associated homogeneous and particular solutions.

$$\Phi(x, s) = \Phi_H(x, s) + \Phi_P(x, s) \qquad (4.17)$$

where the homogeneous solution

$$\Phi_H(x, s) = \sum_m^\infty \phi_{Hm}(x)\cos(\beta_m s) \qquad (4.18)$$

and the particular solution

$$\Phi_P(x, s) = \sum_m^\infty \phi_{Pm}(x)\cos(\beta_m s) \qquad (4.19)$$

4.4.1 Homogeneous Solution

The homogeneous solution for mode m, $\phi_{Hm}(x)$, is expressed as

$$\phi_{Hm}(x) = e^{\gamma_m \beta_m x} \qquad (4.20)$$

The characteristic equation of Eq. (4.20) for mode $m = 0$ is

$$F_8^* \gamma_m{}^8 + F_6^* \gamma_m{}^6 + F_4^* \gamma_m{}^4 = 0 \qquad (4.21)$$

And the homogeneous solution for mode $m = 0$ is

$$\Phi_{H0}(x, s) = C_{10} + C_{20}x + C_{30}x^2 + C_{40}x^3 + [C_{50}\cosh(\gamma_{30}x) + C_{60}\sinh(\gamma_{30}x)]\cos(\gamma_{40}x) + [C_{70}\cosh(\gamma_{30}x) + C_{80}\sinh(\gamma_{30}x)]\sin(\gamma_{40}x) \qquad (4.22)$$

54

The characteristic equation of Eq. (4.20) for mode $m = 1$ is

$$F_8^* \gamma_m{}^8 + F_6^* \gamma_m{}^6 + F_4^* \gamma_m{}^4 + F_2^* \gamma_m{}^2 = 0 \qquad (4.23)$$

And the homogeneous solution for mode $m = 1$ is

$$\Phi_{H1}(x,s) = \left\{ \begin{array}{c} C_{11} + C_{21}x + C_{31}e^{\gamma_{31}x} + C_{41}e^{-\gamma_{31}x} \\ +[C_{51}\cosh(\gamma_{11}x) + C_{61}\sinh(\gamma_{11}x)]\cos(\gamma_{21}x) \\ +[C_{71}\cosh(\gamma_{11}x) + C_{81}\sinh(\gamma_{11}x)]\sin(\gamma_{21}x) \end{array} \right\} \cos(\beta_1 s) \quad (4.24)$$

The characteristic equation of Eq. (4.20) for all other modes ($m = 2, 3, \ldots,\infty$) is

$$F_8^* \gamma_m{}^8 + F_6^* \gamma_m{}^6 + F_4^* \gamma_m{}^4 + F_2^* \gamma_m{}^2 + F_0^* = 0 \qquad (4.25)$$

And the homogeneous solution for all other modes ($m = 2, 3, \ldots, \infty$) is

$$\Phi_{Hm}(x,s) = \left\{ \begin{array}{c} [C_{1m}\cosh(\gamma_{1m}x) + C_{2m}\sinh(\gamma_{1m}x)]\cos(\gamma_{2m}x) \\ +[C_{3m}\cosh(\gamma_{1m}x) + C_{4m}\sinh(\gamma_{1m}x)]\sin(\gamma_{2m}x) \\ +[C_{5m}\cosh(\gamma_{3m}x) + C_{6m}\sinh(\gamma_{3m}x)]\cos(\gamma_{4m}x) \\ +[C_{7m}\cosh(\gamma_{3m}x) + C_{8m}\sinh(\gamma_{3m}x)]\sin(\gamma_{4m}x) \end{array} \right\} \cos(\beta_m s) \quad (4.26)$$

Eq. (4.21), Eq. (4.23), and Eq. (4.25) can be reduced to quartic equations for which the characteristic roots can be solved analytically (Editing Group of the Manual of Mathematics, 1979). The constants C_{dm} ($d = 1,2,\ldots,8$) for each mode ($m = 1,2,\ldots,\infty$) are determined by the boundary conditions at $x = 0$ and $x = x_n$ and the continuity conditions at $x = x_i$ [($i = 1,2,\ldots,n-1$) Figure 4.1].

4.4.2 Particular Solution

The particular solution is dependent upon the load distribution applied to the strip. For a given strip loading, the load distribution function, $q(x,s)$, is expressed as

$$q(x,s) = q_0 f(x)g(s) \qquad (4.27)$$

where q_0 is the load amplitude and $f(x)$ and $g(s)$ are the load distribution functions in the x and s directions.

Substituting into the right hand side of Eq. (4.15) yields,

$$\frac{q_0 f(x)}{2\pi R} \int_0^{2\pi R} g(s)ds \quad \text{for } m = 0 \tag{4.28}$$

and

$$\frac{q_0 f(x)}{\pi R} \int_0^{2\pi R} g(s)\cos(\beta_m s)\,ds \qquad \text{for m} = 1, 2, \ldots, \infty \tag{4.29}$$

The potential function, $\phi_{pm}(x)$, can be derived for a wide range of commonly encountered load distributions. The particular solution for most common strip loadings are presented in Table 4.1.

When a strip is subjected to more than one load, the method of superposition is employed to determine the particular solution.

4.4.3 Edge Loading

For cylinders subjected to point loads and radial line loads distributed along the circumferential direction, the cylinder is divided into strips such that the loads coincide with the edges of the strips (Figure 4.1). These loads are expressed as a Fourier series and incorporated into the solution as shear force discontinuities between strips. Table 4.2 presents the edge loading function $\psi_i(s)$ for several common loadings.

When an edge is subjected to a combination of loads, the method of superposition is employed to determine the edge loading function.

4.4.4 Boundary Conditions

The boundary conditions along the edges $x = 0$ and $x = x_n$ are:

For simply supported edges: $u_x = 0, \quad u_s = 0, \quad w = 0, \quad M_x = 0 \qquad$ (4.30a, b, c, d)

For clamped edges: $u_x = 0$, $\quad u_s = 0$, $\quad w = 0$, $\quad \dfrac{\partial w}{\partial x} = 0$, $\qquad$ (4.31a, b, c, d)

For free edges: $Q_x = \psi$, $\quad N_x = 0$, $\quad N_{xs} = 0$, $\quad M_x = 0$, $\qquad$ (4.32a, b, c, d)

For beam support: $w = w_b$, $\quad \dfrac{dw}{dx} = \phi_b$, $\quad Q_x = q_{rb} + \psi$, $\quad M_x = m_{tb}$ $\quad$ (4.33a, b, c, d)

4.4.5 Continuity Conditions

The following continuity conditions are applied along the shared edge between strips I and $I + 1$ at $x = x_i$

$$u_{xI} = u_{x(I+1)}, \quad u_{sI} = u_{s(I+1)}, \quad w_I = w_{(I+1)}, \quad \frac{\partial w_I}{\partial x} = \frac{\partial w_{(I+1)}}{\partial x} \qquad \text{(4.34a, b, c, d)}$$

and

$$M_{xI} = M_{x(I+1)}, \; N_{xI} = N_{x(I+1)}, \; Q_{xI} = Q_{x(I+1)} + \psi_i, \; N_{xsI} = N_{xs(I+1)} \quad \text{(4.35a, b, c, d)}$$

When a beam is present at $x = x_i$, the following continuity conditions are imposed along the common edge $x = x_i$, between strips I and $I+1$.

$$u_{xI} = u_{x(I+1)}, \quad u_{sI} = u_{s(I+1)}, \quad w_I = w_{(I+1)}, \quad \frac{\partial w_I}{\partial x} = \frac{\partial w_{(I+1)}}{\partial x} = \phi_b \qquad \text{(4.36a, b, c, d)}$$

and

$$m_{tb} = M_{x(I+1)} - M_{xI}, \; q_{xb} = N_{x(I+1)} - N_{xI}, \qquad\qquad\qquad \text{(4.37a, b)}$$

4.5 Solution

A cylindrical shell is divided into N-strips (Figure 4.1) depending on the number of loading discontinuities and the locations of the ring stiffeners. For each of the N-strips, eight equations are generated from the boundary and continuity conditions. This yields a unique $8N$ system of equations for each mode ($m = 0, 1, 2, \ldots, \infty$). Solution of these

systems of equations provide the constants C_{dmI} (d = 1, 2, …, 8) in the homogeneous solution. The potential function Φ_I for each strip I (I = 1, 2, …, N) is derived by summing the homogeneous and particular solutions. The potential function is then back-substituted into the relevant force and displacement equations.

4.6 Application

Because of the ill-conditioned nature of the solution, the ASM is susceptible to numerical instabilities when computing solutions using double precision floating point format. To eliminate this concern, examples are computed with a MATLAB (Mathworks, 2017) program using an arbitrary-precision package.

4.6.1 Example 1: Cylindrical Shell Subjected to Non-Axisymmetric Loads

The purpose of this example is to compare the Analytical Strip Method (ASM) results for cylindrical shells subjected to non-axisymmetric loads to an existing analytical solution developed by Bijlaard (1955) for the design of pressure vessels subjected to point and patch loads.

The shells in Figure 4.3 and Figure 4.4 are simply supported at the ends, $(\partial u_x / \partial x) = u_s = w = M_x = 0$, and are subject to a point load and a patch load at mid-length, respectively. The magnitude of the point load is designated as P, while the resultant (or total) magnitude of the patch load is $P^* = 4pc_1c_2$, where p is the distributed load and c_1 and c_2 are the half-lengths of the patch area in the circumferential and longitudinal direction respectively (Figure 4.4). Poisson's ratio v = 0.30.

Table 4.3 presents the dimensionless radial deflection and force quantities corresponding to bending moments M_s and M_x as well as membrane forces N_s and N_x. The results are presented for prescribed radius-to-thickness ratios (R/t) and length-to-radius ratios (L/R) at $x = L/2$, $s = 0$. The results are presented for an existing analytical solution (Bijlaard,

1955), the Analytical Strip Method (ASM), and a finite-element (FEM) solution generated using SAP2000 (Computers and Structures, Inc., 2015).

The results show excellent agreement between the ASM and FEM solutions; the dimensionless quantities are all within 2% difference. There is also good agreement between the existing analytical solution (Bijlaard, 1955) and the ASM for the dimensionless deflection quantities and the dimensionless force quantities corresponding to M_s and N_x; the values are predominately within 3% difference. The dimensionless force quantities for M_x and N_s show more variation between the existing analytical solution (Bijlaard, 1955) and the ASM; the difference in the two solutions is as much as 10% with the larger differences occurring at larger radius-to-thickness ratios.

In development of the existing analytical solution, Bijlaard's intent was to develop a set of practical equations that could be used in practice for the evaluation of local stresses in pressure vessels. As a result, there were several simplifications made in his formulation at the cost of accuracy in the solution; the most significant being the neglect of the fourth-order terms in his combined eight-order differential equation. The neglected terms correspond to the absence of

$$\frac{t^2}{12R^2}\left[(1-\nu)\frac{\partial^2 v}{\partial x^2} + \frac{\partial^2 v}{\partial s^2}\right] \tag{4.39}$$

in the second of Timoshenko's (1959) three uncoupled differential equations. This term is fully incorporated into the ASM solution. The neglect of this term will not fully capture the membrane stiffness of the shell and is likely a major contributor in the differences in the dimensionless M_x and N_s values between the existing analytical solution (Bijlaard, 1955) and the ASM and FEM.

The ASM results in Table 4.3 are based on summation of the first 51 modes. For the case of radius-to-thickness ratio of 100 and length-to-radius ratio of 3, Table 4.4 presents the cumulative dimensionless deflection and force quantities for selected modes. The solution demonstrates good convergence. The dimensionless force quantity associated with bending moments M_s and M_x converged slower than the other results with variation of 1.7% and 0.6%, respectively, between modes 40 and 50.

4.6.2 Example 2: Cylindrical Shell Subjected to Line Load along the Generator

The purpose of this example is to compare the Analytical Strip Method (ASM) results for a cylindrical shell subjected to a line load with an existing analytical solution developed by Hoff, et al. (1954) with numerical results derived by Kempner (1955).

The shell in Figure 4.5 is simply supported at the ends, $(\partial u_x/\partial x) = u_s = w = M_x = 0$, and is subject to a line load centered at mid-length of the cylinder. The line load has a total magnitude designated as $P^* = 2c_2p$ and a half-length designated at c_2. The modulus of elasticity $E = 2.07\text{x}10^8$ kPa $= 30\text{x}10^6$ psi and Poisson's ratio $v = 0.30$.

Table 4.5 presents the dimensionless radial deflection and force quantities at $x = L/2$, $s = 0$ corresponding to bending moments M_s and M_x as well as membrane forces N_s and N_x. The results presented by Kempner (1955) are compared with ones generated using the ASM and the finite-element method (FEM) solution generated using SAP2000 (Computers and Structures, Inc., 2015). The results of all three methods are in very good agreement.

4.6.3 Example 3: Stiffened Tank

The steel tank in Figure 4.6 has a fixed base and is stiffened with standard W10x49 steel rolled sections having an area $A = 9290$ mm^2 (14.4 in^2) and a moment of inertia $I_x = 1.132\text{x}10^8$ mm^4 (272 in^4). The dimensions and fluid properties for the tank are presented in Table 4.6. The modulus of elasticity of the tank and stiffener $E = 2\text{x}10^8$ kPa (29x10^6 psi) and Poisson's ratio $v = 0.3$.

The inclusion of the stiffeners as well as the variation in wall thickness and loading through the height of the cylinder limits the use of existing analytical solutions. The Analytical Strip Method (ASM) is deployed herein by identifying the six geometric and loading discontinuities, dividing the cylinder into five strips between the discontinuity points, and imposing the boundary and continuity conditions at the ends of each strip. Figure 4.7 through Figure 4.9 present the radial displacement w, bending moment M_x, and

shear Q_x, along the height of the stiffened tank. Comparison with existing analytic methods of solution is not possible. Consequently, the results of the ASM are compared with the finite-element (FEM) results generated using SAP2000 (Computers and Structures, Inc., 2015). To provide a direct comparison, the FEM analysis was performed with stiffeners concentric to the middle surface of the cylinder walls. The two results are in very good agreement. An additional FEM analysis was performed with stiffeners at their true eccentricity. These results correlate well with the FEM results for concentric stiffeners indicating that the eccentricity has minor impact on the deflection and force quantities for this example.

4.6.4 Example 4: Stiffened Tank Subjected to Line Load

The purpose of this example is to demonstrate the application of the Analytical Strip Method (ASM) to a stiffened cylinder subjected to non-axisymmetric loading. Existing analytical solutions to these type problems are not available.

The steel cylinder in Figure 4.10 is stiffened with standard W10x49 steel rolled sections having an area A = 9290 mm^2 (14.4 in^2), a moment of inertia about the section x-axis I_x = 1.132x10^8 mm^4 (272 in^4), a moment of inertia about the section y-axis I_y = 3.888x10^7 mm^4 (93.4 in^4), and a torsion constant J = 5.786x10^5 mm^4 (1.39 in^4). The modulus of elasticity of the cylinder and stiffener E = 2x10^8 kPa (29x10^6 psi) and Poisson's ratio v = 0.3. The ends are simply supported with boundary conditions, $u = s = w = M_x = 0$. The cylinder is subjected to a line load p = 0.01 kN/mm (57.1 lb/in).

The inclusion of the stiffeners, as well as the non-axisymmetric loading, limits the use of analytical solutions. Just as in Example 3, for a shell subjected to axisymmetric loads, the ASM is deployed by identifying four strips between the stiffeners and imposing the boundary and continuity conditions at the ends of each strip. Comparison with existing analytic methods of solution is not possible. Consequently, the results of the ASM are compared with the finite-element (FEM) results generated using SAP2000 (Computers

and Structures, Inc., 2015). Figure 4.11 presents the radial deflection along the generator, $s = 0$. There is excellent agreement between the ASM solution and the FEM solution.
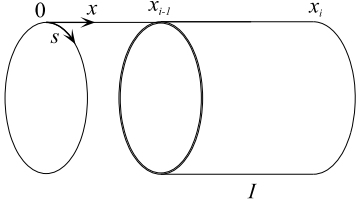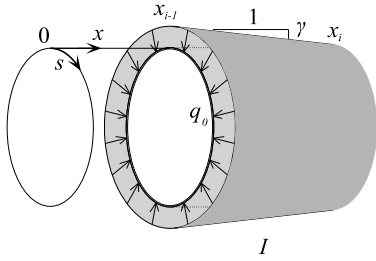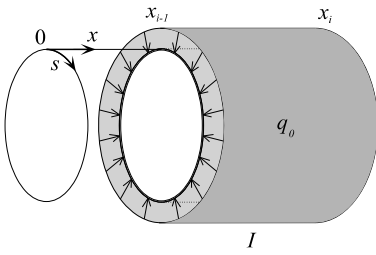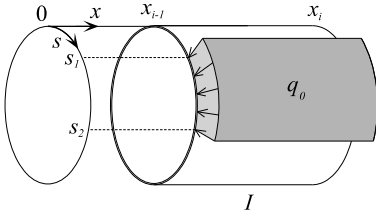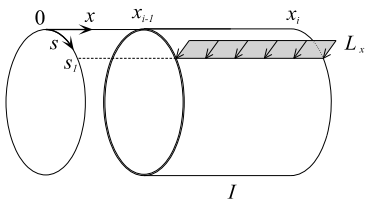
The ASM results are based on summation of the first 51 modes. Table 4.7 presents the radial deflection quantity for several modes at distances of $x = 375$ mm (14.8 in) and $x = 500$ mm (19.7 in) along the generator, $s = 0$. The series shows good convergence characteristics, mode 50 contributes less than 0.04% to the cumulative deflection at both locations presented.

4.7 Conclusions
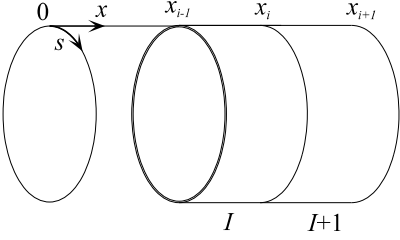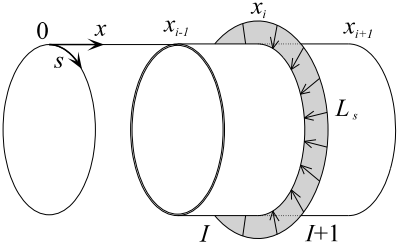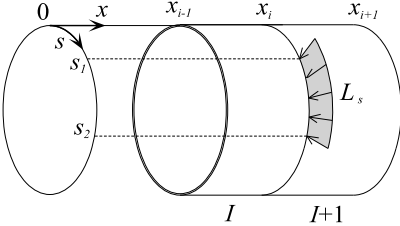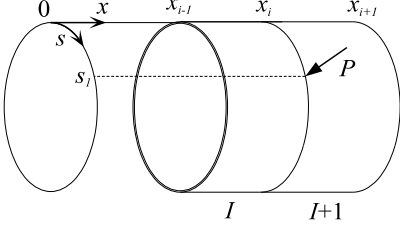
The Analytical Strip Method (ASM) is presented in this paper for stiffened isotropic cylindrical shells. The primary advantage of the ASM is its applicability to any generalized distribution of ring stiffeners along the length of the shell and to any combination of patch, uniform, line, concentrated, and hydrostatic loads. The following are deduced from the derivation of the ASM and the examples presented in this paper:

- The results of the ASM are in good agreement with existing analytical solutions, and the generality of the solution method overcomes many limitations of existing analytical solutions.
- Unlike the finite element method, the ASM does not require significant pre-processing effort. Its accuracy is dependent on the number of modes considered in the solution rather than the fineness of the discretization of the structure.
- The finite element method does offer more flexibility in structure geometry. For instance, the ASM requires stiffeners to be concentric with the shell walls and stepped wall thicknesses to have a coincident middle surface.
- The finite element method has less potential for numerical instabilities than the ASM.

Table 4.1. Particular solution $\Phi_{PI}(x,s)$ for cylindrical strip I

Load Case	$\Phi_{PI}(x,s)$

Case 1 - Zero load

$$\Phi_{PI}(x,s) = 0$$

Case 2 - Linearly varying load (hydrostatic load)

$$q(x,s) = q_0 - \gamma(x - x_{i-1})$$

$$\Phi_{PIm=0}(x,s) = \frac{q_0}{24A_{40}^*}x^4 - \frac{\gamma}{120A_{40}^*}x^5$$

$$\Phi_{PIm=1,2,\dots,\infty}(x,s) = 0$$

Case 3 - Uniform load q_0

$$\Phi_{PIm=0}(x,s) = \frac{q_0}{24A_{40}^*}x^4$$

$$\Phi_{PIm=1,2,\dots,\infty}(x,s) = 0$$

Case 4 - Partial uniform load q_0

$$\Phi_{PIm=0}(x,s) = \frac{q_0}{48\pi RA_{40}^*}(s_2 - s_1)x^4$$

$$\Phi_{PIm=1}(x,s) = \frac{q_0}{2\pi RA_{21}^*}\left[\sin\left(\frac{s_2}{R}\right) - \sin\left(\frac{s_1}{R}\right)\right]x^2\cos\left(\frac{s}{R}\right)$$

$$\Phi_{PIm=2,3,\dots,\infty}(x,s) = \frac{q_0}{m\pi RA_{0m}^*}\left[\sin\left(\frac{m}{R}s_2\right) - \sin\left(\frac{m}{R}s_1\right)\right]\cos\left(\frac{m}{R}s\right)$$

Case 5 - Line load L_x

$$\Phi_{PIm=0}(x,s) = \frac{L_x}{48\pi RA_{40}^*}x^4$$

$$\Phi_{PIm=1}(x,s) = \frac{L_x}{2\pi RA_{21}^*}\cos\left(\frac{s_1}{R}\right)x^2\cos\left(\frac{s}{R}\right)$$

$$\Phi_{PIm=2,3,\dots,\infty}(x,s) = \frac{L_x}{\pi RA_{0m}^*}\cos\left(\frac{m}{R}s_1\right)\cos\left(\frac{m}{R}s\right)$$

63

Table 4.2. Edge loading function $\psi_i(s)$ along the edge $x = x_i$

Load Case	$\psi_i(s)$
Case 1 - Zero load	

$$\psi_i(s) = 0$$

Case 2 - Line load L_s in s direction

$$\psi_{im=0}(s) = L_s$$

$$\psi_{im=1,2,\dots,\infty}(s) = 0$$

Case 3 - Partial line load L_y

$$\psi_{im=0}(s) = \frac{L_s(s_2 - s_1)}{2\pi R}$$

$$\psi_{im=1,2,\dots,\infty}(s) = \frac{2L_s}{m\pi} \sin\left[\frac{m}{2R}(s_2 - s_1)\right] \cos\left[\frac{m}{R}\left(s - \frac{s_1 + s_2}{2}\right)\right]$$

Case 4 - Concentrated point load P

$$\psi_{im=0}(s) = \frac{P}{2\pi R}$$

$$\psi_{im=1,2,\dots,\infty}(s) = \frac{P}{\pi R} \cos\left[\frac{m}{R}(s - s_1)\right]$$

Table 4.3. Dimensionless deflection and forces at $x = L/2$ and $s = 0$ for the cylindrical shell subjected to point load, P, in Figure 4.3 and to patch load, $P^* = 4pc_1c_2$, with $c_1 = c_2$ in Figure 4.4.

R/t	L/R	Method	Point Load $\dfrac{wER}{P}$	Patch Load $\dfrac{wER}{P^*}$	$\dfrac{M_s}{P^*}$	$\dfrac{M_x}{P^*}$	$-\dfrac{N_s R}{P^*}$	$-\dfrac{N_x R}{P^*}$
		Bijlaard[a]	300	272	0.1324	0.1057	2.613	2.320
	3	ASM[b]	296	267	0.1321	0.1045	2.482	2.282
		FEM[c]	299	269	0.1333	0.1052	2.460	2.300
		Bijlaard	468	442	0.1438	0.1100	2.592	2.640
15	6	ASM	463	434	0.1438	0.1079	2.439	2.619
		FEM	469	438	0.1452	0.1086	2.420	2.640
		Bijlaard	601	576	0.1463	0.1102	2.574	2.784
	10	ASM	597	566	0.1473	0.1087	2.428	2.719
		FEM	586	570	0.1486	0.1095	2.420	2.740
		Bijlaard	4352	3645	0.0863	0.0559	6.451	7.120
	3	ASM	4324	3573	0.0857	0.0556	6.367	7.038
		FEM	4350	3596	0.0864	0.0559	6.360	7.060
		Bijlaard	7631	6924	0.0967	0.0614	6.482	8.064
50	8	ASM	7608	6826	0.0956	0.0585	6.310	8.001
		FEM	7656	6844	0.0964	0.0588	6.300	8.020
		Bijlaard	13430	12930	0.1030	0.0634	6.434	8.704
	20	ASM	12667	11853	0.1007	0.0599	6.292	8.466
		FEM	12702	11890	0.1015	0.0603	6.280	8.500
		Bijlaard	20227	15800	0.0626	0.0343	9.578	12.784
	3	ASM	20256	15643	0.0617	0.0341	9.517	12.744
		FEM	20532	15660	0.0627	0.0344	9.520	12.760
		Bijlaard	34350	30136	0.0716	0.0394	9.792	14.192
100	8	ASM	34747	29857	0.0704	0.0366	9.450	14.142
		FEM	35032	29870	0.0711	0.0368	9.460	14.160
		Bijlaard	74379	71448	0.0767	0.0400	9.618	15.472
	30	ASM	74124	68968	0.0760	0.0382	9.432	15.400
		FEM	74472	69020	0.0767	0.0385	9.440	15.420
		Bijlaard	231738	158362	0.0337	0.0137	13.696	29.328
	3	ASM	234848	157615	0.0332	0.0135	13.617	29.188
		FEM	237974	157180	0.0337	0.0136	13.620	29.140
		Bijlaard	402590	313842	0.0406	0.0172	14.963	32.288
	8	ASM	397532	315039	0.0394	0.0154	13.532	32.197
300		FEM	404260	314592	0.0399	0.0155	13.540	32.160
		Bijlaard	625855	566530	0.0440	0.0180	14.584	33.424
	20	ASM	676570	590498	0.0431	0.0165	13.512	34.344
		FEM	683356	590092	0.0436	0.0166	13.520	34.300
		Bijlaard	968910	925438	0.0453	0.0180	14.200	34.128
	40	ASM	1014420	925796	0.0453	0.0171	13.504	35.043
		FEM	1021380	925506	0.0458	0.0172	13.520	35.000

[a] Bijlaard = Existing Analytical Solution (Bijlaard, 1955)
[b] ASM = Analytical Strip Method
[c] FEM = Finite Element Solution (Computers and Structures, Inc., 2015)

Table 4.4. ASM cumulative dimensionless deflections and forces at $x = L/2$ and $s = 0$ for the cylindrical shell subjected to a point load, P, in Figure 4.3 and to a patch load, P^* = $4pc_1c_2$ with $c_1 = c_2$ in Figure 4.4; $R/t = 100$ and $L/R = 3$.

Note: $\mathbf{w} = \sum_0^m \mathbf{w_m}$, $\mathbf{M} = \sum_0^m \mathbf{M_m}$, $\mathbf{N} = \sum_0^m \mathbf{N_m}$

Mode	Point Load	Patch Load				
m	$\dfrac{wER}{P}$	$\dfrac{wER}{P^*}$	$\dfrac{M_s}{P^*}$	$\dfrac{M_x}{P^*}$	$-\dfrac{N_sR}{P^*}$	$-\dfrac{N_xR}{P^*}$
0	102	64	0.0001	0.0004	0.641	0.000
1	371	255	0.0004	0.0012	1.917	0.227
2	1043	842	0.0008	0.0021	3.174	1.127
5	9930	9054	0.0146	0.0098	6.410	7.212
10	16698	14448	0.0435	0.0248	8.972	11.530
20	19401	15648	0.0644	0.0348	9.510	12.738
30	19969	15666	0.0647	0.0350	9.514	12.752
40	20167	15643	0.0627	0.0343	9.516	12.744
50	20256	15643	0.0617	0.0341	9.517	12.744

Table 4.5. Dimensionless deflection and forces at $x = L/2$ and $s = 0$ for the cylindrical shell subjected to a line load with total magnitude of $P^* = 2c_2p$ in Figure 4.5.

Method	$\dfrac{wER}{P^*}$	$\dfrac{M_s}{P^*}$	$\dfrac{M_x}{P^*}$	$-\dfrac{N_sR}{P^*}$	$-\dfrac{N_xR}{P^*}$
Kempner (1955)	6211	0.196	0.107	8.094	9.275
ASM	6201	0.190	0.102	8.031	9.304
FEM	6208	0.196	0.105	8.170	9.337

Table 4.6. Dimensions and fluid properties for the tank in Figure 4.6

Specific	$\gamma_1 =$	9.81 kN/m³ (62.4 pcf)
Gravity	$\gamma_2 =$	7.35 kN/m³ (46.8 pcf)
Wall	$t_1 =$	76.2 mm (3.0 in)
Thickness	$t_2 =$	38.1 mm (1.5 in)
Radius	$R =$	6.1 m (20 ft)
	$H =$	6.08 m (20 ft)
	$H_1 =$	1.52 m (5.0 ft)
	$H_2 =$	0.76 m (2.5 ft)
Height	$H_3 =$	0.76 m (2.5 ft)
	$H_4 =$	1.52 m (5.0 ft)
	$H_5 =$	1.52 m (5.0 ft)

Table 4.7. ASM cumulative deflections $w = \sum_0^m w_m$ along the generator ($s = 0$) at $x = $ 375 mm (14.8 in) and $x = 500$ mm (19.7 in) for the stiffened cylindrical shell in Figure 4.10.

Mode	$x = 375$ mm (14.8 in)		$x = 500$ mm (19.7 in)	
	w	w	w	w
m	(10^{-3} mm)	(10^{-4} in)	(10^{-3} mm)	(10^{-4} in)
0	0.86	0.34	0.03	0.01
1	4.39	1.73	2.23	0.88
2	7.14	2.81	2.78	1.09
5	17.3	6.82	2.91	1.15
10	43.6	17.2	2.92	1.15
20	69.2	27.2	2.93	1.15
30	73.7	29.0	2.93	1.15
40	74.8	29.5	2.93	1.15
50	75.2	29.6	2.93	1.15
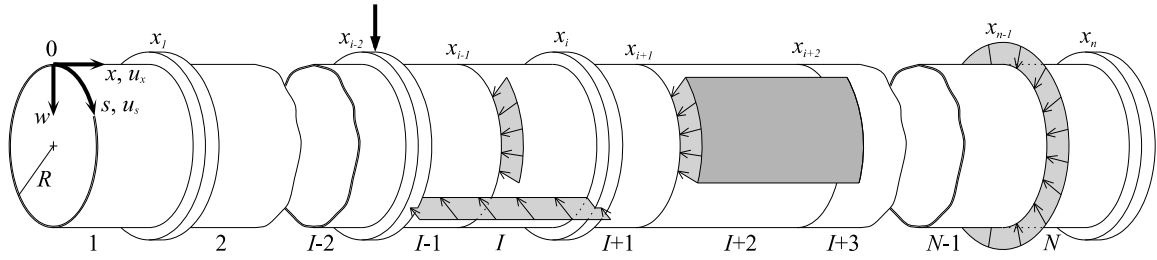
Figure 4.1. Stiffened cylindrical shell with strip and edge loadings
Note: The stiffeners are concentric with the shell
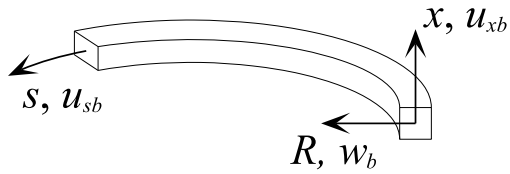
Figure 4.2. Coordinate system for the ring stiffener
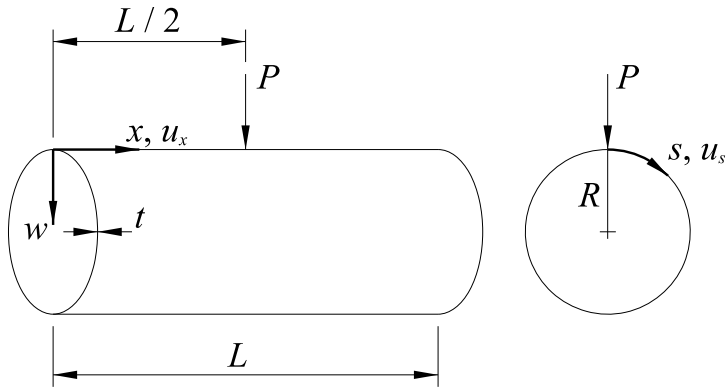
Figure 4.3. Cylindrical Shell Subjected to Point Load

$$c_1 / R = 0.125$$
$$c_2 / R = 0.125$$
$$P* = 4 \, p \, c_1 \, c_2$$
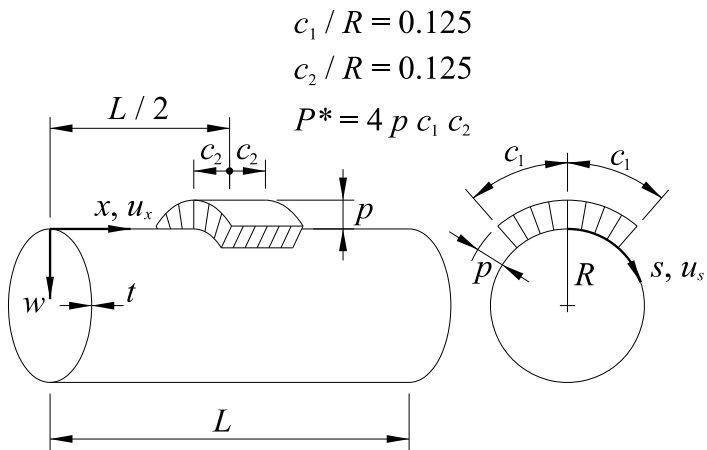
Figure 4.4. Cylindrical Shell Subjected to Patch Load
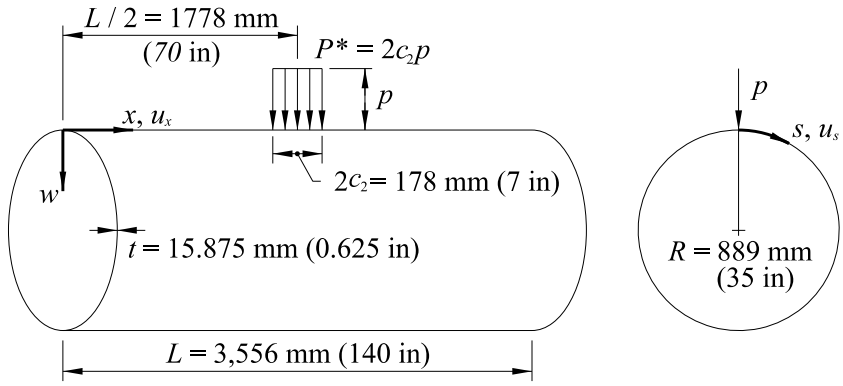
Figure 4.5. Cylindrical shell subjected to a line load
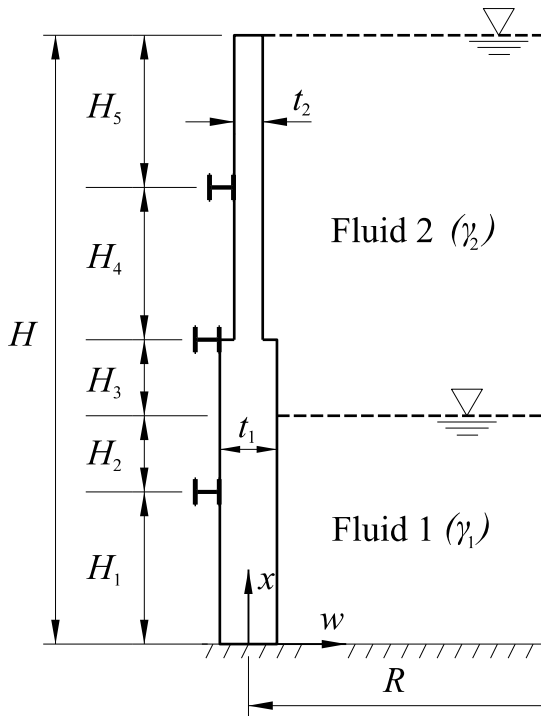
Figure 4.6. Stiffened tank with clamped base
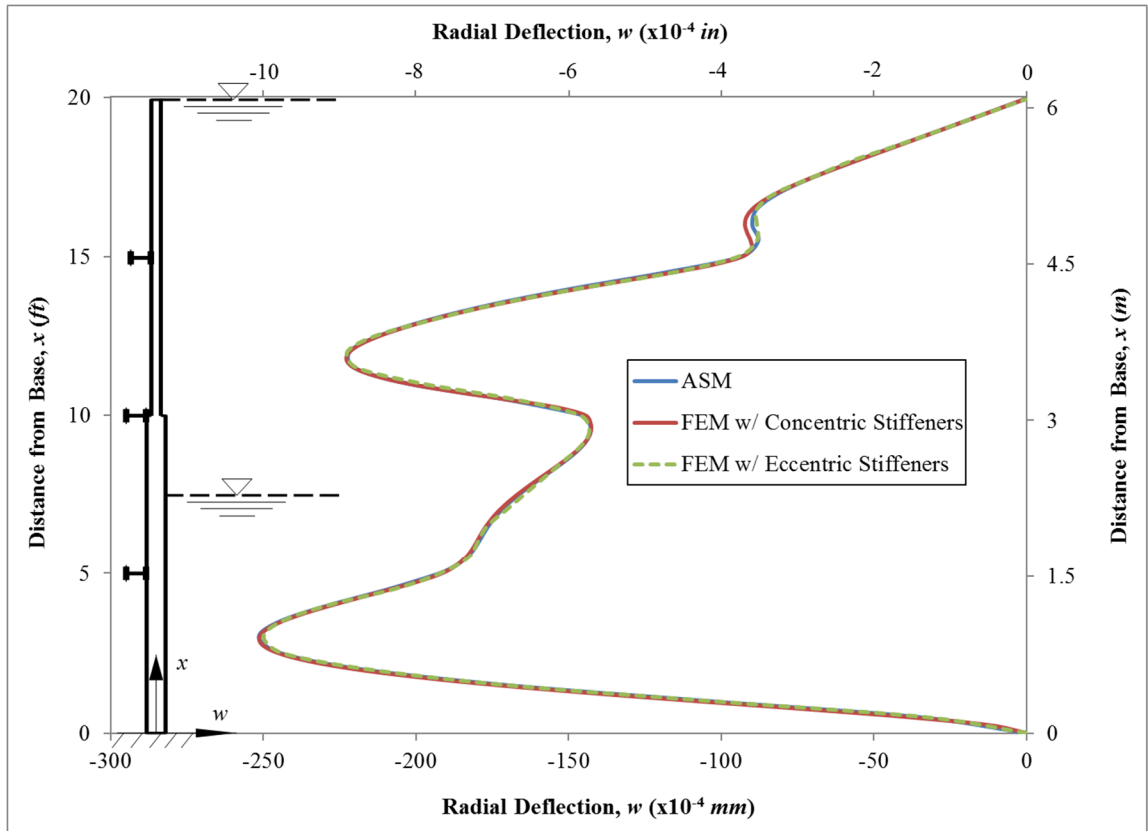
Figure 4.7. Radial deflection for the stiffened tank in Figure 4.6

      Note: The ASM and FEM results are in very good agreement and difficult to discern in the figure
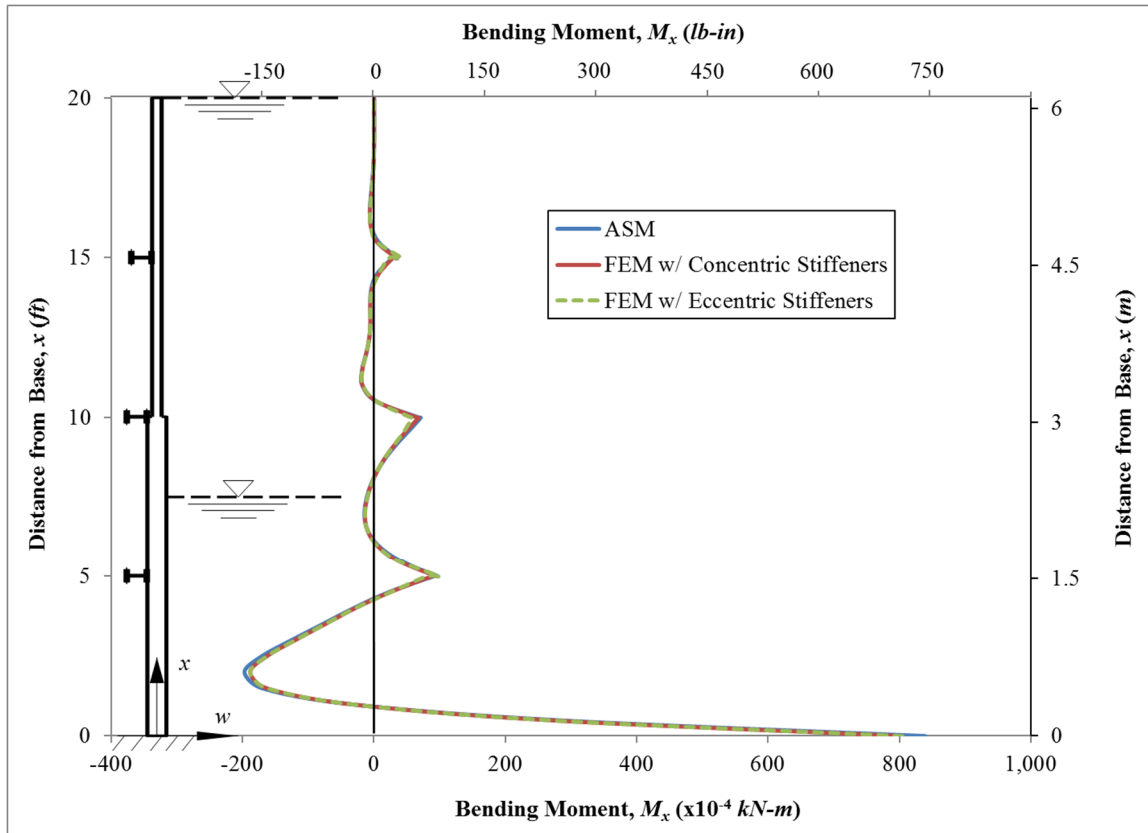
Figure 4.8. Bending moment, M_x, for the stiffened tank in Figure 4.6

        Note: The ASM and FEM results are in very good agreement and difficult

          to discern in the figure
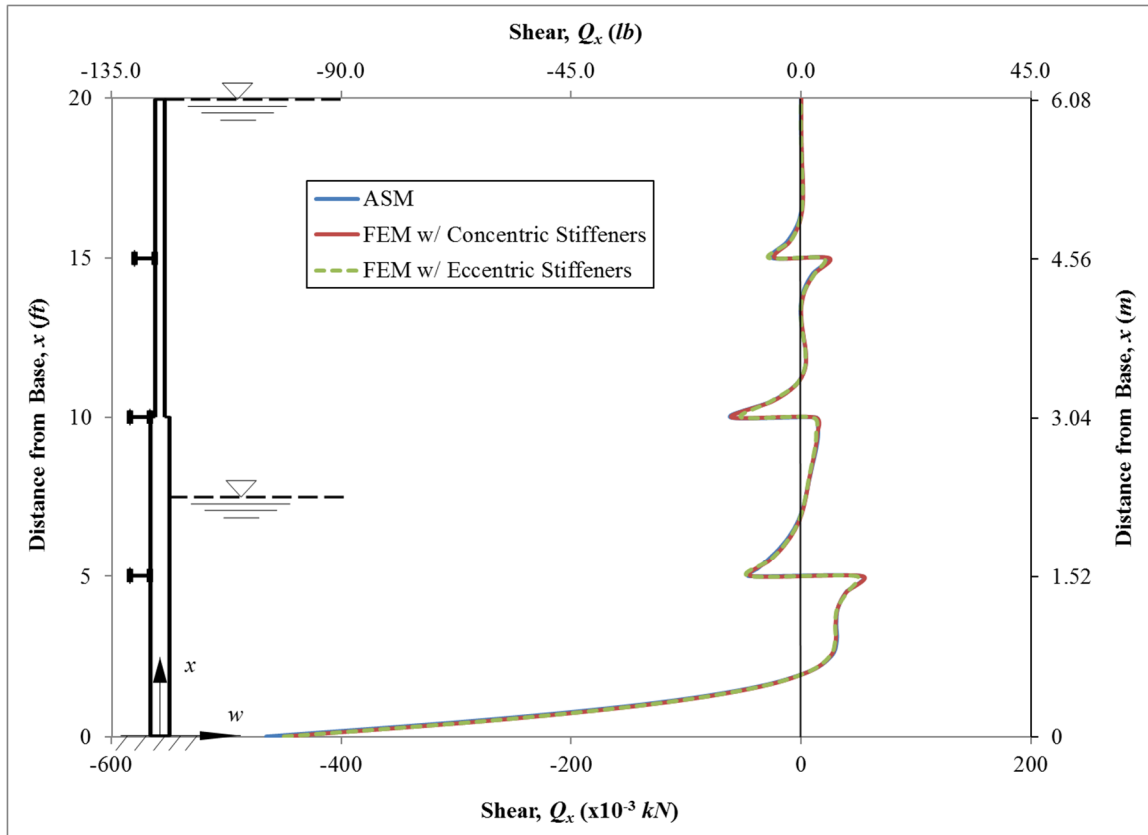
Figure 4.9. Shear, Q_x, for the stiffened tank in Figure 4.6

> *Note: The ASM and FEM results are in very good agreement and difficult to discern in the figure*
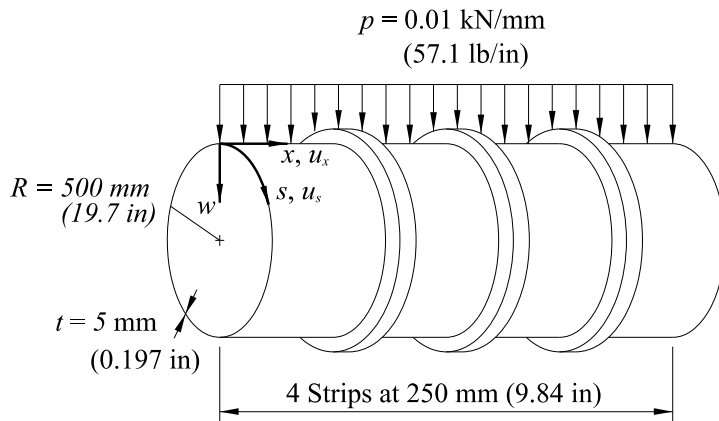
Figure 4.10. Stiffened cylindrical shell subjected to a line load
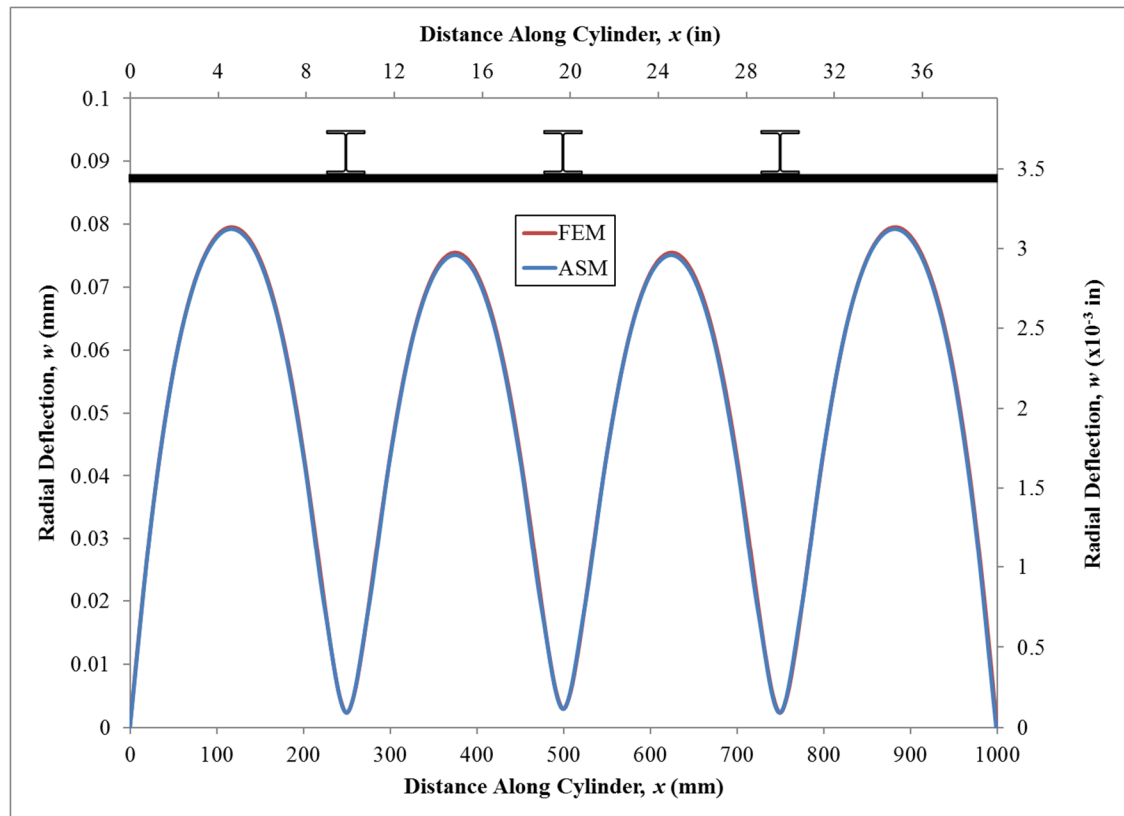
Figure 4.11. Radial deflection, *w*, along the generator (*s* = 0) for the stiffened cylinder in Figure 4.10

> *Note: The ASM and FEM results are in very good agreement and difficult to discern in the figure*

CHAPTER 5

ANALYTICAL STRIP METHOD FOR THIN LAMINATED CYLINDRICAL SHELLS

5.1 Introduction

Laminated shells are widely used in civil, environmental, mechanical, and aerospace applications due to their high stiffness-to-weight ratio. The layered nature of laminates allows for optimal and economical use of the material. Several laminated shell theories have been developed to simplify complex three-dimensional elasticity based solutions. These theories are roughly divided into two categories, thin shell theories which adopt Love's assumptions (Ambartsumian, 1961, 1966; Bert, 1975) and higher order shell theories that relax one or more of Love's assumptions (Vasilenko and Golub, 1984; Reddy, 2004; Barbero et al., 1990).

Three-dimensional elasticity solutions and higher order shell theories are well suited for thick to moderately thick shells. Elasticity solutions for laminated composite shells are widely available (Ren, 1987, 1995; Chandrashekhara and Nanjunda Rao, 1997, 1998; Varadan and Bhaskar, 1991). Noor and Burton (1990) provide and exhaustive review of available solutions. The applicability of these solutions is generally constrained to shells of infinite length or with simplified loading conditions. Although thin shell theories poorly capture the behavior of shells with low radius-to-thickness ratios, they perform reliably for higher radius-to-thickness ratios (Ren, 1987) and the simplifying assumptions in the theory facilitate the incorporation of complex loading and boundary conditions.

The objective of this paper is to develop an analytical strip method (ASM) of solution for stiffened and laminated thin cylindrical shells. The solution is applicable to laminated shells with any generalized layer configuration and ply-angle scheme, such that the shell behaves anisotropically. The ASM was first developed by Harik and Salamoun (1986, 1988) for the analysis of thin orthotropic and stiffened rectangular plates subjected to uniform, partial uniform, patch, line, partial line and point loads or any combination thereof. The solution procedure requires that the structure be divided into strips based on

the geometric discontinuities and applied loads (Figure 5.1). The governing differential equation for each strip is solved analytically and the applicable continuity and boundary conditions are used to combine the solutions for the strips.

The primary contribution of the ASM is in its ability to handle a wide variety of loading and geometric configurations. At present, analytical solutions are limited to axisymmetric and simple non-axisymmetric loadings applied to cylindrical shells of basic geometry. Other more complex cases must utilize numerical or semi-numerical techniques. Unlike numerical based solutions, the accuracy of the ASM does not depend on the number of strips within the structure, but rather the number of modes considered in the series solution.

5.2 Governing Differential Equation for Laminated Cylindrical Shells

The surface coordinate system used in the derivation of the governing equation for a cylindrical strip is shown in Figure 5.1. The strain-displacement equations associated with thin shell theory are given as (Kraus, 1967)

$$\epsilon_x = \frac{\partial u_x}{\partial x} \tag{5.1a}$$

$$\epsilon_s = \frac{\partial u_s}{\partial s} + \frac{w}{R} \tag{5.1b}$$

$$\gamma_{xs} = \frac{\partial u_s}{\partial x} + \frac{\partial u_x}{\partial s} \tag{5.1c}$$

$$\kappa_x = -\frac{\partial^2 w}{\partial x^2} \tag{5.1d}$$

$$\kappa_s = \frac{\partial}{\partial s}\left(\frac{u_s}{R} - \frac{\partial w}{\partial s}\right) \tag{5.1e}$$

$$\kappa_{xs} = \frac{1}{R}\frac{\partial u_s}{\partial x} - 2\frac{\partial^2 w}{\partial x \partial s} \tag{5.1f}$$

And the equilibrium equations are (Kraus, 1967)

$$\frac{\partial N_x}{\partial x} + \frac{\partial N_{sx}}{\partial s} + q_x = 0 \qquad (5.2a)$$

$$\frac{\partial N_{xs}}{\partial x} + \frac{\partial N_s}{\partial s} + \frac{Q_s}{R} + q_s = 0 \qquad (5.2b)$$

$$\frac{\partial Q_x}{\partial x} + \frac{\partial Q_s}{\partial s} - \frac{N_s}{R} + q = 0 \qquad (5.2c)$$

$$\frac{\partial M_x}{\partial x} + \frac{\partial M_{xs}}{\partial s} - Q_x = 0 \qquad (5.2d)$$

$$\frac{\partial M_{xs}}{\partial x} + \frac{\partial M_s}{\partial s} - Q_s = 0 \qquad (5.2e)$$

The five equilibrium equations are reduced to three by substituting Eq. (5.2d) and Eq. (5.2e) into Eq. (5.2c). Substitution of the strain-displacement equations into the equilibrium equations yield a system of three differential equations that may be presented as

$$\begin{bmatrix} L_{11} & L_{12} & L_{13} \\ L_{12} & L_{22} & L_{23} \\ L_{13} & L_{23} & L_{33} \end{bmatrix} \begin{Bmatrix} u_x \\ u_s \\ w \end{Bmatrix} = \begin{Bmatrix} q_x \\ q_s \\ q \end{Bmatrix} \qquad (5.3)$$

where, differential operators L_{ij} are

$$L_{11} = A_{11}\frac{\partial^2}{\partial x^2} + 2A_{16}\frac{\partial^2}{\partial x \partial s} + A_{66}\frac{\partial^2}{\partial s^2} \qquad (5.4a)$$

$$L_{12} = \left(A_{16} + \frac{1}{R}B_{16}\right)\frac{\partial^2}{\partial x^2} + \left(A_{12} + A_{66} + \frac{1}{R}B_{12} + \frac{1}{R}B_{66}\right)\frac{\partial^2}{\partial x \partial s} +$$

$$\left(A_{26} + \frac{1}{R}B_{26}\right)\frac{\partial^2}{\partial s^2} \qquad (5.4b)$$

$$L_{13} = -B_{11}\frac{\partial^3}{\partial x^3} + \frac{1}{R}A_{12}\frac{\partial}{\partial x} - 3B_{16}\frac{\partial^3}{\partial x^2 \partial s} - (B_{12} + 2B_{66})\frac{\partial^3}{\partial x \partial s^2} + \frac{1}{R}A_{26}\frac{\partial}{\partial s} -$$

$$B_{26}\frac{\partial^3}{\partial s^3} \qquad (5.4c)$$

$$L_{22} = \left(A_{66} + \frac{1}{R^2}D_{66} + \frac{2}{R}B_{66}\right)\frac{\partial^2}{\partial x^2} + 2\left(\frac{1}{R^2}D_{26} + \frac{2}{R}B_{26} + A_{26}\right)\frac{\partial^2}{\partial x \partial s} +$$

$$\left(A_{22} + \frac{2}{R}B_{22} + \frac{1}{R^2}D_{22}\right)\frac{\partial^2}{\partial s^2} \qquad (5.4d)$$

$$L_{23} = \left(-B_{16} - \frac{1}{R}D_{16}\right)\frac{\partial^3}{\partial x^3} + \frac{1}{R}\left(\frac{1}{R}B_{26} + A_{26}\right)\frac{\partial}{\partial x} -$$

$$\left(\frac{2}{R}D_{66} + \frac{1}{R}D_{12} + B_{12} + 2B_{66}\right)\frac{\partial^3}{\partial x^2 \partial s} + \left(-3B_{26} - \frac{3}{R}D_{26}\right)\frac{\partial^3}{\partial x \partial s^2} +$$

$$\frac{1}{R}\left(A_{22} + \frac{1}{R}B_{22}\right)\frac{\partial}{\partial s} + \left(-B_{22} - \frac{1}{R}D_{22}\right)\frac{\partial^3}{\partial s^3} \tag{5.4e}$$

$$L_{33} = \frac{1}{R^2}A_{22} + D_{11}\frac{\partial^4}{\partial x^4} + 4D_{16}\frac{\partial^4}{\partial x^3 \partial s} + (2D_{12} + 4D_{66})\frac{\partial^4}{\partial x^2 \partial s^2} - \frac{2}{R}B_{12}\frac{\partial^2}{\partial x^2}$$

$$-\frac{4}{R}B_{26}\frac{\partial^2}{\partial x \partial s} + 4D_{26}\frac{\partial^4}{\partial x \partial s^3} - \frac{2}{R}B_{22}\frac{\partial^2}{\partial s^2} + D_{22}\frac{\partial^4}{\partial s^4} \tag{5.4f}$$

where A_{ij} are the extensional stiffnesses, B_{ij} are the bending-extensional coupling stiffnesses, and D_{ij} are the bending stiffnesses. The stiffness coefficients are given by Reddy (2004) and are defined as

$$\{A_{ij}, B_{ij}, D_{ij}\} = \int_{-\frac{t}{2}}^{\frac{t}{2}} \bar{Q}_{ij}\{1, z, z^2\}dz; \quad i, j = 1,2,6 \tag{5.5}$$

where t is the thickness of the shell and $\bar{Q}_{ij}$ are the lamina stiffness coefficients (Reddy, 2004).

In symmetric laminates, $B_{ij} = 0$ in Eq. (5.4). In antisymmetric cross-ply laminates, $B_{12} = B_{16} = B_{26} = B_{66} = 0$ and $B_{22} = -B_{11}$ in Eq. (5.4). In antisymmetric angle-ply laminates, $B_{11} = B_{12} = B_{22} = B_{66} = 0$ in Eq. (5.4).

The displacements in the x, s, and r direction, u_x, u_s, and w, are presented in terms of the potential function $\Phi(x, s)$ (Sharma et al., 1980)

$$u_x = (L_{12}L_{23} - L_{13}L_{22})\Phi(x, s) \tag{5.6a}$$

$$u_s = (L_{13}L_{21} - L_{23}L_{11})\Phi(x, s) \tag{5.6b}$$

$$w = (L_{11}L_{22} - L_{12}L_{21})\Phi(x, s) \tag{5.6c}$$

For the case of radial loads only, the three equations can be combined into a single eighth order differential equation expressed in terms of the potential function Φ (Sharma et. al., 1980).

$$F_{80}\frac{\partial^8\Phi}{\partial x^8} + F_{71}\frac{\partial^8\Phi}{\partial x^7\partial s} + F_{62}\frac{\partial^8\Phi}{\partial x^6\partial s^2} + F_{53}\frac{\partial^8\Phi}{\partial x^5\partial s^3} + F_{44}\frac{\partial^8\Phi}{\partial x^4\partial s^4} + F_{35}\frac{\partial^8\Phi}{\partial x^3\partial s^5} + F_{26}\frac{\partial^8\Phi}{\partial x^2\partial s^6} +$$

$$F_{17}\frac{\partial^8\Phi}{\partial x\partial s^7} + F_{08}\frac{\partial^8\Phi}{\partial s^8} + F_{60}\frac{\partial^6\Phi}{\partial x^6} + F_{51}\frac{\partial^6\Phi}{\partial x^5\partial s} + F_{42}\frac{\partial^6\Phi}{\partial x^4\partial s^2} + F_{33}\frac{\partial^6\Phi}{\partial x^3\partial s^3} + F_{24}\frac{\partial^6\Phi}{\partial x^2\partial s^4} +$$

$$F_{15}\frac{\partial^6\Phi}{\partial x\partial s^5} + F_{06}\frac{\partial^6\Phi}{\partial s^6} + F_{40}\frac{\partial^4\Phi}{\partial x^4} + F_{31}\frac{\partial^4\Phi}{\partial x^3\partial s} + F_{22}\frac{\partial^4\Phi}{\partial x^2\partial s^2} + F_{13}\frac{\partial^4\Phi}{\partial x\partial s^3} + F_{04}\frac{\partial^4\Phi}{\partial s^4} = q(x,s)$$

$$(5.7)$$

The coefficients F_{ij} are presented in Eq. (2.25).

5.3 Isotropic Beam Equations

The following differential equations can be derived from the equilibrium of an isotropic curved beam element (Vlasov, 1961)

$$q_{xb} = E_b I_r\left(\frac{d^4 u_{xb}}{ds^4} - \frac{1}{R}\frac{d^2\phi_b}{ds^2}\right) + \frac{E_b C_w}{R}\left(\frac{d^4\phi_b}{ds^4} + \frac{1}{R}\frac{d^4 u_{xb}}{ds^4}\right) - \frac{G_b J_b}{R}\left(\frac{d^2\phi_b}{ds^2} + \frac{1}{R}\frac{d^2 u_{xb}}{ds^2}\right) \qquad (5.8)$$

$$q_{rb} = E_b I_x\left(\frac{d^4 w_b}{ds^4} - \frac{1}{R}\frac{d^3 u_{sb}}{ds^3}\right) + \frac{E_b A_b}{R}\left(\frac{du_{sb}}{ds} + \frac{1}{R}w_b\right) \qquad (5.9)$$

$$q_{sb} = \frac{E_b I_x}{R}\left(\frac{d^3 w_b}{ds^3} - \frac{1}{R}\frac{d^2 u_{sb}}{ds^2}\right) - E_b A_b\left(\frac{d^2 u_{sb}}{ds^2} + \frac{1}{R}\frac{dw_b}{ds}\right) \qquad (5.10)$$

$$m_{xb} = \frac{E_b I_r}{R}\left(-\frac{d^2 u_{xb}}{ds^2} + \frac{1}{R}\phi_b\right) + E_b C_w\left(\frac{d^4\phi_b}{ds^4} + \frac{1}{R}\frac{d^4 u_{xb}}{ds^4}\right) - G_b J_b\left(\frac{d^2\phi_b}{ds^2} + \frac{1}{R}\frac{d^2 u_{xb}}{ds^2}\right) \qquad (5.11)$$

The terms q_{xb}, q_{rb}, and q_{sb} are the distributed forces per unit length applied to the beam in the x, r, and s directions (Figure 5.2); m_{xb} is the twisting moment per unit length applied to the beam; u_{xb}, u_{sb}, and w_b are the deflections of the beam in the x, r, and s directions (Figure 5.2); ϕ_b is the twist angle of the beam; R is the radius measured to the centroid of the beam; $E_b I_r$ = flexural rigidity about the r-axis (Figure 5.2); $E_b I_x$ = flexural rigidity about the x-axis (Figure 5.2); $E_b A_b$ = axial stiffness of the beam; $G_b J_b$ = torsional rigidity of the beam; $E_b C_w$ = warping rigidity of the beam.

5.4 Analytical Strip Method

The solution of the differential equation for a general strip I assumes that the form for the potential function Φ_I satisfies continuity at the surface coordinate $s = 0$ and $s = 2\pi R$. Let

$$\Phi = \sum_n^{\infty} \phi_n(x) \cos(\beta_n s) \tag{5.12}$$

Where

$$\beta_n = \frac{n}{R} \tag{5.13}$$

Substituting Eq. (5.12) into the governing differential equation [Eq. (5.7)], multiplying both sides of the equation by $\cos(\beta_m s)$, integrating from $s = 0$ to $s = 2\pi R$, and summing from $m = 0$ to $m = \infty$ yields the following equation by orthogonality

$$\sum_m^{\infty} \left\{ F_{8m}^* \frac{d^8 \phi_m(x)}{dx^8} + F_{6m}^* \frac{d^6 \phi_m(x)}{dx^6} + F_{4m}^* \frac{d^4 \phi_m(x)}{dx^4} + F_{2m}^* \frac{d^2 \phi_m(x)}{dx^2} + F_{0m}^* \phi_m(x) \right\} =$$

$$\frac{1}{2\pi R} \int_0^{2\pi R} q(x, s) ds + \sum_{m=1}^{\infty} \frac{1}{\pi R} \int_0^{2\pi R} q(x, s) \cos(\beta_m s) \, ds \tag{5.14}$$

Where:

$$F_{8m}^* = F_{80} \tag{5.15a}$$

$$F_{6m}^* = -F_{62}\beta_m^{\ 2} \tag{5.15b}$$

$$F_{4m}^* = F_{44}\beta_m^{\ 4} - F_{42}\beta_m^{\ 2} + F_{40} \tag{5.15c}$$

$$F_{2m}^* = -F_{26}\beta_m^{\ 6} + F_{24}\beta_m^{\ 4} - F_{22}\beta_m^{\ 2} \tag{5.15d}$$

$$F_{0m}^* = F_{08}\beta_m^{\ 8} - F_{06}\beta_m^{\ 6} + F_{04}\beta_m^{\ 4} \tag{5.15e}$$

For $m = 0$, $F_{20}^* = F_{00}^* = 0$ and for $m = 1$, $F_{01}^* = 0$.

Eq. (5.14) is an infinite set of linear 8th order ordinary differential equations for $\phi_m(x)$ with $m = 0, 1, 2, \ldots, \infty$. The solution is obtained by superposition of the associated homogeneous and particular solutions.

$$\Phi(x,s) = \Phi_H(x,s) + \Phi_P(x,s) \tag{5.16}$$

where the homogeneous solution

$$\Phi_H(x,s) = \sum_m^\infty \phi_{Hm}(x)\cos(\beta_m s) \tag{5.17}$$

and the particular solution

$$\Phi_P(x,s) = \sum_m^\infty \phi_{Pm}(x)\cos(\beta_m s) \tag{5.18}$$

5.4.1 Homogeneous Solution

The homogeneous solution for mode m, $\phi_{Hm}(x)$, is expressed as

$$\phi_{Hm}(x) = e^{\gamma_m \beta_m x} \tag{5.19}$$

The characteristic equation of Eq. (5.19) for mode $m = 0$ is

$$F_8^* \gamma_m{}^8 + F_6^* \gamma_m{}^6 + F_4^* \gamma_m{}^4 = 0 \tag{5.20}$$

And the homogeneous solution for mode $m = 0$ is

$$\Phi_{H0}(x,s) = C_{10} + C_{20}x + C_{30}x^2 + C_{40}x^3 + [C_{50}\cosh(\gamma_{30}x) +$$
$$C_{60}\sinh(\gamma_{30}x)]\cos(\gamma_{40}x) + [C_{70}\cosh(\gamma_{30}x) + C_{80}\sinh(\gamma_{30}x)]\sin(\gamma_{40}x)$$
$$\tag{5.21}$$

The characteristic equation of Eq. (5.19) for mode $m = 1$ is

$$F_8^* \gamma_m{}^8 + F_6^* \gamma_m{}^6 + F_4^* \gamma_m{}^4 + F_2^* \gamma_m{}^2 = 0 \tag{5.22}$$

And the homogeneous solution for mode $m = 1$ is

$$\Phi_{H1}(x,s) = \begin{Bmatrix} C_{11} + C_{21}x + C_{31}e^{\gamma_{31}x} + C_{41}e^{-\gamma_{31}x} \\ +[C_{51}\cosh(\gamma_{11}x) + C_{61}\sinh(\gamma_{11}x)]\cos(\gamma_{21}x) \\ +[C_{71}\cosh(\gamma_{11}x) + C_{81}\sinh(\gamma_{11}x)]\sin(\gamma_{21}x) \end{Bmatrix}\cos(\beta_1 s) \tag{5.23}$$

The characteristic equation of Eq. (5.19) for all other modes ($m = 2, 3, \ldots, \infty$) is

$$F_8^* \gamma_m{}^8 + F_6^* \gamma_m{}^6 + F_4^* \gamma_m{}^4 + F_2^* \gamma_m{}^2 + F_0^* = 0 \qquad (5.24)$$

And the homogeneous solution for all other modes ($m = 2, 3, \ldots, \infty$) is

$$\Phi_{Hm}(x, s) = \begin{cases} [C_{1m} \cosh(\gamma_{1m}x) + C_{2m} \sinh(\gamma_{1m}x)] \cos(\gamma_{2m}x) \\ +[C_{3m} \cosh(\gamma_{1m}x) + C_{4m} \sinh(\gamma_{1m}x)] \sin(\gamma_{2m}x) \\ +[C_{5m} \cosh(\gamma_{3m}x) + C_{6m} \sinh(\gamma_{3m}x)] \cos(\gamma_{4m}x) \\ +[C_{7m} \cosh(\gamma_{3m}x) + C_{8m} \sinh(\gamma_{3m}x)] \sin(\gamma_{4m}x) \end{cases} \cos(\beta_m s) \qquad (5.25)$$

Eq. (5.20), Eq. (5.22), and Eq. (5.24) can be reduced to quartic equations for which the characteristic roots can be solved analytically (Editing Group of the Manual of Mathematics, 1979). The constants C_{dm} ($d = 1, 2, \ldots, 8$) for each mode ($m = 1, 2, \ldots, \infty$) are determined from the boundary conditions at $x = 0$ and $x = x_n$ and the continuity conditions at $x = x_i$ [$i = 1, 2, \ldots, n-1$, Figure 5.1].

5.4.2 Particular Solution

The particular solution is dependent upon the load distribution applied to the strip. For a given strip loading, the load distribution function, $q(x, s)$, is expressed as

$$q(x, s) = q_0 f(x) g(s) \qquad (5.26)$$

where q_0 is the load amplitude and $f(x)$ and $g(s)$ are the load distribution functions in the x and s directions.

Substituting into the right hand side of Eq. (5.14) yields,

$$\frac{q_0 f(x)}{2\pi R} \int_0^{2\pi R} g(s) ds \qquad \text{for } m = 0 \qquad (5.27)$$

and

$$\frac{q_0 f(x)}{\pi R} \int_0^{2\pi R} g(s) \cos(\beta_m s) ds \qquad \text{for } m = 1, 2, \ldots, \infty \qquad (5.28)$$

The potential function, $\phi_{pm}(x)$, can be derived for a wide range of commonly encountered load distributions. The particular solution for most common strip loadings are presented in Table 4.1.

When a strip is subjected to more than one load, the method of superposition is employed to determine the particular solution.

5.4.3 Edge Loading

For cylinders subjected to point loads and radial line loads distributed along the circumferential direction, the cylinder is divided into strips such that the loads coincide with the edges of the strips (Figure 5.1). These loads are expressed as a Fourier series and incorporated into the solution as shear force discontinuities between strips. Table 4.2 presents the edge loading function $\psi_i(s)$ for several common loadings.

When an edge is subjected to a combination of loads, the method of superposition is employed to determine the edge loading function.

5.4.4 Boundary Conditions

The boundary conditions along the edges $x = 0$ and $x = x_n$ are:

For simply supported edges: $u_x = 0,\quad u_s = 0,\quad w = 0,\quad M_x = 0$ (5.29a, b, c, d)

For clamped edges: $u_x = 0,\quad u_s = 0,\quad w = 0,\quad \dfrac{\partial w}{\partial x} = 0,$ (5.30a, b, c, d)

For free edges: $Q_x = \psi,\quad N_x = 0,\quad N_{xs} = 0,\quad M_x = 0,$ (5.31a, b, c, d)

For beam support: $w = w_b,\quad \dfrac{dw}{dx} = \phi_b,\quad Q_x = q_{rb} + \psi,\quad M_x = m_{tb}$ (5.32a, b, c, d)

Difficulties arise when the coefficients on the odd derivatives of the s terms in Eq. (2.32), Eq. (2.34), and Eq. (2.36) are non-zero. Expansion of these equations lead to both $\cos(\beta_m s)$ and $\sin(\beta_m s)$ in the expressions for u_x, u_s, and w when $m = 1, 2, \ldots, \infty$. This necessitates two constraint equations to impose any one of the boundary conditions in Eq. (5.29) through Eq. (5.32). For these cases, only four boundary conditions can be assigned per strip, in contrast to the eight conditions allowed for the alternative case.

5.4.5 Continuity Conditions

The following continuity conditions are applied along the shared edge between strips I and $I + 1$ at $x = x_i$

$$u_{xI} = u_{x(I+1)}, \quad u_{sI} = u_{s(I+1)}, \quad w_I = w_{(I+1)}, \quad \frac{\partial w_I}{\partial x} = \frac{\partial w_{(I+1)}}{\partial x} \qquad \text{(5.33a, b, c, d)}$$

and

$$M_{xI} = M_{x(I+1)}, \quad N_{xI} = N_{x(I+1)}, \quad Q_{xI} = Q_{x(I+1)} + \psi_i, \quad N_{xsI} = N_{xs(I+1)} \qquad \text{(5.34a, b, c, d)}$$

When a beam is present at $x = x_i$, the following continuity conditions are imposed along the common edge $x = x_i$, between strips I and I+1.

$$u_{xI} = u_{x(I+1)}, \quad u_{sI} = u_{s(I+1)}, \quad w_I = w_{(I+1)}, \quad \frac{\partial w_I}{\partial x} = \frac{\partial w_{(I+1)}}{\partial x} = \phi_b \qquad \text{(5.35a, b, c, d)}$$

and

$$m_{tb} = M_{x(I+1)} - M_{xI}, \quad q_{xb} = N_{x(I+1)} - N_{xI}, \qquad \text{(5.36a, b)}$$

$$q_{rb} = Q_{x(I+1)} - Q_{xI} + \psi_i, \quad q_{sb} = N_{xs(I+1)} - N_{xsI} \qquad \text{(5.37c, d)}$$

5.5 Solution

A cylindrical shell is divided into N-strips (Figure 5.1) depending on the number of loading discontinuities and the locations of the ring stiffeners. For each of the N-strips, eight equations are generated from the boundary and continuity conditions. This yields a unique $8N$ system of equations for each mode ($m = 0, 1, 2, …, \infty$). Solution of these systems of equations provide the constants C_{dmI} ($d = 1, 2, …, 8$) in the homogeneous solution. The potential function Φ_I for each strip I ($I = 1, 2, …, N$) is derived by summing the homogeneous and particular solutions. The potential function is then back-substituted into the relevant force and displacement equations.

5.6 Application

Because of the ill-conditioned nature of the solution, the ASM is susceptible to numerical instabilities when computing solutions using double precision floating point format. To eliminate this concern, examples are computed with a MATLAB (Mathworks, 2017) program using an arbitrary-precision package.

5.6.1 Example 1: Laminated Cylindrical Shells Subjected to Axisymmetric Loads

The purpose of this example is to compare the Analytical Strip Method (ASM) results for laminated cylindrical shells subjected to axisymmetric loads to an existing analytical solution developed by Ren (1995).

Three laminated shells are considered:

Case 1: Single layer with lamina fibers oriented at an angle of $\beta = 45°$.

Case 2: Two-layer antisymmetric angle-ply laminate with inner layer oriented with fibers at an angle of $\beta = 45°$ and outer layer oriented with fibers at an angle of $\beta = -45°$.

Case 3: Three-layer symmetric angle-ply laminate with inner and outer layers oriented with fibers at an angle of $\beta = 45°$ and middle layer oriented at an angle of $\beta = -45°$. The thickness of the inner, middle, and outer layers is t/2, t/4, and t/2.

Orientation angle of the lamina, β, is measured counterclockwise from the x-axis of the cylinder. For the layer material, the elastic modulus in the direction of the fibers $E_1 = 172$ GPa $= 25 \times 10^6$ psi, the elastic modulus perpendicular to the direction of the fibers $E_2 = 7$ GPa $= 10^6$ psi, shear modulus $G_{12} = 3.4$ GPa $= 0.5 \times 10^6$ psi, and Poisson's ratio $v_{12} = 0.25$.

The shells are simply supported with length-to-radius ratio $L/R = 6$ and are subjected to an axisymmetric sinusoidal load $q = q_0 \sin(\pi x/L)$. Table 5.1 presents the dimensionless deflection, $\overline{w} = \frac{100 E_2 t^3 w}{q_0 R^4}$, at $x = L/2$ for prescribed radius-to-thickness ratios (R/t). The results are presented for an exact elasticity based solution (Ren, 1995), an existing classical shell theory (CST) solution for thin shells (Ren, 1995), and the Analytical Strip Method (ASM).

As expected, the ASM and CST results are in excellent agreement regardless of the radius-to-thickness ratios. The ASM and CST solutions are within 2% of the Exact solution for radius-to-thickness ratios up to 10. For the thicker shells, the difference between the Exact and thin shell solutions increases to 15% for $R/t = 2$.

5.6.2 Example 2: Laminated Cylindrical Shells Subjected to Non-Axisymmetric Loads

The purpose of this example is to compare the Analytical Strip Method (ASM) results for laminated cylindrical shells subjected to non-axisymmetric loads to an existing analytical solution developed by Ren (1987).

Three laminated shells are considered:

Case 1: Single layer with lamina fibers oriented in the s-direction, $\beta = 90°$.

Case 2: Two-layer antisymmetric cross-ply laminate with inner layer oriented with fibers in the *x*-direction, $\beta = 0°$, and outer layer oriented with fibers in the *s*-direction, $\beta = 90°$.

Case 3: Three-layer symmetric cross-ply laminate with inner and outer layers oriented with fibers in the *s*-direction, $\beta = 90°$, and middle layer oriented with fibers in the *x*-direction, $\beta = 0°$. All three layers are of equal thickness.

For the layer material, the elastic modulus in the direction of the fibers $E_1 = 172$ GPa = 25×10^6 psi, the elastic modulus perpendicular to the direction of the fibers $E_2 = 6.9$ GPa = 10^6 psi, shear modulus $G_{12} = 3.4$ GPa = 0.5×10^6 psi, and Poisson's ratio $v_{12} = 0.25$.

The loading on the shells is uniform in the *x*-direction but has a sinusoidal distribution $q = q_0 \cos(3s/R)$ in the circumferential direction. The cylinders are infinite in length and have a radius $R = 10$. Table 5.2 present the dimensionless deflection, $\bar{w} = \frac{100 E_2 t^3 w}{q_0 R^4}$, at $s = 0$ for prescribed radius-to-thickness ratios (R/t). The results are presented for an exact elasticity based solution (Ren, 1987), an existing classical shell theory (CST) solution for thin shells (Ren, 1987), and the Analytical Strip Method (ASM). Because the ASM is not constrained by the infinite length requirement, the solution is obtained by increasing the length of the simply supported shells until the dimensionless deflection quantity converges.

As expected, the ASM and CST results are in excellent agreement regardless of the radius-to-thickness ratios. The thin shell theories give reliable results for radius-to-thickness ratios down to 50, as the dimensionless deflection quantities are within 3%. As the thickness of the shell increases, the thin shell theories tend to significantly under predict the deflection. At $R/t = 10$, the exact solution predicts nearly twice the deflection as given by the thin shell theories; and at R/t = 2, the exact solution predicts 18 times the deflection of the thin shell theories.

5.6.3 Example 3: Retrofit of a Water Storage Tank

The purpose of this example is to demonstrate the use of the ASM to optimize the design of a retrofit for a steel water storage tank.

An existing water storage tank has a radius $R = 4.572$ m (15 ft), a height $H = 12.192$ m (40 ft), and is simply-supported at the base. The tank is constructed from steel with a uniform wall thickness $t_1 = 6.350$ mm (0.25 in), modulus of elasticity $E = 2.0 \times 10^5$ MPa (29×10^3 ksi) and Poisson's ratio $v = 0.3$. The owner wants to increase the storage capacity by raising the height of the tank by $H_3 = 9.144$ m (30 ft). The raised portion is constructed from steel with a uniform wall thickness $t_2 = 3.175$ mm (0.125 in).

The increased height of the tank produces a maximum Von Mises stress $\sigma_v = 167$ MPa (24.2 ksi), which is more than the maximum allowable stress $\sigma_{all} = 124$ MPa (18 ksi). To reduce the stresses below the allowable, the steel is wrapped with a fiber-reinforced polymer (FRP) from the base to a height $H_1 = 4.572$ m (15 ft). The FRP has elastic moduli $E_1 = 1.724 \times 10^5$ MPa (25×10^3 ksi) and $E_2 = 1.724 \times 10^4$ MPa (2.5×10^3 ksi), shear modulus $G_{12} = 3.792 \times 10^4$ MPa (5.5×10^3 ksi), and Poisson's ratio $v_{12} = 0.25$. The thickness of each lamina layer is $t_L = 0.991$ mm (0.039 in). The retrofitted tank is shown in Figure 5.3.

The ASM is deployed by dividing the tank into three strips, corresponding to the geometric discontinuities, and imposing the boundary and continuity conditions at the ends of each strip. The strip at the base of the tank will behave anisotropically due to the FRP layers, while the other two strips are isotropic. The ASM is used to analyze the structure for 1, 2, 3, and 4 layers of FRP with ply-orientations of β, $\beta/-\beta$, $\beta/-\beta/\beta$, and $\beta/-\beta/\beta/-\beta$, where β varies from 0° to 90°. Due to the variations in the geometry of the structure and the anisotropic behavior, no existing analytical methods are suitable for the analysis.

Figure 5.4 shows the ratio of maximum Von Mises stress within the steel portion of the tank to the allowable stress, σ_v / σ_{all}, for the range of FRP configurations analyzed. The optimal design of the retrofit uses three layers of FRP with ply-angle oriented at $71^\circ \le \beta \le$

90°. The optimal orientation is at $\beta = 90°$, which orients the fibers in the circumferential direction of the tank. Figure 5.5 shows the variation in Von Mises stress within the steel along the height of the structure for the optimal retrofit. The results are compared with a finite element (FEM) solution generated using ANSYS (ANSYS, Inc., 2016). The results are in good agreement.

5.6.4 Example 4: Stiffened Tank Subjected to Line Load

The purpose of this example is to demonstrate the use of the ASM for stiffened and laminated cylindrical shells.

The cylinder in Figure 5.6 is stiffened with standard W10x49 steel rolled sections having an area $A = 9290$ mm^2 (14.4 in^2), a moment of inertia about the section x-axis $I_x = 1.132 \times 10^8$ mm^4 (272 in^4), a moment of inertia about the section y-axis $I_y = 3.888 \times 10^7$ mm^4 (93.4 in^4), and a torsion constant $J = 5.786 \times 10^5$ mm^4 (1.39 in^4). The modulus of elasticity of the stiffener E $= 2 \times 10^8$ kPa (29×10^6 psi) and Poisson's ratio $v = 0.3$. The ends are simply supported with boundary conditions, $u = s = w = M_x = 0$. The cylinder is subjected to a line load $p = 0.01$ kN/mm (57.1 lb/in) along the generator, $s = 0$.

Table 5.3 presents dimensionless deflections along the generator, $s = 0$, at $x = L/8$, $x = L/4$, $x = 3L/8$, and $x = L/2$ for the shell in Figure 5.6. Results are presented for an isotropic steel shell as well as cross-ply laminated shells with the number of layers ranging from 2-ply to 8-ply. For the isotropic steel shell, the modulus of elasticity E $= 2 \times 10^8$ kPa (29×10^6 psi), Poisson's ratio $v = 0.3$, and thickness $t = 5$ mm (0.197 in). For the cross-ply laminated shells, the lamina has elastic moduli $E_1 = 1.724 \times 10^5$ MPa (25×10^3 ksi) and $E_2 = 1.724 \times 10^4$ MPa (2.5×10^3 ksi), shear modulus $G_{12} = 3.792 \times 10^4$ MPa (5.5×10^3 ksi), and Poisson's ratio $v_{12} = 0.25$. Results are presented for the ASM solution as well as a finite-element method (FEM) solution generated using ANSYS (ANSYS, Inc., 2016). The results are in good agreement.

One of the primary advantages of laminated composites is their high weight-to-stiffness ratio. Table 5.3 shows that a 7-layer laminate with total thickness 39% greater than the

thickness of the steel shell yields deflections within 15% of steel. Since the unit weight of FRP is ¼ the weight of steel, the reduction in the weight, exclusive of the stiffeners, is approximately 36%. High weight-to-stiffness ratio along with other performance characteristics, such as corrosion resistance, make laminated composites a desirable construction material.

The ASM results are based on summation of the first 51 modes. Table 5.4 presents the dimensionless radial deflection quantity for several modes at distances of $x = L/8$, $x = L/4$, $x = 3L/8$, and $x = L/2$ along the generator, $s = 0$, for the 7-layer cross-ply laminated shell. The series shows good convergence characteristics, mode 50 contributes less than 0.05% to the cumulative deflection at all locations presented. Deflections at the ring stiffeners show faster convergence than at other locations.

5.7 Conclusion

The Analytical Strip Method (ASM) is presented in this chapter for stiffened and laminated cylindrical shells. The primary advantage of the ASM is its applicability to any laminated shell, any generalized distribution of ring stiffeners along the length of the shell, and to a wide variety of axisymmetric and non-axisymmetric loads. The following are deduced from the derivation of the ASM and the examples presented in this chapter:

- The results of the ASM are in good agreement with existing analytical solutions based on classical thin shell theory, and the generality of the solution method overcomes many limitations of existing analytical solutions.
- The ASM produces reliable results for shells with a large radius-to-thickness ratio; however, as the ratio drops below 50, significant deviations from the exact elasticity solution are likely.
- The ASM can be used to efficiently optimize the design of laminated cylinders and structure retrofits.
- The ASM shows good convergence characteristics.

Table 5.1. Dimensionless deflections, $\overline{w} = \frac{100E_2 t^3 w}{q_0 R^4}$, at $x = L/2$ for angle-ply laminated cylindrical shells subjected to axisymmetric loading with sinusoidal distribution, $q = q_0 \sin(\pi x/L)$, along the length of the shell.

	Case 1 - β = 45°			Case 2 - β = 45° / -45°			Case 2 - β = 45° / -45° / 45°		
	$\overline{w}$			$\overline{w}$			$\overline{w}$		
R/t	ASM[a]	CST[b]	EXACT[c]	ASM	CST	EXACT	ASM	CST	EXACT
2	18.968	18.600	19.882	13.852	13.469	16.184	13.741	13.361	16.184
5	3.072	3.012	3.154	2.213	2.151	2.341	2.210	2.149	2.341
10	0.7693	0.7545	0.7784	0.5530	0.5377	0.5624	0.5528	0.5375	0.5624
20	0.1924	0.1887	0.1922	0.1382	0.1344	0.1376	0.1382	0.1344	0.1376
50	0.0308	0.0302	0.0304	0.0221	0.0215	0.0217	0.0221	0.0211	0.0217

[a] ASM = Analytical Strip Method
[b] CST = Classical Shell Theory solution for thin shells (Ren, 1995)
[c] EXACT = Three-dimensional elasticity solution (Ren, 1995)

Table 5.2. Dimensionless deflections, $\overline{w} = \frac{100E_2 t^3 w}{q_0 R^4}$, at $s = 0$ for cross-ply laminated cylindrical shells subjected to sinusoidal load distribution, $q = q_0 \cos(3s/R)$, along the circumference of the shell.

	Case 1 - β = 90°			Case 2 - β = 0° / 90°			Case 2 - β = 90° / 0° / 90°		
	$\overline{w}$			$\overline{w}$			$\overline{w}$		
R/t	ASM[a]	CST[b]	EXACT[c]	ASM	CST	EXACT	ASM	CST	EXACT
2	0.7659	0.7640	9.9860	4.9991	4.9900	20.7900	0.8004	0.7790	14.3600
4	0.7543	0.7520	3.1200	4.4742	4.4700	8.5400	0.7838	0.7810	4.5700
10	0.7509	0.7490	1.1500	4.1814	4.1700	4.9300	0.7791	0.7770	1.4400
50	0.7503	0.7480	0.7700	4.0307	4.0200	4.0900	0.7779	0.7760	0.8080
100	0.7503	0.7480	0.7550	4.0117	4.0000	4.0300	0.7782	0.7760	0.7870
500	0.7503	0.7480	0.7490	3.9910	3.9900	3.9900	0.7779	0.7760	0.7730

[a] ASM = Analytical Strip Method
[b] CST = Classical Shell Theory solution for thin shells (Ren, 1987)
[c] EXACT = Three-dimensional elasticity solution (Ren, 1987)

Table 5.3. Dimensionless deflections, $\widehat{w} = \frac{wE_1R}{pL}$, at $s = 0$ for stiffened cylindrical shell in Figure 5.6 subjected to line load, p, along the generator of the shell.

| Shell Material	R/t	$\widehat{w}$ at $x = L/8$ ASM[a]	FEM[b]	$\widehat{w}$ at $x = L/4$ ASM	FEM	$\widehat{w}$ at $x = 3L/8$ ASM	FEM	$\widehat{w}$ at $x = L/2$ ASM	FEM
Isotropic	100	790	793	23	27	752	756	29	33
2 Layer - Cross-Ply	252	13943	14058	77	79	13998	14092	101	103
3 Layer - Cross-Ply	168	7389	7458	53	57	6810	6868	70	73
4 Layer - Cross-Ply	126	2604	2608	41	45	2549	2554	54	57
5 Layer - Cross-Ply	101	1936	1947	35	38	1772	1785	45	48
6 Layer - Cross-Ply	84	1098	1103	30	33	1052	1058	38	42
7 Layer - Cross-Ply	72	883	890	27	30	798	807	34	37
8 Layer - Cross-Ply	63	599	605	24	27	563	570	30	34

[a] ASM = Analytical Strip Method
[b] FEM = Finite Element Method

Table 5.4. ASM cumulative deflections $\widehat{w} = \sum_0^m \widehat{w}_m$, where $\widehat{w}_m = \frac{w_m E_1 R}{pL}$, along the generator ($s = 0$) for the stiffened 7-layer cross-ply cylindrical shell in Figure 5.6.

Mode m	$\widehat{w}$ at $x = L/8$	$\widehat{w}$ at $x = L/4$	$\widehat{w}$ at $x = 3L/8$	$\widehat{w}$ at $x = L/2$
0	13	0	12	0
1	50	21	61	28
2	83	26	95	33
5	218	27	218	34
10	534	27	480	34
20	814	27	731	34
30	865	27	781	34
40	878	27	794	34
50	883	27	798	34
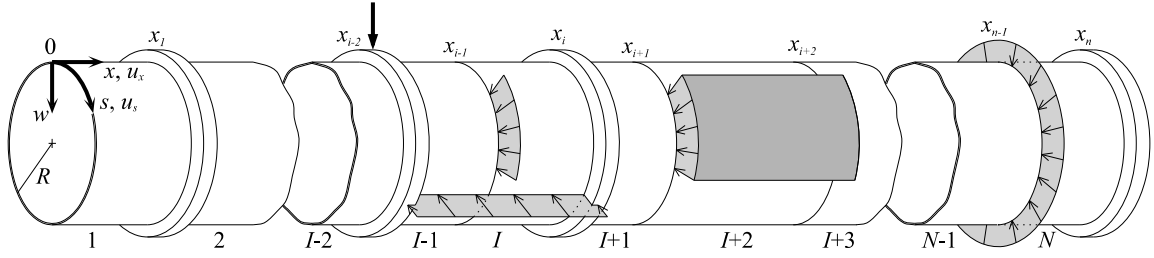
Figure 5.1. Stiffened cylindrical shell with strip and edge loadings
Note: The stiffeners are concentric with the shell
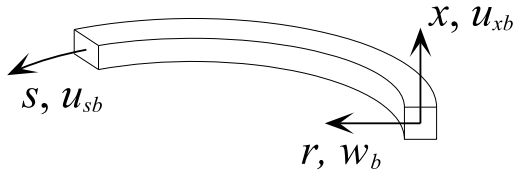
Figure 5.2. Coordinate system for the ring stiffener
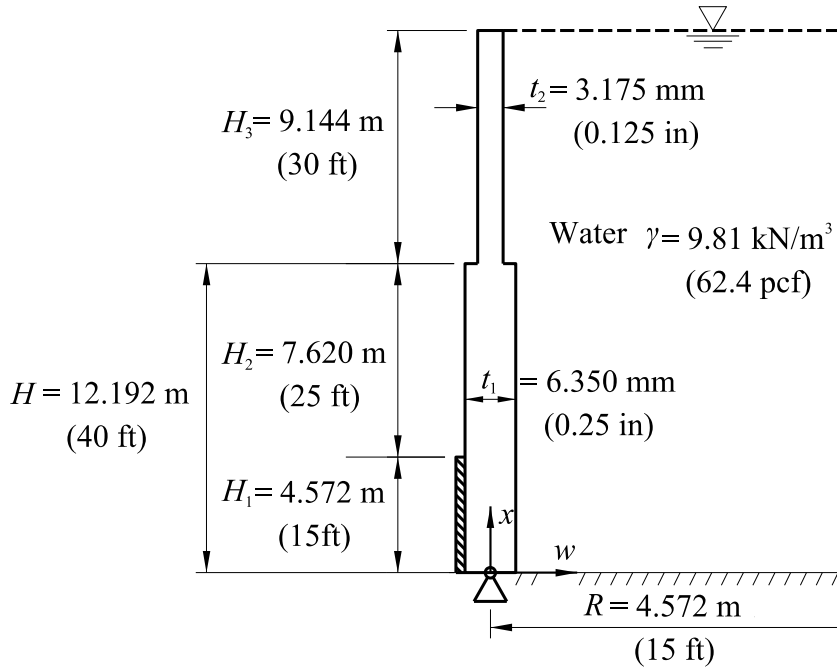
Figure 5.3. Retrofitted water storage tank with simply supported base
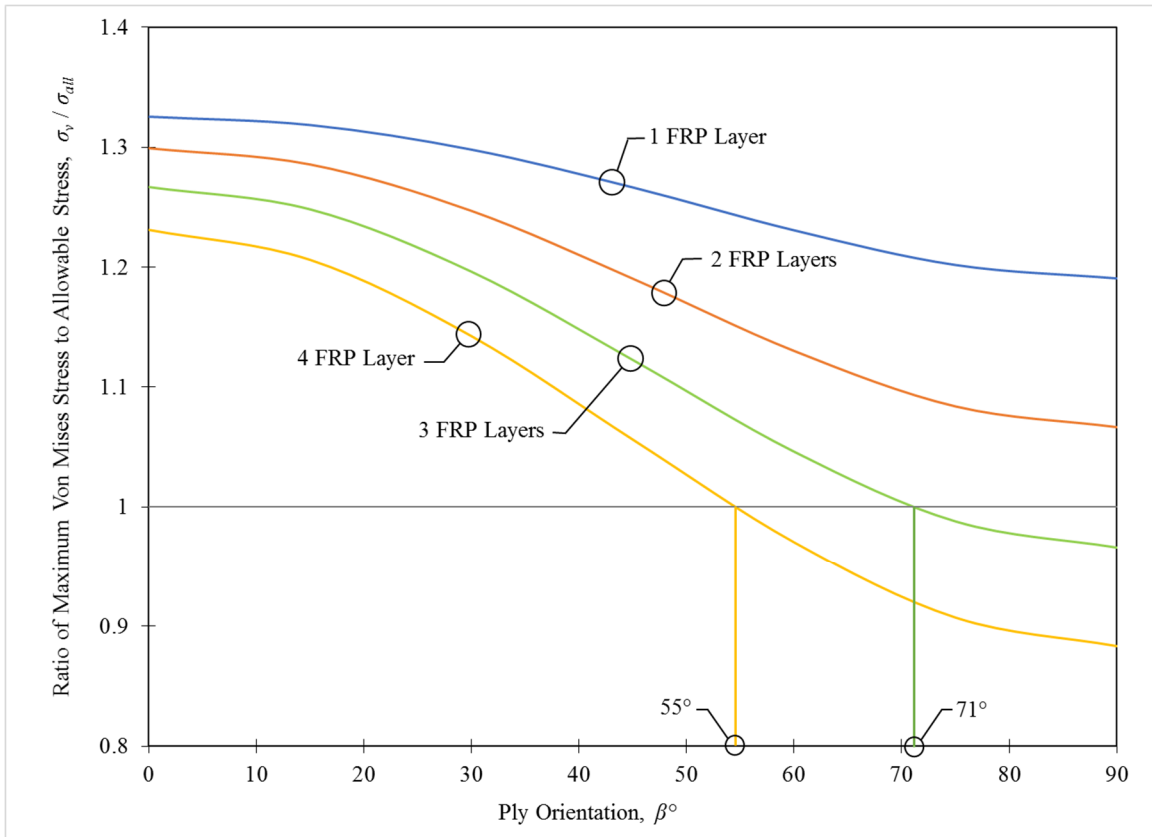
Figure 5.4. Ratio of maximum Von Mises stress to allowable stress, σ_v/σ_{all}, for the water storage tank in Figure 5.3 retrofitted with layers of FRP laminate at varying ply-angle orientations.

94
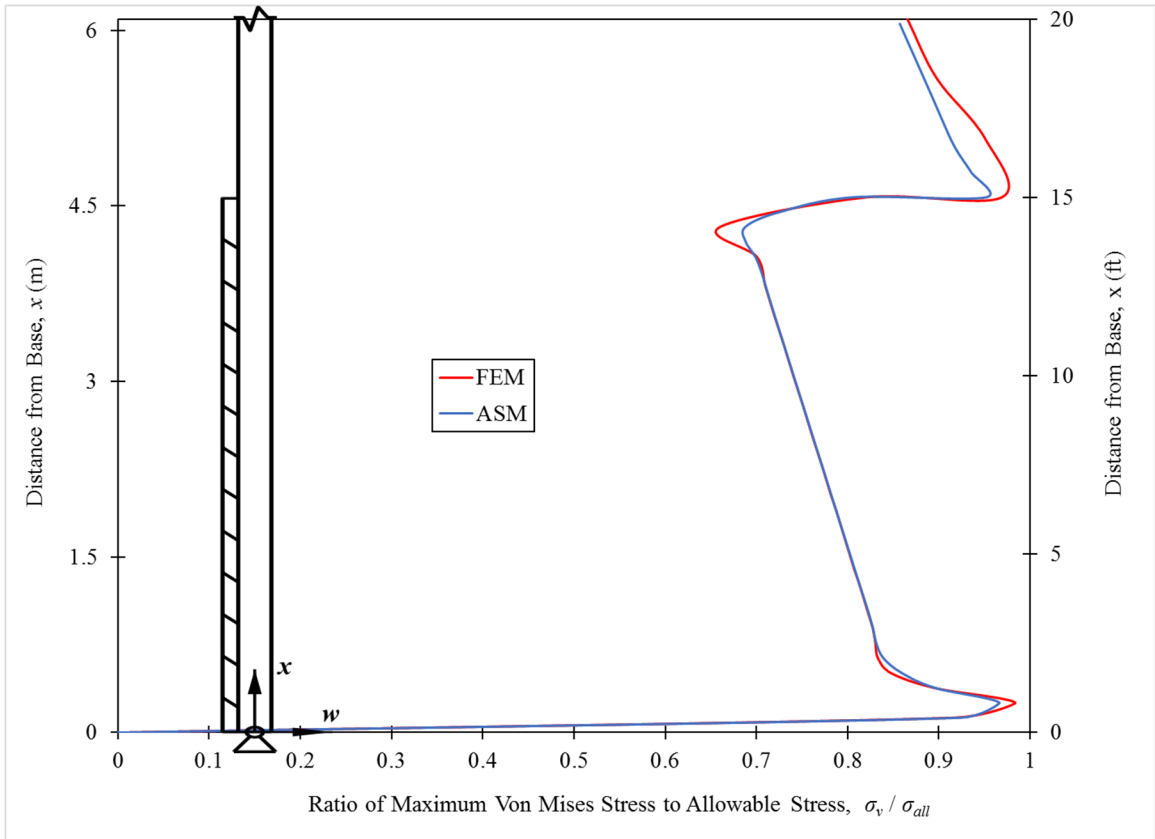
Figure 5.5. Ratio of maximum Von Mises stress to allowable stress, σ_v / σ_{all}, along the height of the water storage tank in Figure 5.3 retrofitted with three layers of FRP laminate with fibers oriented in the circumferential direction of the tank.
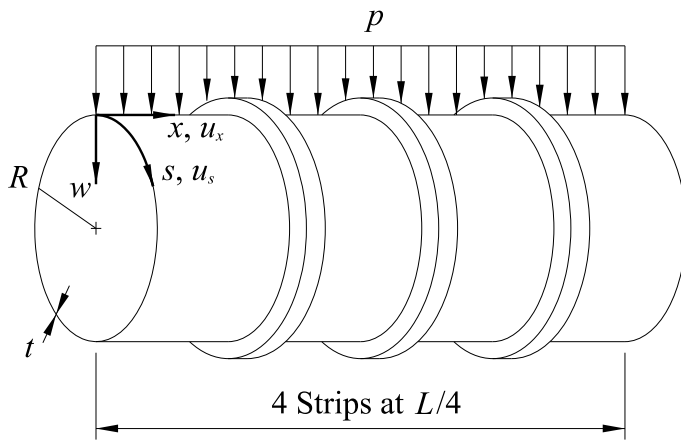
Figure 5.6. Stiffened cylindrical shell subjected to a line load

CHAPTER 6
CONCLUSIONS AND FUTURE RESEARCH NEEDS

6.1 General Summary

An Analytical Strip Method (ASM) has been derived for isotropic and laminated cylindrical shells. Laminated shells can have any generalized layer configuration and ply-angle scheme, such that the shell behaves anisotropically. The ASM can handle any combination of fixed, simply supported, and beam supported boundary conditions, as well as any variations in wall thickness and distribution of ring stiffeners. The ASM can be applied to any combination of radially applied point loads, patch loads, line loads, and hydrostatic loads. The following are deduced from the derivation of the ASM and the examples presented in Chapter 4 and Chapter 5:

- The results of the ASM are in good agreement with existing analytical solutions, and the generality of the solution method overcomes many limitations of existing analytical solutions.
- Unlike the finite element method, the ASM does not require significant pre-processing effort. Its accuracy is dependent on the number of modes considered in the solution rather than the fineness of the discretization of the structure.
- The finite element method offers more flexibility in structure geometry.   For instance, the ASM requires stiffeners to be concentric with the shell walls and stepped wall thicknesses to have a coincident middle surface.
- The finite element method has less potential for numerical instabilities than the ASM.

6.2 Isotropic Cylindrical Shells

Existing analytical solutions for isotropic shells are limited to simplified loading conditions and shell geometry; the ASM overcomes these limitations. Unlike many existing analytical solutions, the ASM does not require elimination of terms from the

governing equations to simplify the solution. Examples in Chapter 4 show up to 10% difference between the ASM and existing analytical solution. Finite Element results are in very good agreement with the ASM results. Convergence studies show good convergence characteristics of the ASM series solution. In general, force quantities require more modes for convergence when compared to the displacement quantities.

6.3 Laminated Cylindrical Shells

The ASM is derived for laminated shells with any generalized layer scheme and ply-angle orientation, such that the shell behaves anisotropically. This includes the special cases of symmetric and anti-symmetric laminates with cross-ply or angle-ply orientations. ASM results were compared to results from existing classical shell theory (CST) solutions for thin shells, as well as exact elasticity solutions. As expected, the results between the ASM and CST were in excellent agreement. For shells with large radius-to-thickness ratios, the ASM solution closely matched the exact solution. Thicker shells, with small radius-to-thickness ratios, exhibited a significant deviation between the ASM and exact solution.

A major benefit of the ASM is the ability to optimize the design of laminated cylindrical shells. Chapter 5 demonstrated the use of the ASM to find the optimal design of a retrofit for and cylindrical water storage tank. The isotropic steel tank, wrapped with fiber-reinforced polymer laminates leads to an anisotropic response, for which there are no existing analytical solutions available.

6.4 Recommendations for Future Research

Based on the current work, recommendations for future work include:

- Eccentricity of stiffeners: The solution is derived with stiffeners concentric to the mid-surface of the shell. The ASM can be modified to incorporate an eccentricity between the ring stiffener and the mid-surface of the shell.

- Non-isotropic stiffeners: The governing equations for the stiffeners are derived based on isotropic beams. Laminated stiffeners or stiffeners with non-isotropic properties can be incorporated in the same fashion using revised governing equations.

- Eccentricity of reference surface: The ASM requires that adjacent strips have a coincident middle surface, even in the case where the wall thickness changes. The solution method can be modified to incorporate arbitrary definition of the reference surface within each strip.

- Axial and circumferential loading: The ASM is currently derived for radial loads only. The solution method can be extended to incorporate axial and circumferential loading. This would require the incorporation of q_x and q_s in the three coupled differential equations of Eq. (2.16).

- Thermal loading: The ASM can be extended to handle thermal loading, which is of considerable interest in laminated shells.

- Free vibration: The ASM could be used to determine the fundamental frequencies of a cylindrical shell by incorporating the equations of motion into the governing differential equations. Free vibration analysis of stiffened and laminated cylindrical shells would be a significant advancement in the analysis and design of shell structures.

- Buckling: By incorporating axial loading into the solution method, the ASM can be further extended to the bucking of stiffened and laminated cylindrical shells. Buckling analysis of cylindrical shells is of great interest due to the high number of cylindrical shell structures designed to carry axial loads.

REFERENCES

Ambartsumian, S. A. (1961). *Theory of Anisotropic Shells*. State Publishing House for Physical and Mathematical Literature, Moscow.

Ambartsumian, S. A. (1966). "Some Current Aspects of the Theory of Anisotropic Layered Shells." *Applied Mechanics Surveys*, Spartan Books, Washington, DC, 301-303.

ANSYS, Inc. (2016). ANSYS, version 17.

Barbero, E. J., Reddy, J. N., Teply J. L. (1990). "A General Two-Dimensional Theory of Laminated Cylindrical Shells." *AIAA J.*, 28(3), 544-553.

Bert, C. W. (1975). "Analysis of Shells." *Composite Material – Structural Design and Analysis*, *Part I, vol. 7*, Academic Press, New York, 207-258.

Bijlaard, P. (1955). "Stresses From Local Loadings in Cylindrical Pressure Vessels." *Trans. Am. Soc. Mech. Engrs*, 77, 805-814.

Byrne, R. (1944). "Theory of Small Deformations of a Thin Elastic Shell. Seminar Reports in Math." *Univ. of Calif. Pub. In Math.*, 2(1), 103-152.

Computers and Structures, Inc. (2015). Sap2000, version 18.

Chandrashekhara, K., Nanjunda Rao, K. S (1997). "Approximate Elasticity Solution for a Long and Thick Laminated Circular Cylindrical Shell of Revolution." *Int. J. Solids Struct.*, 34, 1327-1341.

Chandrashekhara, K., Nanjunda Rao, K. S. (1998). "Method of Initial Functions for the Analysis of Laminated Circular Cylindrical Shells Under Axisymmetric Loading." *Mechanics of Composite Materials and Structures*, 5, 187-201.

Cheng, S., Ho, B. P. C. (1963). "Stability of Heterogeneous Aeolotropic Cylindrical Shells Under Combined Loading." *AIAA Journal*, 1(4), 892-898.

Cooper, R. M (1957). "Cylindrical Shells Under Line Load." *Journal of Applied Mechanics*, 24, 553-558.

Dong, S. B., Pister, K. S., Taylor, R. L. (1962). "On the Theory of Laminated Anisotropic Shells and Plates." *Journal of Aerospace Sciences*, 29, 969-975.

Donnell, L. H. (1933). "Stability of Thin Walled Tubes Under Torsion." *NACA Rept. No. 479*.

Donnell, L. H. (1938). "A Discussion of Thin Shell Theory." *Proc. Fifth Intern. Congr. Appl. Mech.*.

Editing Group of the Manual of Mathematics (1979). "Roots for Quartic Equation." *Manual of Mathematics*, People's Education Press, Beijing, China, (Chinese), 87-90.

Flügge, W. (1934). *Statik und Dynamik der Schalen*. Julius Springer, Berlin, (Reprinted by Edwards Brothers Inc., Ann Arbor, Mich., 1943.)

Flügge, W. (1962). *Stresses in Shells*. Springer-Verlag, Berlin.

Goldenveizer, A. L. (1961). *Theory or Thin Shells*. Pergamon Press, New York.

Harik, I. E., Salamoun, G. L. (1986). "Analytical Strip Solution to Rectangular Plates." *Journal of Engineering Mechanics*, 112(1), 105-118.

Harik, I. E, Salamoun, G. L. (1988). "The Analytical Strip Method of Solution for Stiffened Rectangular Plates." *Computers & Structures*, 29(2), 283-291.

Hildebrand, F. B., Reissner, E., Thomas, G. B. (1949). "Notes on the Foundations of the Theory of Small Displacements or Orthotropic Shells." *NACA-TN-1833*.

Hoff, N. J., Kempner, J., Pohle, F. V. (1954). "Line Load Applied Along Generators of Thin-Walled Circular Cylindrical Shells of Finite Length." *Quarterly of Applied Mathematics*, 11, 411-425.

Jones, R. M. (1999). *Mechanics of Composite Materials*, 2nd ed., Taylor & Francis Group, New York.

Kempner, J. (1955). "Remarks on Donnell's Equations." *Journal of Applied Mechanics*. 22, 117-118.

Kraus, H. (1967). *Thin Elastic Shells*. John Wiley & Sons, Inc., New York.

Leissa, A. W. (1973). "Vibration of Shells." *NASA SP-288*.

Liew, K. M., Ng, T. Y., Zhao, X. (2002). "Vibration of Axially Loaded Rotating Cross-Ply Laminated Cylindrical Shells via Ritz Method." *Journal of Engineering Mechanics*, 128(9), 1001-1007.

Love, A. E. H. (1892). *A Treatise on the Mathematical Theory of Elasticity. 4th Ed.*, Dover Pub., Inc., New York.

Love, A. E. H. (1888). "The Small Free Vibrations and Deformations of a Thin Elastic Shell." *Phil. Trans. Roy. Soc. (London), ser. A*, 179, 491-549.

Lur'ye, A. I. (1940). "General Theory of Elastic Shells." *Prikl. Mat. Mekh.*, 4(1), 7-34. (In Russian.)

Mathworks (2017). MATLAB, version R2017a

Meck, H. R. (1961). "Bending of a Thin Cylindrical Shell Subjected to a Line Load Around a Circumference." *Journal of Applied Mechanics*, 28, 427-433.

Mushtari, Kh. M. (1938). "On the Stability of Cylidrical Shells Subjected to Torsion." *Trudy Kaz. avais in-ta*, 2. (In Russian.)

Mushtari, Kh. M. (1938). "Certain Generalizations of the Theory of Thin Shells." *Izv. Fiz. Mat. ob-va. Pri Kaz. un-te.*, 11(8), (In Russian.)

Naghdi, A. K. (1968). "Bending of a Simply Supported Circular Cylindrical Shell Subjected to Uniform Line Load Along a Generator." *Int. J. Solids Structures*, 4, 1067-1080.

Naghdi, P. M. (1957). "On the Theory of Thin Elastic Shells." *Q. Appl. Math.* 14, 369-380.

Naghdi, P. M., Berry, J. G. (1964). "On the Equations of Motion of Cylindrical Shells." *J. Appl. Mech.*, 21(2), 160-166.

Noor, A. K., Burton, W. S. (1990). "Assessment of Computational Models for Multilayered Composite Shells." *Appl. Mech. Rev.*, 43, 67-96.

Novozhilov, V. V. (1964). *The Theory of Thin Elastic Shells*. P. Noordhoff Lts, Groningen, The Netherlands.

Odqvist, F. (1946). "Action of Forces and Moments Symmetrically Distributed along a Generatrix of Thin Cylindrical Shell." *Trans. Am. Soc. Mech. Engrs*, 68A, 106-108.

Reddy, J. N. (1984). "Exact Solutions of Moderately Thick Laminated Shells." *Journal of Engineering Mechanics*, 110(5), 794-809.

Reddy, J. N. (2004). *Mechanics of Laminated Composite Plates and Shells: Theory and Analysis 2nd ed.*, CRC Press, Boca Raton.

Reissner, E. (1941). "A New Derivation of the Equations of the Deformation of Elastic Shells." *Amer. J. Math.*, 63(1), 177-184.

Reissner, E. (1952). "Stress Strain Relations in the Theory of Thin Elastic Shells." *J. Math. Phys.*, 31, 109-119.

Ren, J. G. (1987). "Exact Solution for Laminated Cylindrical Shells in Cylindrical Bending." *Composites Science and Technology*, 29, 169-187.

Ren, J. G. (1995). "Analysis of Laminated Circular Cylindrical Shells Under Axisymmetric Loading." *Composite Structures*, 30, 271-280.

Sanders, J. L., JR. (1959). "An Improved First Approximation Theory for Thin Shells." *NASA TR-R24*.

Saviz, M. R., Shakeri, M., Yas, M. H. (2009). "Layerwise Finite Element Analysis of Laminated Cylindrical Shell with Piezoelectric Rings Under Dynamic Load." *Mechanics of Advanced Materials and Structures*, 16, 20-32.

Saviz, M. R., Mohammadpourfard, M. (2010). "Dynamic Analysis of a Laminated Cylindrical Shell with Piezoelectric Layers under Dynamic Loads." *Finite Elements in Analysis and Design*, 46, 770-781.

Sharma, S., Iyengar, N. G. R, Murthy, P. N. (1980). "Buckling of Antisymmetric Cross- and Angle-ply Laminated Plates." *International Journal of Mechanical Sciences*, 22(10), 607-620.

Singha, M. K., Ramachandra, L. S., Bandyopadhyay, J. N. (2006). "Nonlinear Response of Laminated Cylindrical Shell Panels Subjected to Thermomechanical Loads." *Journal of Engineering Mechanics*, 132(10), 1088-1095.

Stewart, J. (1995). *Calculus, 3rd ed.*, Brooks/Cole, Pacific Grove, Ca.

Sun, L. (2009). *Analytical Strip Method to Antisymmetric Laminated Plates.* University of Kentucky, Doctoral Dissertation.

Timoshenko, S., Woinowsky-Krieger, S. (1959). *Theory of Plates and Shells, 2nd Ed.*, McGraw-Hill Book Company, Inc, York.

Timoshenko, S., Gere, J. M. (1961). *Theory of Elastic Stability, 2nd ed.*, McGraw-Hill, New York.

Varadan, T. K, Bhaskar, K. (1991). "Bending of Laminated Orthotropic Cylindrical Shells – An Elasticity Approach." *Composite Structures*, 17, 141-156.

Vasilenko, A. T., Golub, G. P. (1984). "Stressed State of Anisotropic Shells of Revolution with Transverse Shear." *Sov. Appl. Mech.*, 19(9), 759-763.

Vlasov, V. Z. (1944). "Osnovnye Differentsialnye Uravnenia Obshche Teorii Uprugikh Obolochek." *Prikl. Mat. Mekh.*, 8, (English transl.: *NACA TM 1241*, "Basic Differential Equations in the General Theory of Elastic Shells." Feb. 1951.)

Vlasov, V. Z. (1961). *Thin-Walled Elastic Beams, 2nd Ed.*, Israel Program for Scientific Translations Ltd, Jerusalem.

Vlasov, V. Z. (1949). "Obshchaya teoriya obolochek; yeye prilozheniya v tekhnike." *Gos. Izd. Tekh.-Teor. Lit.*, Moscow-Leningrad. (English transl.: *NASA TT F-99*, "General Theory of Shells and Its Applications in Engineering." Apr. 1964.)

Whitney, J. M., Sun, C. T. (1974). "A Refined Theory for Laminated Anisotropic, Cylindrical Shells." *Journal of Applied Mechanics*, 41, 471-476.

John (Taylor) Perkins was born in Louisville, KY. After graduating high school in May of 2002, he began his undergraduate education at the University of Kentucky. He graduated Summa Cum Laude in May 2007 with a BS in Civil Engineering and in May 2008 with a MS in Civil Engineering. Beginning in August 2008, he began pursuing a doctoral degree in Structural Engineering at the University of Kentucky.

Since May 2007, Taylor has worked full-time as a Senior Structural Engineer for Stantec Consulting Services in Lexington, KY. He carries the NCEES Model Law Structural Engineer designation, is a licensed Structural Engineer in IL, and holds Professional Engineering licensure in KY, MN, GA, FL

Taylor Perkins is a co-author of the following publications:

1. J. Taylor Perkins and Issam E. Harik, "*Analytical Strip Method for Thin Isotropic Cylindrical Shells*", IOSR Journal of Mechanical and Civil Engineering, 14(4.3) (Jul. – Aug. 2017), pp. 24-38
2. J. Taylor Perkins and Issam E. Harik, "*Analytical Strip Method for Thin Laminated Cylindrical Shells*", (in preparation)
3. J. Taylor Perkins, Husein A. Hasan, and Daniel A. Gilbert, "*Pseudo-Nonlinear Finite Element Analysis of Concrete Gravity Dams*", United States Society of Dams Conference 2017, Anaheim, CA (April 3 – April 7, 2017)
4. J. Taylor Perkins and Jim Bader, "*Direct Fixation Challenges for the North Metro Rail Line Skyway Bridge*", International Bridge Conference 2017, National Harbor, MD (June 5 – June 8, 2017)
5. J. Taylor Perkins, Jim Bader, and Jennifer Whiteside, "*Lessons Learned from Colorado's Longest Direct Fixation Bridge*", AREMA Annual Conference 2017, Indianapolis, IN (September 17 – September 20, 2017) (accepted for publication)
6. J. Taylor Perkins, C. Tony Hunley, and Matthew Hyner, "*US 60 Smithland Bridge – Navigation Modeling*", 39th IABSE Symposium, Vancouver, BC (September 21 – September 23, 2017) (accepted for publication)